Good Practice Guide on the operation of AC quantum voltage standards

Book · June 2018

CITATIONS
0

READS
335

14 authors, including:

Javier Diaz de Aguilar
Centro Español de Metrología. España
19 PUBLICATIONS **6** CITATIONS
SEE PROFILE

Martin Šíra
Czech Metrology Institute
54 PUBLICATIONS **290** CITATIONS
SEE PROFILE

A. Sosso
INRIM Istituto Nazionale di Ricerca Metrologica
49 PUBLICATIONS **279** CITATIONS
SEE PROFILE

J.M. Williams
National Physical Laboratory
75 PUBLICATIONS **1,032** CITATIONS
SEE PROFILE

Good Practice Guide on the operation of AC quantum voltage standards

Javier Díaz de Aguilar, Raúl Caballero, Yolanda A. Sanmamed
Centro Español de Metrología (CEM)

Martin Šíra
Czech Metrology Institute (CMI)

Patryk Bruszewski
Główny Urząd Miar (GUM)

Andrea Sosso
Istituto Nazionale di Ricerca Metrologica (INRIM)

Vitor Cabral, Luís Ribeiro
Instituto Português da Qualidade (IPQ)

Helge Malmbekk
Justervesenet (JV)

Jonathan M. Williams
National Physical Laboratory (NPL)

Ralf Behr, Oliver Kieler
Physikalisch-Technische Bundesanstalt (PTB)

Recep Orhan
Türkiye Bilimsel ve Teknolojik Araştırma Kurumu (TUBITAK)

Grégoire Bonfait
Faculdade de Ciências e Tecnologia Universidade Nova de Lisboa (FCT)

Javier Díaz de Aguilar, Raúl Caballero, Yolanda A. Sanmamed, Martin Šíra, Patryk Bruszewski, Andrea Sosso, Vitor Cabral, Luís Ribeiro, Helge Malmbekk, Jonathan M. Williams, Ralf Behr, Oliver Kieler, Recep Orhan, Grégoire Bonfait

Good Practice Guide on the operation of AC quantum voltage standards

Published by Czech Metrology Institute
Okružní 31, Brno, 636 00, Czech Republic
Typeset by Martin Šíra using pdfLaTeX

First edition, 21.6.2018
ISBN 978-80-905619-2-2
2018

Abstract

This Good Practice Guide is intended for both National and Industrial Metrology Laboratories who wish to invest in the development of a quantum standard for alternating voltage based on the Josephson effect. It gives a detailed description of the components required to construct a practical system as well as information on measurement techniques, uncertainty estimation, software tools and safe operation of cryogenic equipment. The text in the Guide is supported by a comprehensive list of references to material already published in scientific literature.

Contents

1 Introduction **5**

2 Binary-divided arrays **6**
2.1 Cryoprobe and microwave source 6
2.2 Binary bias source 8
2.3 Binary arrays 8

3 Pulse-driven arrays **12**
3.1 Cryoprobe and microwave source 12
3.1.1 PPGs, power amplifiers 12
3.1.2 IV-box 12
3.1.3 Array bias lines; twisted pairs, coaxial lines, types and suppliers 13
3.1.4 RF waveguides; coaxial and semi rigid cables, DC-blocks 13
3.1.5 Array mounting, cable termination, heater for removing trapped flux 13
3.2 Bias source 13
3.3 Pulse driven array 14
3.3.1 Junction technology, critical current, operating frequency, Shapiro step width as a function of microwave power and pulse repetition frequency 14
3.3.2 Output voltage, number of junctions 14
3.3.3 Cable correction at high frequencies 14
3.3.4 Sigma-Delta simulation, quality of codes, SNR, quantisation noise 15
3.4 Low frequency synthesizer 15
3.5 Null detector 15
3.6 Measurement system and procedures 15
3.7 Software 15

4 Reference system **16**
4.1 Introduction 16
4.2 Equipment list 16
4.3 Operating principle 17
4.4 Connection of the DAC source 17
4.5 Common-mode-rejection-ratio of the digitizer 18
4.6 Data collection and analysis 18
4.7 Numerical correction factors 19

5 Cryocoolers in voltage metrology **21**
5.1 Introduction . . . 21
5.2 Basic thermodynamics . . . 22
5.3 Gifford-McMahon Cryocoolers . . . 23
5.4 Pulse tube cryocoolers . . . 25
5.5 Cryocooler is just the "bare engine" . . . 25
5.5.1 Vacuum chamber . . . 26
5.5.2 Vacuum system . . . 26
5.5.3 Thermometry . . . 28
5.6 Optimized heat transmission . . . 30
5.6.1 Thermal conductivity . . . 30
5.6.2 Thermal contact & insulation . . . 32
5.6.3 Contact thermal resistance . . . 32
5.7 Sample holder and coldplate . . . 33
5.8 Security rules . . . 33
5.9 Recomended bibliography . . . 34

6 A standard voltmeter referenced to an AC Josephson standard **35**

7 AC Voltage Measurements using PJVS and Differential Sampling **38**

8 Procedure for calibration ac-dc transfer standards using AC quantum voltage standards **42**
8.1 Scope . . . 42
8.2 Method . . . 42
8.3 Calibration Procedure . . . 43
8.3.1 PJVS, RMS Calibration . . . 43
8.3.2 PJVS, Sampling . . . 44
8.3.3 JAWS . . . 45
8.3.4 Uncertainty . . . 45

9 Calibrating voltmeters with PJVS **46**

10 Procedure for metrology grade characterization of analog-to-digital converters frequency response using ac quantum voltage standards **48**
10.1 Scope . . . 48
10.2 Method . . . 48
10.3 Quantum standards . . . 48
10.3.1 PJVS . . . 48
10.3.2 JAWS . . . 49
10.4 Measurand definition . . . 49
10.5 Configuration . . . 50
10.6 Data acquisition . . . 51
10.7 Data processing . . . 51
10.8 Uncertainty . . . 52
10.9 Probability density functions (PDFs) . . . 53
10.10 Selected biography . . . 53

11 Calibration of thermal converters, voltmeters and AC sources **55**
11.1 Principles of AC/DC converters . . . 55
11.1.1 Single Junction Thermal Voltage Converters (SJTVC) . . . 55
11.1.2 Multi Junction Thermal Voltage Converters (MJTVC) . . . 56
11.1.3 Semiconductor TVC . . . 56
11.2 Measurement system of the thermal converter based AC voltage standard . . . 58
11.2.1 AC/DC converters . . . 58
11.2.2 Voltmeters . . . 58
11.2.3 Voltage sources . . . 58
11.2.4 AC/DC switching and timing . . . 58
11.3 Comparison of thermal voltage converters . . . 61
11.3.1 Comparison principle . . . 61
11.3.2 Sources of inaccuracies . . . 61
11.4 Literature . . . 62

12 Software **63**
12.1 Array characterisation and optimisation . . . 63
12.2 Binary array waveform synthesis . . . 63
12.3 Binary array waveform synthesis – source voltages . . . 63
12.4 Null detector data collection and processing . . . 64
12.5 Device control . . . 64
12.6 System control, automated measurements and calibrations . . . 64
12.7 Interoperability of software components . . . 65
12.8 Data storage: content and format . . . 65
12.9 Data analysis, measurement parameters, measurement uncertainty . . . 65

Appendices **74**

A Safety rules in cryogenics **75**
A.1 Disclaimer . . . 75
A.2 Generalities . . . 75
A.3 Security risks . . . 75
A.3.1 Levels of oxygen . . . 76
A.3.2 Cold burn hazards . . . 77
A.3.3 Collective protection devices . . . 77
A.3.4 Clothing and personal protective equipment . . . 78
A.3.5 Rules of conduct for the use of cryogenic liquids . . . 79
A.3.6 Transfer of cryogenic liquids . . . 79
A.3.7 Storage of dewar or tanks containing cryogenic liquids . . . 81
A.3.8 Transport and lifting of dewar or tanks containing cryogenic liquids . . . 81
A.3.9 In the event of an accident, spillage, emergency, natural disaster, evacuation . . . 81
A.3.10 Work alone . . . 82
A.3.11 Interference with other workers in the same room . . . 83
A.3.12 Normative and bibliographic references . . . 83

Foreword

This Good Practice Guide was prepared during the ACQ-PRO EMPIR project and can be accessed on the website of the ACQ-PRO project:

`http://www.acqpro.cmi.cz`

The project ACQ-PRO has received funding from the EMPIR programme co-financed by the Participating States and from the European Union's Horizon 2020 research and innovation programme. This guide reflects only the author's view and EURAMET is not responsible for any use that may be made of the information it contains.

Chapter 1

Introduction

NPL

Josephson junction arrays have been in use as a primary standard for voltage metrology for over 30 years. A number of review articles have been written which summarise the main aspects of the design of junction arrays and their associated measurement systems to form a practical quantum standard of voltage [1], [2], [3]. The development of non-hysteretic junctions paved the way for quantum metrology of dynamic voltages using either programmable arrays of Josephson junctions arranged in a binary sequence [4] or linear arrays of Josephson junctions with a pulse train bias [5]. This Good Practice Guide gives a detailed description of the components and systems required to realise a practical ac quantum voltage standard. It refers extensively to material already available in scientific literature and complements this with practical details and illustrations.

Chapter 2

Binary-divided arrays

NPL

2.1 Cryoprobe and microwave source

If the Josephson array is to be operated in a liquid helium cryostat at $4.2\,\mathrm{K}$, a cryoprobe is required to support the array in the cryostat and to supply both the necessary microwave bias current and low frequency bias currents. The cryoprobe design is a compromise between ideal properties for the microwave and low frequency conductors and liquid helium consumption.

If the array is operated at microwave frequencies around $70\,\mathrm{GHz}$ then either a dielectric waveguide can be used to achieve for example a loss of $2.2\,\mathrm{dB}$ at $75\,\mathrm{GHz}$ for a waveguide length of $1.25\,\mathrm{m}$ [6] or $1.2\,\mathrm{dB}$ over a frequency range of $67.5\,\mathrm{GHz}$ to $77.5\,\mathrm{GHz}$ for a waveguide length of $1\,\mathrm{m}$ and a liquid helium consumption of $0.2\,\mathrm{l}$ per day[7] or alternatively an over-moded waveguide fitted with WR-12 launching horns, achieving a loss at $75\,\mathrm{GHz}$ of $0.7\,\mathrm{dB}$ per metre and a liquid helium consumption of $0.5\,\mathrm{l}$ per day [1].

Waveguide components suitable for interfacing a rectangular waveguide to an over-moded circular waveguide are shown in figures 2.1 and 2.2. The brass ring around the waveguide taper supports the circular waveguide tube as well as a larger cylinder which forms the cryoprobe outer shield. The three slots in the brass ring are to accommodate the cables which pass down the gap between the two tubes to carry the low frequency bias currents.

If the array is to be operated at frequencies around $20\,\mathrm{GHz}$ then a coaxial waveguide can be used. Figure 2.3 shows an example cryoprobe fitted with a coaxial waveguide for microwave bias.

Each segment of a binary-divided array needs to be connected to an electronic bias source at room temperature so that the array can be biased to an arbitrary voltage to within the resolution set by the step voltage for the smallest segment. The use of coaxial cables for these connections guarantees a transmission line impedance and if the bias source output impedance is matched to the cable impedance, the effect of cable capacitance on the transition time between different array bias configurations is minimized. For example, the bias source developed at NPL uses a $50\,\Omega$ system for connections to the Josephson array [8]. The effect of reflections in the cables can also be greatly reduced by introducing terminating impedances. In this way, a transition time between quantized voltages of less than $100\,\mathrm{ns}$ can be achieved [9]. The coaxial cables create a further heat load on the cryostat so have to be chosen carefully to achieve a frequency response in the MHz range in combination with an acceptable thermal conductivity. An example solution is coaxial cable type 'C' provided by LakeShore Cryotronics which has a characteristic impedance of $50\,\Omega$ and a reduced heat load through use of an aluminized polyester shield conductor.

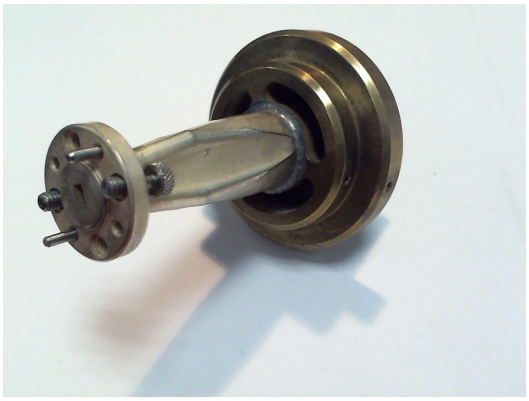

Figure 2.1: Rear view of waveguide taper from rectangular to over-moded circular waveguide.

Figure 2.2: Front view of waveguide taper showing central hole for location of the waveguide tube and three slots in the brass supporting ring to carry the low frequency coaxial cables.

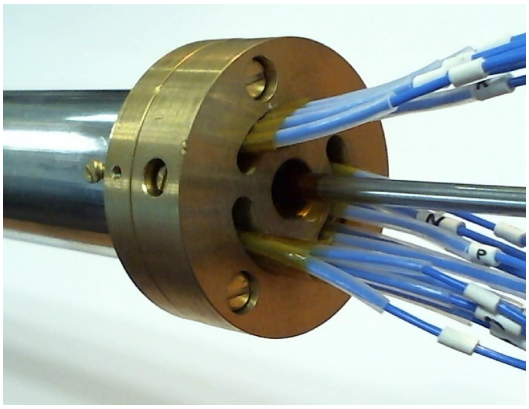

Figure 2.3: Cryoprobe end showing central coaxial waveguide for microwave power at 20 GHz and coaxial cables for low frequency bias currents.

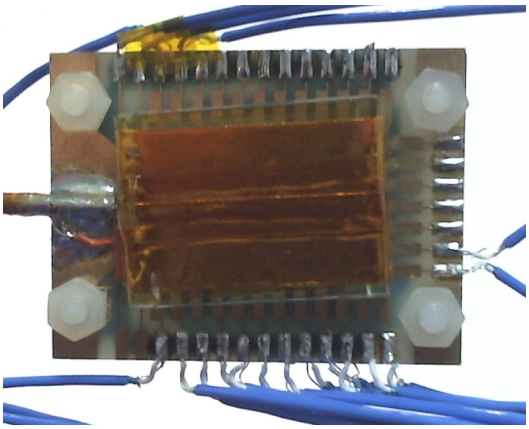

Figure 2.4: Array chip carrier showing connection of coaxial cables for the low frequency bias currents. The drain wires in the cables are connected to a common ground wire behind the carrier.

2.2 Binary bias source

For waveform synthesis, a bias source is required for the programmable Josephson array which has individual outputs for each binary array segment and which can store a sequence of array bias conditions so that a waveform can be generated as a series of discrete quantised voltage values. For highest accuracy, the bias source should be able to change from one bias condition to the next with a minimum rise time and also have the capability of synchronisation with an external frequency reference so that the generated waveform can be phase-locked to other parts of the measurement system.

The bias source designed by NPL[8] is shown in figure 2.5. Bias connections to individual Josephson array segments are provided on SMB coaxial connectors and the source is powered by dc-dc converters with low electrical leakage to reduce the effect of ground loops. The source contains a waveform memory with a capacity of 32 768 waveform points and is connected to a PC for programming via two optical fibres.

The array bias outputs on the source have a $50\,\Omega$ output impedance for use with coaxial connecting cables. A connection scheme for the bias source and Josephson array is given in figure 2.6. In this example, there is no direct connection between the Josephson array and the common screen provided by the coaxial cables, instead a bias channel is used to sink the return current from the lower end of the array. The common screen is isolated from the chassis of the bias source and also from the exterior metal of the cryoprobe. The coaxial cables are isolated from the cryoprobe and form an independent screen, as illustrated in figure 2.7.

With this connection scheme, the bias conditions for each bias channel are interdependent. The required settings of the voltage sources in the bias source, V_{b_j}, counting up from the bottom of the array, have to take account of the Josephson array segment voltages, V_{a_i} and the segment bias currents, I_i according to equation 2.1 where $R = 50\,\Omega$. In this equation, the bias source channels count from index zero and the array segments from index one (array segment zero does not exist so is defined as having zero voltage). For each quantised voltage in the synthesized waveform, the set of voltages V_i are calculated in the PC and transferred to the bias source memory.

$$V_{\mathrm{b}_j} = \sum_{i=0}^{j} V_{\mathrm{a}_i} + R(I_i - I_{i+1}) \tag{2.1}$$

2.3 Binary arrays

Binary-divided arrays of Josephson junctions are fabricated in one or more microwave transmission lines so that all the junctions receive approximately the same microwave bias current. Separate connections to the junctions are provided for low frequency bias currents to select the Shapiro constant-voltage step required. The microwave current is continuously applied and control of the junction array voltage is provided by the low frequency bias currents. The over-damped Josephson junctions are designed to have a single-valued I-V characteristic so that there is a unique correspondence between the applied bias currents and the voltage generated by the array. An example characteristic curve is shown in figure 2.8. Constant-voltage Shapiro steps can clearly be seen at ± 1 V and a bias current of ± 3 mA. The width of the Shapiro steps depends on the level of microwave bias current. Ideally, the microwave power from the source should be adjusted so that the zero voltage and the ± 1 V steps have approximately the same width in terms of the bias current.

It is important to ensure that there is no trapped magnetic flux in the array of junctions. Flux trapped in just one junction can compromise the accuracy of the voltage generated by the array. The most effective way to test for trapped flux is to measure the voltage across the whole array using a voltmeter with at least seven digits of resolution. The voltage generated should be recorded when the bias current is adjusted to the centre of the Shapiro step and then compared with the voltage generated for a change in the bias

Figure 2.5: NPL Josephson array bias source.

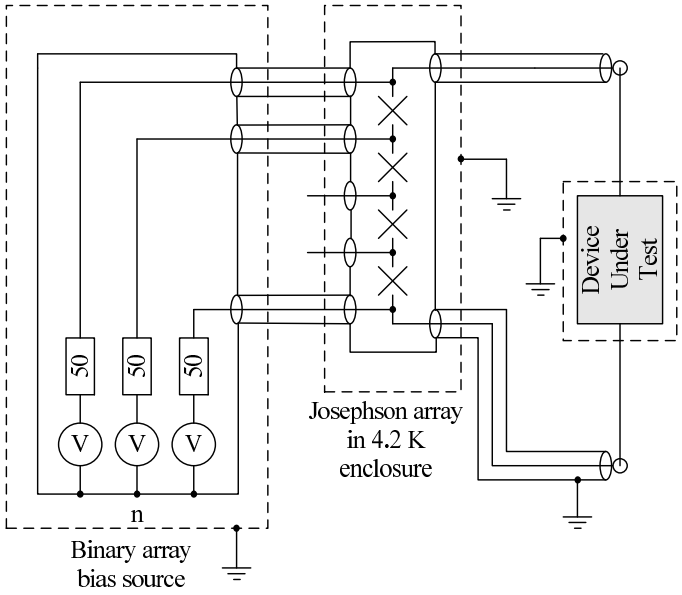

Figure 2.6: Bias source connections.

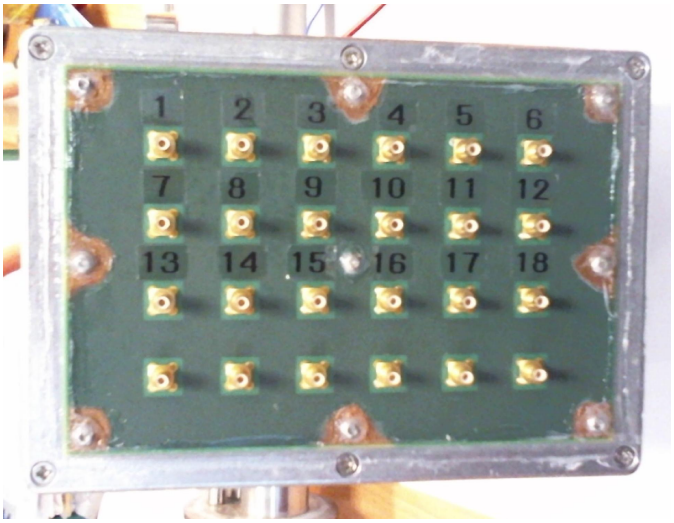

Figure 2.7: Insulating panel on the cryoprobe for the coaxial cable connections.

current of ± 0.5 mA. The recorded voltages should be the same to within 1 μV for all three bias currents. If a change in voltage is observed, then trapped magnetic flux is a likely explanation. The array should be raised to a temperature above 20 K for a few seconds with all bias currents reduced to zero and the microwave power turned off. The procedure for testing the step width should then be repeated to confirm that any trapped flux has been removed.

Binary-divided arrays are normally sub-divided so that the number of junctions in the individual segments follows the series 1, 1, 2, 4, 8, 16 etc up to half the maximum number of junctions. Two single junctions are often provided so that a build-up of voltage can be performed by comparing a single junction against a single junction in opposition and then the two single junctions in series against a segment with two junctions, etc. This is a useful procedure for verifying system performance but is not necessary to verify the accuracy of the array of junctions itself.

The voltage resolution of a binary-divided array depends on the number of Josephson junctions in the smallest segment and the frequency of the microwave bias. For example, if the smallest segment consists of a single junction and the bias frequency is 70 GHz, then the voltage resolution is approximately $140\,\mu$V. In some designs, the bias frequency is lower and the number of junctions in a single segment is larger. For example if there are 32 junctions in the smallest segment and the bias frequency is 16 GHz, then the voltage resolution is approximately 1 mV. The inherent symmetry of the positive and negative Shapiro steps means that the array effectively has an extra binary bit of resolution and bipolar waveforms are straightforward to generate. For example, an binary-divided array of 8192 Josephson junctions biased at 70 GHz with the smallest segment having a single junction as a voltage range of $\pm 1.2\,\mu$V.

A schematic diagram of a complete measurement system is shown in figure 2.9, see also [10]. The quantum reference is provided by a programmable Josephson array and associated bias source in the same way as shown earlier in figure 2.1. The quantized voltage from the array is present between terminals b and c which are shown as coaxial connections. A reference waveform for characterising the device under test is provided by a digital synthesizer. The voltage across the device under test $a - f$ is compared with the quantized voltage using a null detector consisting of an amplifier and analog to digital converter (ADC).

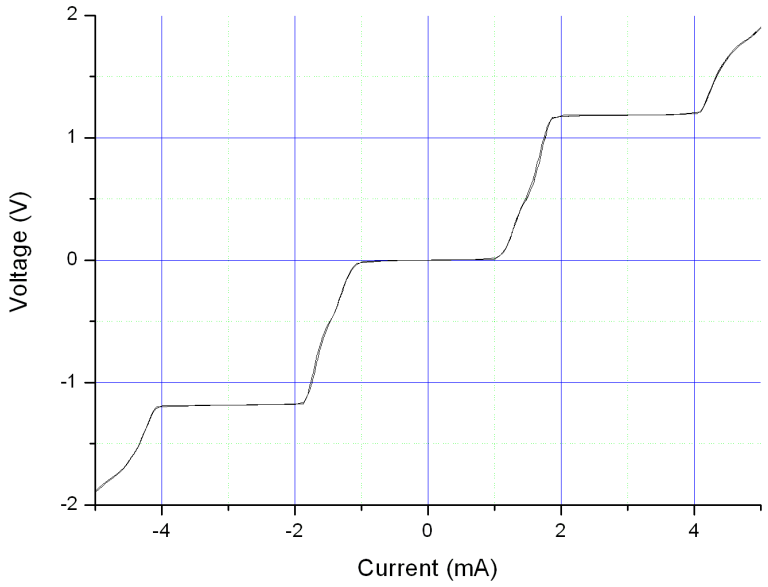

Figure 2.8: Example current-voltage characteristic for a binary-divided array with microwave bias applied.

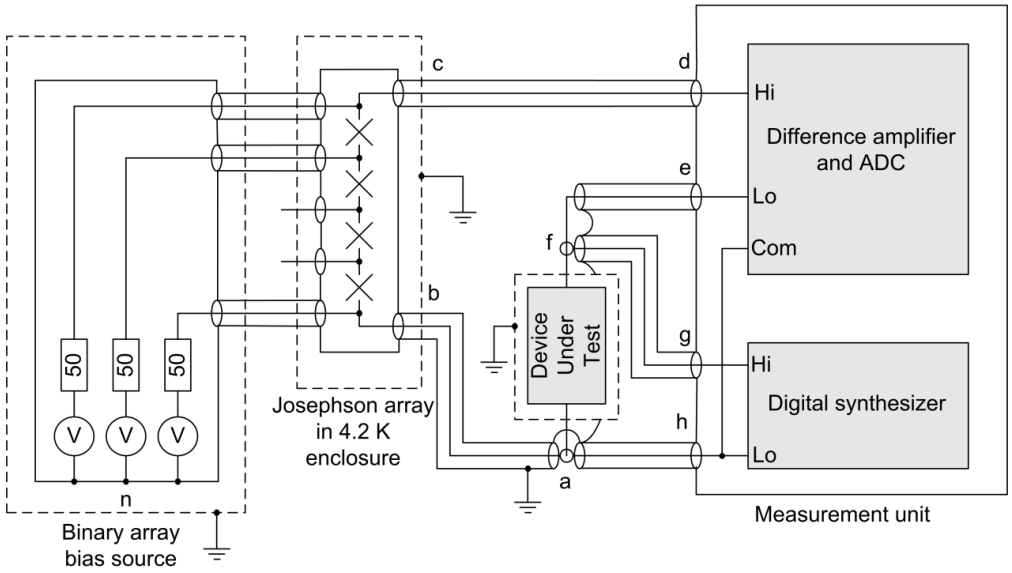

Figure 2.9: Schematic diagram of a basic measurement system consisting of a programmable Josephson array and bias source, a digital synthesizer, a null detector and a device under test.

Chapter 3

Pulse-driven arrays

PTB

The pulse-driven Josephson voltage standard has been introduced more than 20 years ago [5], [11]. Recent developments in Josephson Arbitrary Waveform Synthesizer (JAWS) led to the breakthrough of achieving 1 V RMS output voltages [12]–[15]. The JAWS are already used in several National Metrology Institutes (NMIs) in special applications where only 100 mV levels are required e.g. for ac-dc transfer measurements [16]–[19] and for calibrating ac voltage standards and instruments [20]–[24]. The increase to the 1 V level is important for many metrological applications, as instruments and measurement methods are consequently more accurate in that range. More information about comparisons can be in [25], [26] and reference therein. The step towards higher voltages was possible due to constant technology improvements [27]–[31]. Towards higher frequencies the output voltage needs corrections due to long cables and impedance mismatch – research is on-going [32]–[35]. New optical methods are aiming for a different driving approach [36]–[39], as well as ideas for using multilevel pulse codes [29]. A pulse-driven system has also lead to the new definition of the Boltzmann constant (see e.g. [40]).

Due to the ongoing research activities such as to increase the bandwidth and the voltage or to simplify systems this paper only can give a snapshot of the present status. We will give details about the instruments to drive the arrays and the array technology. As most details have already been published the aim of this paper is not to be exhaustive but to give references and links.

3.1 Cryoprobe and microwave source

3.1.1 PPGs, power amplifiers

Presently different PPGs (Sympuls AG, Keysight, Anritsu,...) are used for the driving arrays with pulses. This is a still developing field with a need from faster communication techniques. Nowadays multilevel PPGs are available, see Keysight manufacturer, and optical ones are also in development [39].

Very often the pulse amplitudes must be amplified using a broadband amplifier. Good experience has been made with the PSPL5882 from Tektronix.

3.1.2 IV-box

IV-boxes are used for isolating the low-frequency part in 'AC-coupling technique' [30]. Usually such electronics is home-made.

3.1.3 Array bias lines; twisted pairs, coaxial lines, types and suppliers

All this wires/cables can be used at low frequencies. Of course, thermal EMFs must be taken into account for DC while for high frequencies impedance match is most important [35]. Low temperature cables from Lake Shore type SC are suitable at cost of helium consumption.

3.1.4 RF waveguides; coaxial and semi rigid cables, DC-blocks

At PTB waveguides from Huber + Suhner and Elspec are used showing suitable margins (at 4 K), see figure 3.1. Depending on your application you must decide between attenuation and heat input. In general, high conductivity means wide margins at costs of heat input. Therefore, copper cables cannot be used for cryocoolers.

At PTB, we have made good experience with Sucoflex cables from Huber + Suhner (at 300 K).

Suitable DC blocks are DCB-3510 (inner) and DSCB-3511 (inner/outer) from Midwest Microwaves.

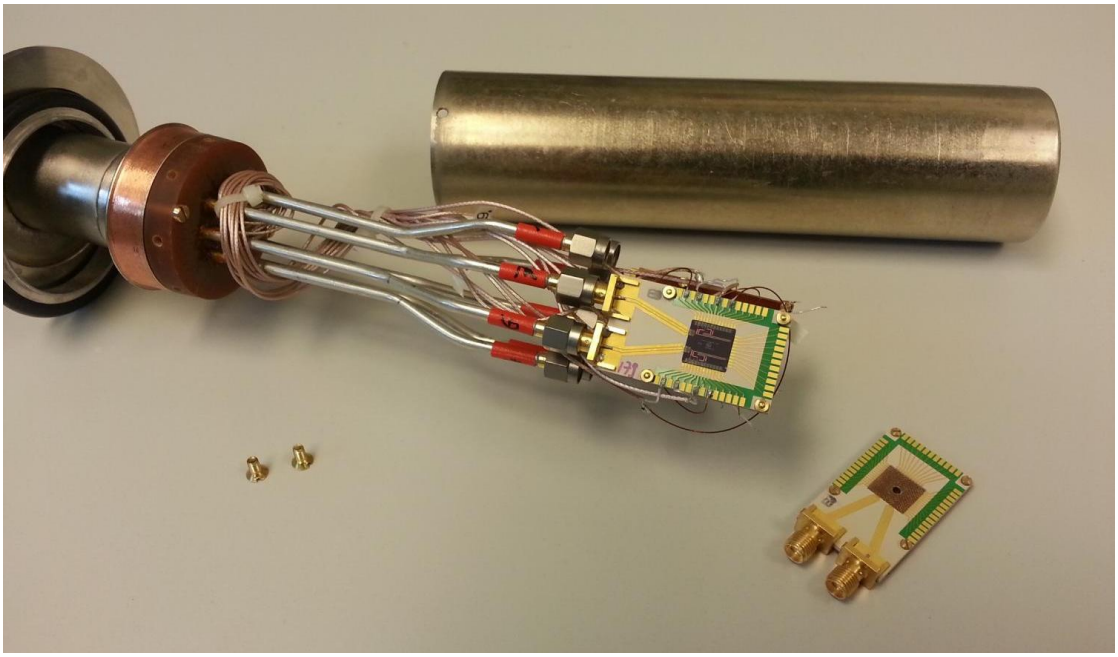

Figure 3.1: Pulse driven array with waveguides designed in PTB.

3.1.5 Array mounting, cable termination, heater for removing trapped flux

Arrays are usually mounted by chip suppliers [30]. Such chips come with an on-chip termination. So far, we do not use a heater for pulse-driven arrays as we do not trap flux often. We prevent chips from trapping flux by always using flexible grounding straps.

3.2 Bias source

For pulse-driven Josephson arrays a bias source in only required for testing the arrays and for verifying margins. Such a source can be like the ones for binary arrays without additional requirements.

3.3 Pulse driven array

3.3.1 Junction technology, critical current, operating frequency, Shapiro step width as a function of microwave power and pulse repetition frequency

Details about junction technology can be found in [20] and many cited articles. A very nice example for Shapiro step measurements as function of pulse height is given in [31], [36] further theoretical background is given in early NIST papers, see [11]. The on-chip filters have been optimized by NIST, see [28] and figure 3.2.

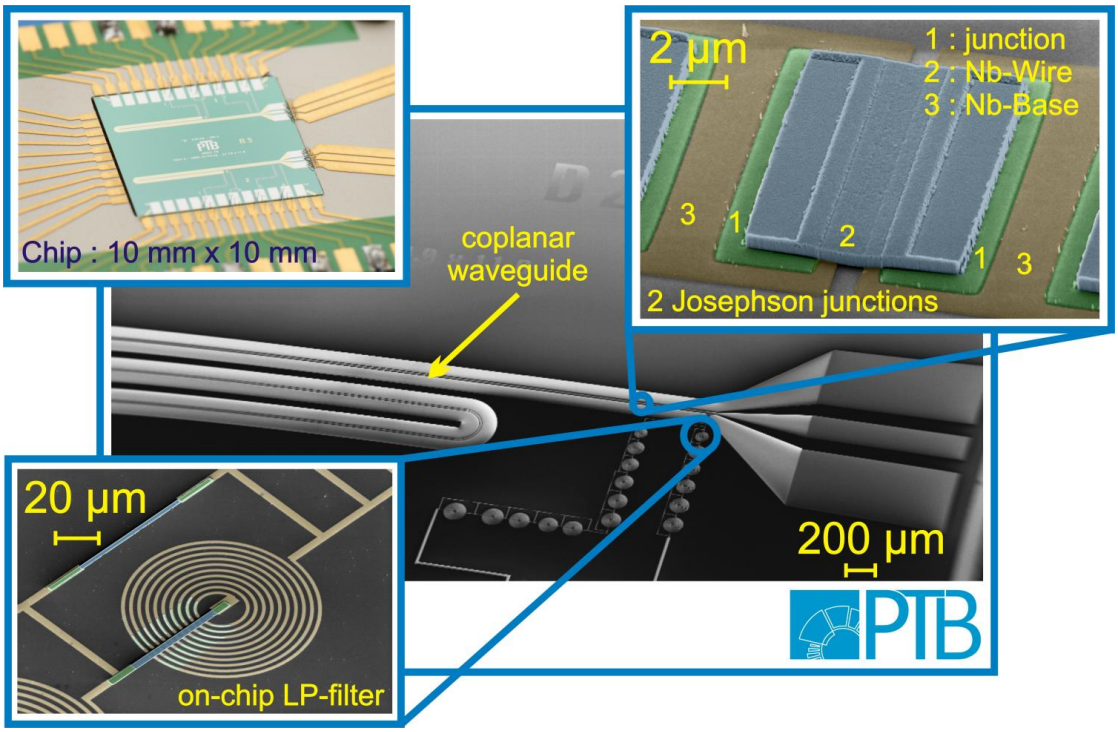

Figure 3.2: Josephson junctions of pulse driven arrays and on-chip filters developed by PTB.

3.3.2 Output voltage, number of junctions

The output peak-to-peak voltage VPP for a series array of m junctions is given by

$$V_{\mathrm{pp}}(t) = 2mn\Phi_0 f_{\text{clock-PPG}} A_{\Sigma\Delta} \tag{3.1}$$

with Φ_0 the magnetic flux quantum and $n = 0, \pm 1, \pm 2, \ldots$ the integer step number and m the number of junctions in the array. $f_{\text{clock-PPG}}$ is the clock frequency of the pulse pattern generator (PPG), $A_{\Sigma\Delta}$ ($0 < A_{\Sigma\Delta} < 1$), the $\Sigma\Delta$-code amplitude factor. The amplitude factor must be < 1 to ensure a stable $\Sigma\Delta$-simulation.

3.3.3 Cable correction at high frequencies

The latest paper on this topic comes from VSL, see [35] citations. A cable correction and load compensation method is under development by METAS within the QuADC project, see [41].

3.3.4 Sigma-Delta simulation, quality of codes, SNR, quantisation noise

A good description of all this is given in an early paper by the NIST group [11].

3.4 Low frequency synthesizer

At PTB, low frequency synthesizers of the 33500B series from Keysight are used for the low frequency part of the AC-coupling technique [30]. We have little knowledge how much specifications e.g. harmonic distortion or phase stability are important for operating margins.

3.5 Null detector

Following NIST, PTB uses the NI PXI 5922 cards as fast sampling system and to for spectrum analysis. However, any other sampler or spectrum analyser could be used.

In case of comparisons or in the pulse-driven Josephson impedance bridges a phase sensitive detector (Lock-in amplifier) is required. So far, no Lock-in amplifier has been found which limits the operational capability of the pulse-driven Josephson system.

3.6 Measurement system and procedures

Cables and interconnections, screening, current equalisation, mutual inductance, current and voltage paths etc. are details which depend on the measurement application. Therefore, the JAWS should be assumed just as an isolated synthesiser to replace a conventional one a common experiment.

3.7 Software

At PTB, LabVIEW software is used for all applications. This includes special software for arrays characterization, waveform synthesis, spectral measurements, data collection and system control. Matlab is used for fast calculation of the encoded waveforms by $\Sigma\Delta$-simulation.

Chapter 4

Reference system

NPL

4.1 Introduction

This chapter describes the configuration for a new general AC quantum voltage standard including the best choices of equipment, Josephson junction arrays, voltage waveforms and sampling parameters. It brings together the experience of NMIs who have been conducting research in this area over several years. This design of quantum voltage standard is intended to serve the interest of a range of institutes involved precision AC metrology and the metrology community in general. It is designed to underpin the calibration uncertainties regularly required to deliver state of the art measurement services.

4.2 Equipment list

1. Binary Josephson array bias source
2. RF bias source, GHz frequencies
3. Cryogenic enclosure, 4.2 K
4. Cryoprobe and Josephson junction array
5. Stable DAC synthesizer
    - Aivon source
    - Fluke 5720A calibrator
    - Custom hardware e.g. NPL DAC source
6. Digitizer for difference voltage measurement
    - Sampling voltmeter, e.g. Agilent model 3458A
    - Flexible resolution digitizer, e.g. National Instruments model 5922
    - Custom hardware, e.g. NPL difference amplifier and ADC
7. Optional second digitizer
8. Synchronisation oscillator
9. Power for DAC source

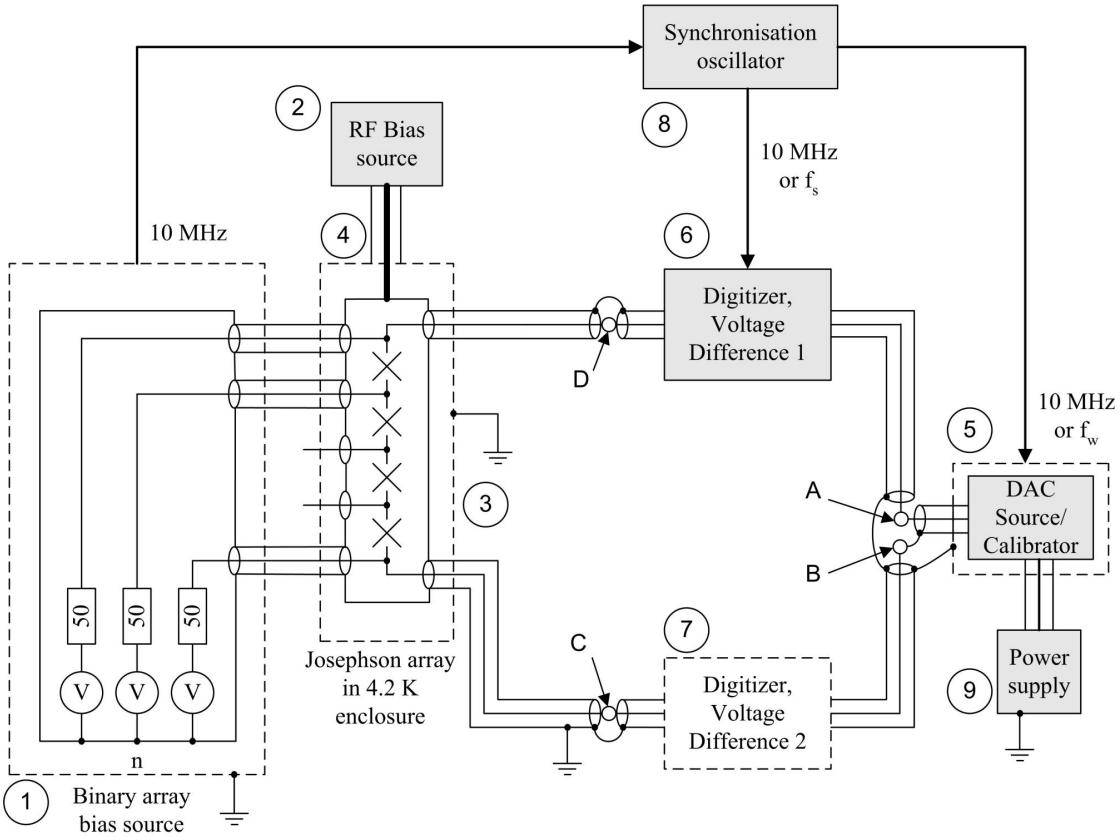

Figure 4.1: Schematic diagram of the reference system.

4.3 Operating principle

In figure 4.1, the stable DAC source or calibrator (5) generates a smooth sine wave with the same period and amplitude as the step-wise waveform from the Josephson waveform synthesizer (JWS), consisting of items (1) to (4) in the Equipment List. The Josephson array high frequency bias is supplied by the RF bias source (2), operating at 20 GHz or 70 GHz, depending on the type of Josephson array. The DAC source or calibrator is frequency-locked to the Josephson synthesizer using a synchronisation oscillator (8) operating at 10 MHz or the synthesis frequency, f_w depending on the type of voltage source. The difference voltage between the DAC source and the Josephson synthesizer is measured using the digitizer (6) at the high potential terminals. There is an option of using a second digitizer (7) at the low potential terminals. The digitizer (6) is synchronised from the oscillator using either a 10 MHz frequency or the sampling frequency of the Josephson synthesizer, depending on the model of the digitizer. The second digitizer (7) is synchronised in a similar way.

4.4 Connection of the DAC source

The connection scheme for the DAC source or calibrator (5) depends on the quality of the associated power supply (9). The high potential terminal of the DAC source or calibrator is connected to the digitizer (6)

at node A. If the second digitizer (7) is not used, then the low potential terminal of the DAC source or calibrator is directly connected to the low potential terminal of the Josephson array via nodes B and C. As a consequence, any common-mode current from the DAC source or calibrator power supply will flow into the low potential terminal of the Josephson array, C, and can affect the accuracy of the quantised voltage. Note that this problem is not solved by using a single digitizer in the low potential connection between nodes B and C instead. Due to the low output impedance of the source, the common-mode current from the power supply will now flow through the high potential connection to the Josephson array via nodes A and D. There are two solutions:

1. The DAC source can be powered with a supply having a common-mode current of less than 1 μA or a calibrator with low common-mode current can be used

2. The common-mode current can be diverted to a safe route (note that a common-mode current of this kind comes from a high impedance so needs to have a path to return it to its source). For this solution, node B has to be connected to the measurement system screen (represented by the coaxial cables) at the source output. The second digitizer (7) is then also required to isolate the low potential terminal of the Josephson array from the measurement system screen.

4.5 Common-mode-rejection-ratio of the digitizer

The digitizer (6) is measuring a voltage difference but at an elevated potential equal to the amplitude of the voltage waveform being generated. It therefore requires a high common-mode rejection ratio (CMRR) if the output of the DAC source or calibrator is to be calibrated accurately against the Josephson reference. For example, an accuracy of 1 part in 10^6 on amplitude requires a CMRR of 120 dB. Alternatively, if the digitizer has an internal guard which is effective at the frequency of the waveform being synthesized, then this guard can be driven by the source by making a connection between the guard and node A (this will have a negligible loading effect on the source).

4.6 Data collection and analysis

When using a binary-divided array as the Josephson reference, it is essential that the data collected by the digitizers is correctly synchronised and that voltages associated with Josephson array transients are eliminated to the required uncertainty level. If an integrating voltmeter, such as a model 3458A is used, then normally the integration time of the voltmeter is set to be slightly less than the duration of a JWS sample interval and the voltmeter trigger delay adjusted to avoid the transients. If a high speed digitizer, such as a National Instruments model 5922 is used, then many samples for a given JWS sample are acquired and selected samples are eliminated to avoid the Josephson array transients.

Figure 4.2 shows example voltage samples acquired by a sampling digitizer of the type employed at NPL for the comparison of a sine wave from the DAC source with a JWS waveform consisting of 38 samples. The digitizer is recording 8 samples per JWS value making a total of 304 digitizer sample points per period of the waveform. The digitizer trigger is adjusted so that all of the samples occur in the time interval between the QWS transients. To test the rejection of the transients, the first and last sample in each set can be deleted from the data and the waveform recalculated to test for a significant change in the result. This procedure can be repeated for further pairs of sample points.

The data collected by the digitizer, after processing to eliminate the JWS transients, is used to reconstruct the voltage waveform generated by the DAC source or calibrator. Figure 4.2 also shows the calculated voltage differences between the JWS and an ideal sine wave, due to the finite quantisation of the binary-divided Josephson array. When these are subtracted from the digitizer data, a reconstructed difference waveform is obtained which represents the difference between the waveform from the DAC

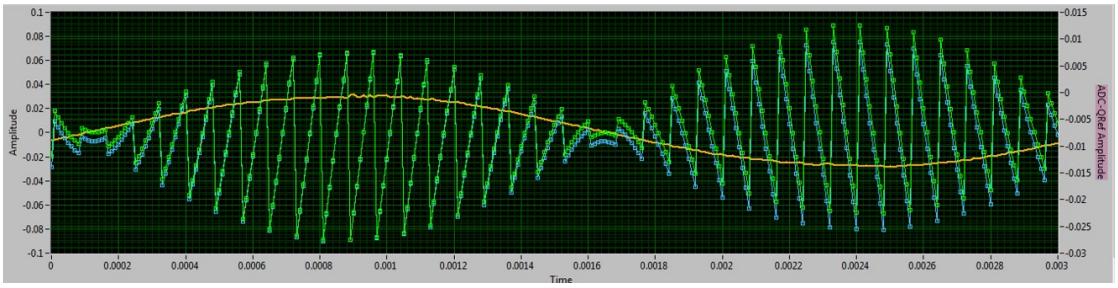

Figure 4.2: Example plot for a sine wave with 38 Josephson voltage samples per period showing (i) difference voltage waveform measured by digitizer (blue), calculated voltage differences from PJVS values (green) and reconstructed difference voltage (yellow).

N	Formula	Value	sinc
1	1	1.000000	1.000000
2	$\cos(\pi f\tau)$	0.999947	0.999982
3	$(2\cos(2\pi f\tau)+1)/3$	0.999858	0.999929
4	$(\cos(3\pi f\tau)+\cos(\pi f\tau))/2$	0.999733	0.999840
5	$(2\cos(4\pi f\tau)+2\cos(2\pi f\tau)+1)/5$	0.999573	0.999715
6	$(\cos(5\pi f\tau)+\cos(3\pi f\tau)+\cos(\pi f\tau))/3$	0.999377	0.999555
7	$(2\cos(6\pi f\tau)+2\cos(4\pi f\tau)+2\cos(2\pi f\tau)+1)/7$	0.999146	0.999359
8	$(\cos(7\pi f\tau)+\cos(5\pi f\tau)+\cos(3\pi f\tau)+\cos(\pi f\tau))/4$	0.998879	0.999128

Table 4.1: Formulae and correction values for an average taken over a number of discrete samples, N for a waveform with a total of 304 samples. The equivalent correction for the sinc function over a time interval $(N-1)\tau$ is given for comparison.

source and a perfect sine wave of known amplitude, given by the number of junctions operating in the Josephson array and the frequency of the applied microwave bias current. The reconstructed waveform can be used to determine both the rms value of the sine wave generated by the DAC source as well as it harmonic content.

4.7 Numerical correction factors

If an average of the difference voltage is taken over a period of time, for example due to the integration time of a sampling voltmeter, then a correction needs to be applied to the data to account for the fact that the waveform from the DAC source or calibrator is continuously changing with time. If the voltmeter has a rectangular averaging window of width τ, then for a sinusoidal voltage of frequency, f, the measured voltage is reduced by the factor $\sin(\pi f\tau)/(\pi f\tau)$. If, however, an average is formed by taking an average of N discrete samples each separated by a time interval τ then the factor is given by the formulae in table 4.1. These corrections are similar but not the same. Corrections for an average of discrete samples are compared with a rectangular average function in table 4.1 and also plotted in figure 4.3.

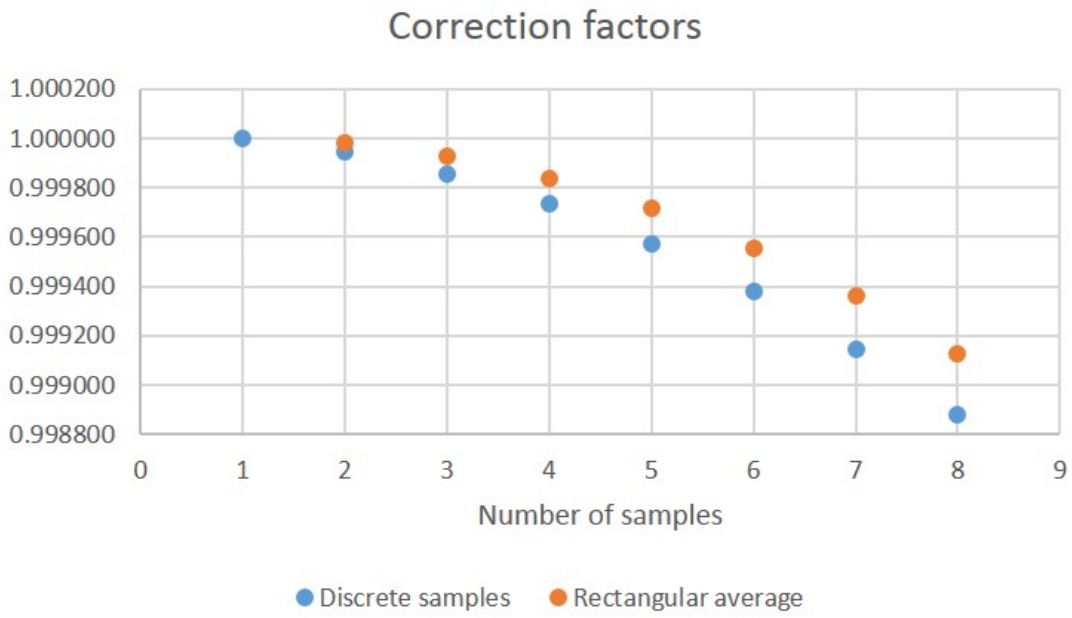

Figure 4.3: Graph showing data from table 4.1.

Chapter 5

Cryocoolers in voltage metrology

INRIM, FCT

5.1 Introduction

There is mainly two ways to perform (electrical) measurements at low temperature. The first one is to use as a cold source a cryogenic liquid stored in a dewar and to connect thermally the "sample" to this cold source. The sample temperature can be controlled (PID control for instance) using an adequate thermal connection to the liquid bath or varying the bath temperature by pumping or pressurizing it. Such systems, usually called "cryostat", are used from a very long time for low temperature research (since Dewar, $\approx$1880) and are, from more than 50 years, largely commercialized. Beside their reliability and the large know-how acquired during all these years, this type of system presents some inconvenient (table 5.1). In the 70's, a new way has been developed and avoids the necessity to use a cryogenic liquid: many "closed cycle engine" using compression and expansion of a gas can lead to thermodynamic cooling, not very efficient (Carnot oblige), but presenting the main advantage that low temperature can be obtained using a push-button machine! This type of "thermal machines" are nowadays very reliable and widely used for low temperature (from 2 K up to 300 K) set-up. They are also widely commercialized. Some inconvenient and advantage of these type of machine are presented in table 5.1. Let us note that these cryocoolers relief many cryogenics-related pains and usually turn cryogenics much more easily accessible. However, for very precise measurements, their uses is limited by the mechanical and thermal oscillations due to their intrinsic principle (the expansion-compression cycles create mechanical vibrations and temperature oscillations). For metrology, up to now, these limitations restricted their uses. However, due to improvements of these machine, benefits are more and more and could, in some cases, outweighing the disadvantages. In particular, the development of the so-called Pulse Tube (PT) cryocooler with no moving part at low temperature led to a significant decrease of the vibration level.

We present here a simple introductory guide on cryocoolers focusing on voltage metrology. A cryocooler reduces the temperature of a dedicated piece (called as "Cold finger") by through a proper exploitation of a thermodynamic cycle. In this text, we will focus on the cryocoolers that can be useful for metrology in the temperature range 2 K to 4 K. We will describe the basic operating principles, avoiding any complications related to detailed thermophysical principles. As the cryocooler is just a thermal machine, we will also describe the mandatory instrumentation that must accompanied it to turn it functional. The main technical problems related to work at low temperature will be mentioned.

	Cryostat	Cryocooler
Pro's	No intrinsic mechanical vibrations Temperature stability Large choice of cryostats Easy integration of super-conducting magnet (QHE)	Large community of people using cryo-coolers More compact (can reduce cable length) Push-button system No refilling No helium logistic
Contra's	Periodic refill Liquid helium logistic Gas helium logistic (if recuperated) Helium cost (increasing) Increasing difficulty for helium procure-ment	Thermalization Temperature fluctuations Usually: Electric step motor not far of experimental space (can be separated)

Table 5.1: Advantages and disadvantages of cryostats and cryocoolers.

5.2 Basic thermodynamics

The basic principle of a cryocooler (refrigerator) is summarized in Figure 5.1 (Index "C" and "H" refer at "cold" and "hot", respectively). The cooling effect is used to remove heat from the cold source (Q_{C}, T_{C}). At the equilibrium, T_{C} is constant then Q_{C} is equal to the heating power dissipated by the electrical measurements at the cold finger level. In usual cryocoolers, this heat removing is obtained by a cycle of compression-expansion of a gas. This cycle is driven by a motor consuming energy (W in Figure 5.1). The energy conservation law implies $Q_{\mathrm{C}} + W + Q_{\mathrm{H}} = 0$ (in this equation, Q_{C} and W are positive whereas Q_{H} is negative). Q_{H} is released to the "hot source" (generally, the hot source is at the room temperature). It can be shown that the most efficient thermal machine (Carnot machine) is based on two isothermal and two adiabatic processes (2 compressions and 2 expansions). If all the process are reversible, the entropy conservation implies:

$$\frac{Q_{\mathrm{H}}}{T_{\mathrm{H}}} + \frac{Q_{\mathrm{C}}}{T_{\mathrm{C}}} = 0\,. \tag{5.1}$$

These two equations allow to calculate the "Coefficient of Performance" (COP) defined, to make it short, as the ratio (What we want)/(What we pay) for a Carnot Machine:

$$COP = \frac{Q_{\mathrm{C}}}{W} = \frac{T_{\mathrm{C}}}{T_{\mathrm{H}} - T_{\mathrm{C}}}\,. \tag{5.2}$$

As it can be seen from this last expression, The COP decreases with T_{C}. For instance, for a machine working between 77 K and 300 K, the is equal to $0.3\,\mathrm{W\,W^{-1}}$ (1 W (W) supplied to the engine leads to a heat removing of 0.3 W (Q_{C}) at the cold source). If the machine has to work at 4 K, the decreases by a factor ≈ 20 ($\approx 0.014\,\mathrm{W\,W^{-1}}$).Taking into account that the various processes are far to be reversible and that the Carnot cycle is not easy to implement, the of a cryocooler working around 4 K is about 10 to 100 times smaller in existent cryocoolers. The commercial cryocoolers working in the 4 K temperature range, range useful for voltage metrology, are based on Ericsson cycles (Gifford McMahon cryocooler (GMM)) or Pulse tube cycles and use helium as working gas.

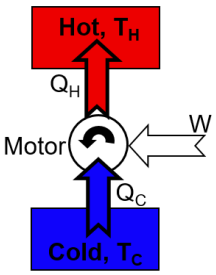

Figure 5.1: Basic principle of a refrigerator.

5.3 Gifford-McMahon Cryocoolers

The Gifford-McMahon Cryocoolers (Figure 5.2) were intensively developed during the end of last century (1960–2000). Its main use was as the cold source of cryopumps ($T \approx 20\,\mathrm{K}$) and then largely found in semiconductor industries. Continuous developments and improvements in the material used allowed to reach temperature as low as 2 K. Up to recently, they were the most usual cryocooler for the $4\,\mathrm{K}$ range. Actually, this cycle allows to build two (or three) Cryocoolers (stages) in series using the same compression machine and the same mechanical parts (Figure 5.3): two stages Gifford-McMahon Cryocoolers having a cooling power more than $1\,\mathrm{W}$ at $4\,\mathrm{K}$ are nowadays commercialized as "usual" cryocooler. A somewhat detailed explanation of the cycle can be found in [42]. In such machines, the gas compression is obtained by an external compressor (electric power typically 6 kW). This compressor is highly vibrating and noisy but can be installed quite far (20 meters for instance) of the cryocooler itself. The expansion-compression cycles are obtained by a distributing valve connecting the cold gas volume alternatively to the input or the output of the compressor. Beside the compressor, the main piece of such a machine is the so-called "regenerator-displacer". This fundamental piece, driven by the motor driven the valve, allows to transfer the gas back and forth from the hot part to the cold part whereas it also allows to precool the working gas before the cooling expansion. The displacement of the "regenerator-displacer" inside the system is the main source of mechanical vibrations of such a machine.

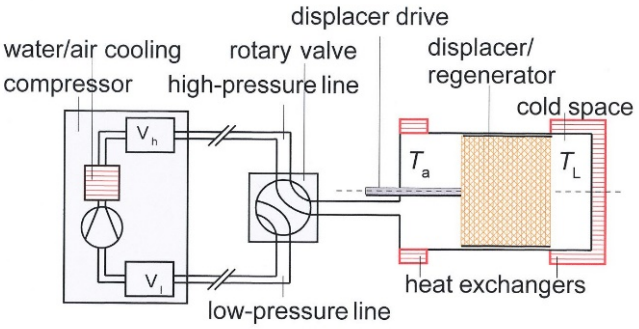

Figure 5.2: Principle of the Gifford McMahon Cryocoolers using a "regenerator-displacer". In some system this unique piece is substituted by a fixed regenerator and a moving displacer. From [42].

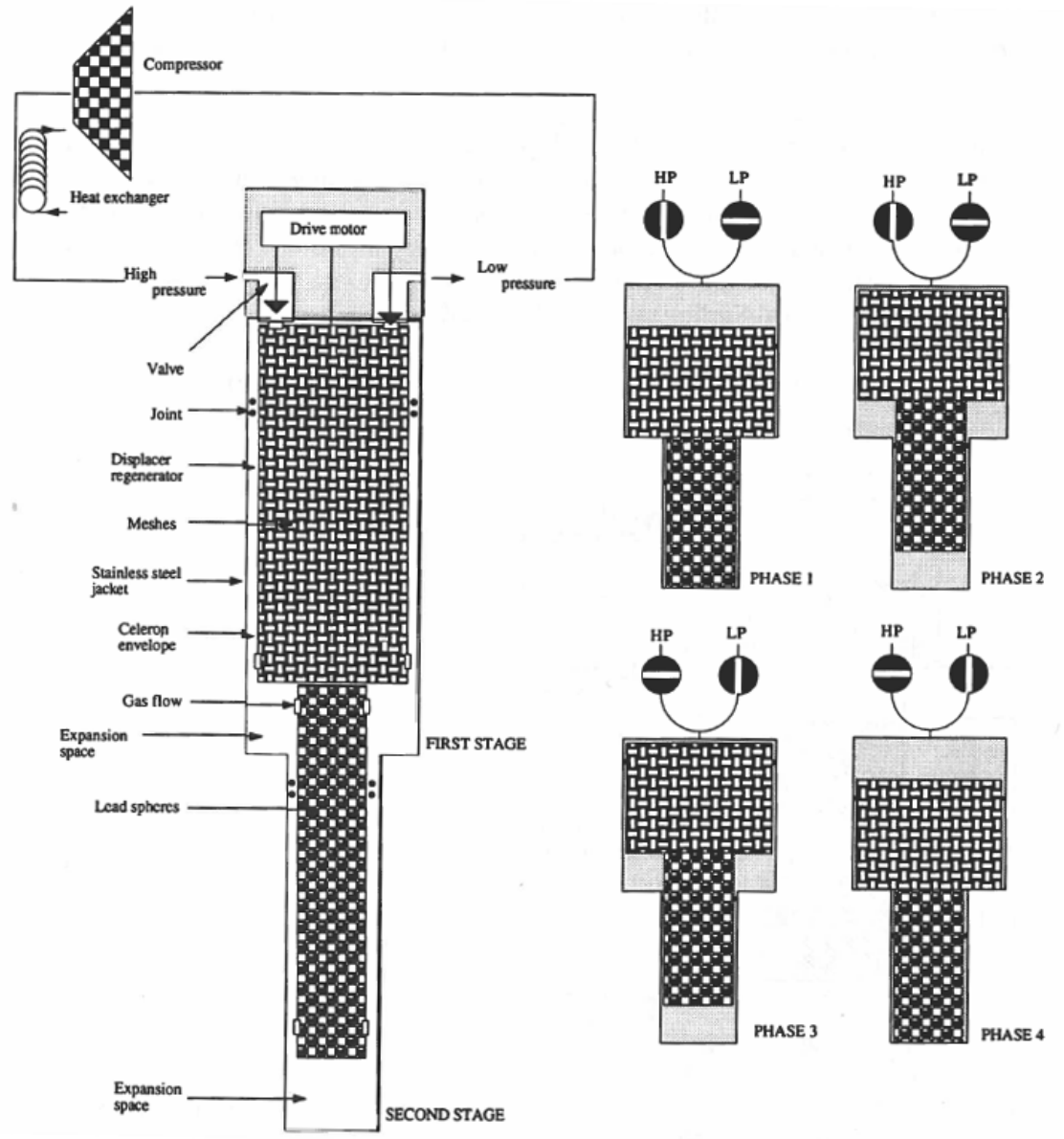

Figure 5.3: Two stage Gifford McMahon Cryocoolers using a ""regenerator-displacer" [43]. This machine corresponds actually to two cryocoolers in series: the second stage (low temperature stage), uses as hot source the cold source of the first stage cryocooler. This type of system allows a cooling power of more than 1 W at 4 K.

Figure 5.4: Typical 1 W at 4 K commercial Gifford-McMahon (two stages) cryocoolers [44]. The typical intermediate stage temperatures are around 30 K to 35 K (with no thermal charge). It can provide about 40 W at 45 K.

Figure 5.5: Typical commercial 1 W at 4 W Pulse Tube (two stages) cryocoolers [45].

5.4 Pulse tube cryocoolers

Whereas the Stirling cryocoolers – based on the well-known Stirling cycle – are widely used for the 80 K range, its impossibility to build two Stirling cycle in series as in Gifford McMahon machines disqualified it (up to now) for lower temperature range. However, from end of 70's, a cryocooler based on this type of cycle – Pulse Tube Cooler – was developed and more and more efficient version are nowadays commercialized. The theory behind Pulse Tube Coolers is similar to that of the Stirling/Gifford McMahon Refrigerators (2 expansion and 2 compression processes) but its understanding is a little more subtle (see for instance [46]): the gas displacement mechanism being replaced by a cold volume – orifice – buffer volume system, the orifice-buffer volume induces a phase shift between the pressure and the mass waves that ensures the cooling effect. For instance the Figure 5.6 shows the comparison between the Stirling cooler processes and those of the pulse tube. As it can be seen on this figure, no mobile piece exists at low temperature: no mobile piece in the low temperature part means less vibrations, less mechanical adjustment issues and less maintenance issues. Then, despite its performance generally worse than the original GMM or Stirling coolers, this feature was found important enough to boost the technical efforts on this type of cooler. The Figure 5.7 shows the schematic of the main pieces of a PT cryocooler and the Figure 5.5 its materialization for the case of a two stage PT cooler (≈ 0.5 W at 4 K).

5.5 Cryocooler is just the "bare engine"

When you buy a cryocooler you still need the setup to operate the cooling engine. Many companies commercialize turnkey machines in which all the basic for "elementary measurements" are installed, namely, thermometers, heater for temperature control and free wiring. However, for many special types of measurements, needing special requirements, these standard commercial solutions are not often immediately suitable.

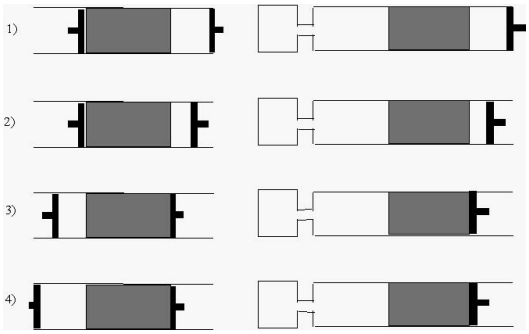

Figure 5.6: Analogy between Pulse Tube and Stirling Cycle. Piston compresses from 1) to 2) and from 2) to 3) when near-isochoric process occurs. The compressor piston becomes stationary 3) to 4), gas continues to flow into the surge volume. Near-isochoric process, 4) to 1) completes the cycle. From [47].

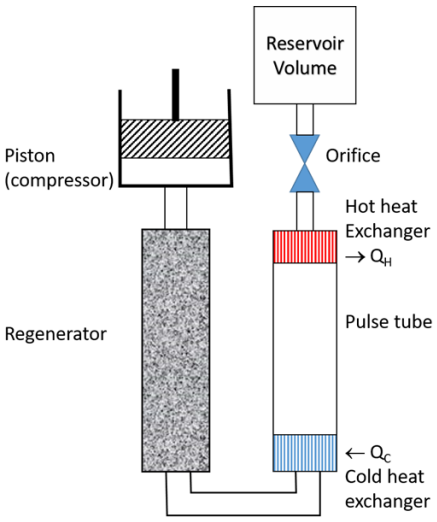

Figure 5.7: Scheme of a Pulse Tube. From [48].

5.5.1 Vacuum chamber

For thermal isolation between room temperature and the cold part, the inner parts of the cryocooler is installed in a vacuum chamber. This vacuum chamber must be equipped with different access to atmospheric pressure at RT (Ports). For instance:

- Vacuum pumping ports (+ eventually a pressure security valve port).
- Wiring port(s) for thermometry (low-current connectors).
- Wiring port for heaters (high current connectors).
- Special ports for special needs (wave guide for instance).

All these ports must be leaktight. Leaktight connectors are commercially available. Normalized flange and usual o-rings can be used if dismountable flanges are adequate. Figure 5.8 shows the drawing of the vacuum chamber existing in INRIM laboratory.

5.5.2 Vacuum system

The thermal isolation between cold system and RT surroundings becomes acceptable if the pressure in the vacuum chamber is about or below $10\,\mathrm{mbar}$ to $5\,\mathrm{mbar}$. Because, generally, the vacuum chamber volume is relatively small (often less than 100 liters), compact vacuum system with relatively low pumping speed ($50\,\mathrm{l\,s^{-1}}$ to $80\,\mathrm{l\,s^{-1}}$ is generally enough) are quite adequate. Pressure sensors are generally integrated to the system. It is recommended to connect this system to computer to record the vacuum level in order to detect any pressure anomaly. To minimize vibrations coming from this vacuum system to the cryocooler, corrugated stainless steel $25\,\mathrm{mm}$ tube can be used to connect these two parts, this tube being fixed somewhere by to a massive block. If very long tubes are used, care must be taken to use a not to small diameter that could increase significantly the pressure drop. Pressure drop calculation in this molecular regime can be found, for instance, in [51].

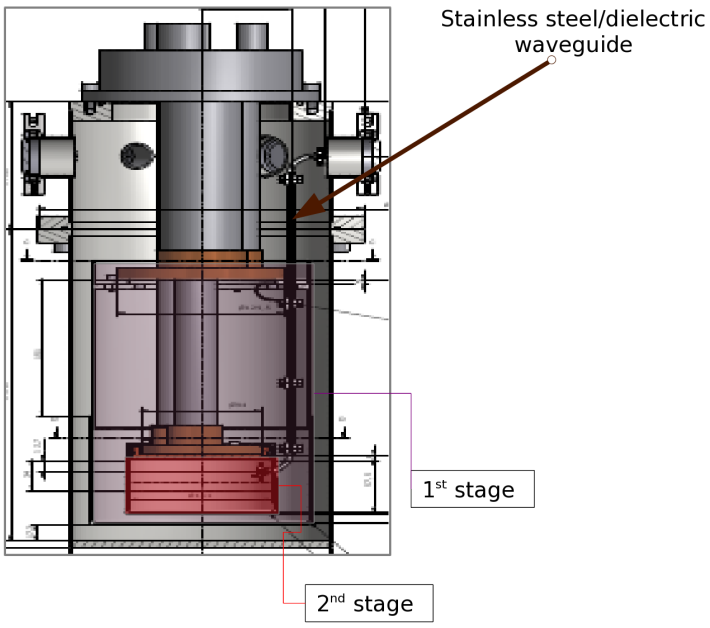

Figure 5.8: Vacuum chamber design example (INRIM) [49].

Figure 5.9: Typical turbo vacuum system. Rough dimensions: $60\,\text{cm} \times 60\,\text{cm} \times 60\,\text{cm}$ [50].

Type	Range[1,2]	Inter-changeable?	Typical Applications	B sens.[3] $\Delta T/T$ @ B, T	Radiation Sensitivity
Carbon Resistor	0.01 K to 100 K	N	R&D, $T < 1$ K	5%, 4.2 K, 8 T	low
Cernox™ Resistor	0.1 K to 420 K	N	R&D, $T < 1$ K Process Control	3%, 2 K, 8 T	low
RuO_2 Resistor	0.01 K to 40 K	Some	R&D, $T < 1$ K	5%, 2 K, 8 T	low
Platinum Resistor	14 K to 873 K	Y	Process Control	4%, 30 K, 8 T	low
Rh-Fe Resistor	0.65 K to 500 K	N	R&D, reference	12%, 40 K, 8 T	low
Si Diode	1.4 K to 500 K	Y	Process Control	10%, 10 K, 8 T	high
Vapor Pressure Bulb	0.5 K to 5.2 K, 13.8 K to 44 K, > 68 K	Y	R&D, reference	none[4]	none[5]

1. Lower limit will depend on installation.
2. Not necessarily covered by a single device.
3. Effect may depend on individual device and orientation.
4. Oxygen vapor pressure is affected by an external field.
5. For compounds such as methane chemical decomposition would produce and effect at very high doses. Helium vapor pressure bulbs are highly resistant to radiation.

Table 5.2: Main thermometers used at low temperature. From [52].

5.5.3 Thermometry

During years, the temperature measurement at low temperature has been a hot topic and filled many chapters in cryogenics books. The Table 5.2 shows a selection of thermometers that can be used below room temperature. Nowadays, in the 2 K to 300 K temperature range, this issue can be solved by many reliable ways and the recommended technique is thermometry using temperature dependent resistances.

Platinum resistors

100 Ω or 1 kΩ (Pt100 or Pt1k), 70 K to 400 K

This type of thermometers are recommended and are a low-cost and reliable solution. These thermometers are widely used (for low and high (< 800 K) temperature) and are commercialized by many companies. They have a good reproducibility and a standard calibration curve $T(R)$. Below 50 K to 70 K, the $T(R)$ characteristic becomes dependent of their values at 4 K.

Silicon/GaAlAs diodes

2 K to 300 K

More expensive than the Platinum thermometers, the have a good sensitivity down to 2 K. They are not properly resistance but are measured using a $V(I)$ method. They have a good reproducibility and

a standard calibration curve $T(V)$ (usually using $I = 10\,\mu A$). They are commercialized by companies specialized in Cryogenics material (see below). Because they do not need calibration, they are a good alternative to the Platinum thermometers in the range 2 K to 70 K.

Cernox resistances

50 mK – 300 K

Commercialized in the 90's, they are nowadays widely used in cryogenics due to their high sensitivity and reproducibility [53]. Note however that:

1. No standard calibration curve are available. Calibration (home made / commercial) process is needed.
2. The high sensitivity is obtained in a determined temperature range. Table or graphs gives the sensitivity versus temperature for the various model.

Germanium resistor

0.05 K to 30 K

In this temperature range they are the most stable thermometer, expensive but very stable calibration curve. Nowadays, they are used mainly as secondary standard.

Thermocouples

(Not mentioned in the Table 5.2)

The thermocouples were also often used in cryogenics. In principle, they have a standard calibration curve. However, they have a relative poor sensitivity below 10 K and need special technique for installation. Due to the easier solutions mentioned in the previous paragraphs, we do not find reason to use this more complicated solution. As far as requirements on temperature precision are not extreme, the thermometry is this temperature range is no more a problem.

Packaging

The sentence "the thermometer measured its own temperature" is often referred in cryogenics meaning that it is not difficult to measure "a" temperature, more difficult is to measure the temperature of the device! As a matter of fact, to measure the device temperature, the thermometer must be quite well (thermally) coupled to it. Usually, in cryocooler, the device and the thermometer are in vacuum and then the thermal coupling is made by solid-solid contact. To optimize this thermal contact, the solid-solid contact must be achieved through two plane surfaces with a significant forces between these two surfaces (see section 5.6.2). The good thermal contact between the thermometer and the other surface can then be obtained if the packaging provides these two possibilities. Once again, this problem being recognized from a long time, the thermometers are nowadays available in many type of packaging allowing good contacts. Figure 5.10 shows some type of the packaging proposed by Lakeshore-Cryogenics [54]. Note that if none of this packaging is judged satisfactory, a bare thermometer can be bought and a homemade casing adapted to the specific application can be built.

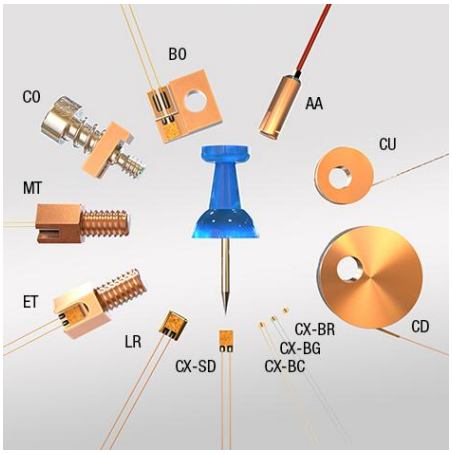

Figure 5.10: Various type of thermometers packaging proposed by Lakeshore cryogenics [54].

Cryogenic Temperature Monitors and controllers

As previously explained, the measurement of the temperature in the 2 K to 300 K temperature range is performed by measuring a resistance R and using a $T(R)$ calibration curve. Many Cryogenic Temperature Monitors and controllers are commercially available. Usually, they are able to measure two or four sensors simultaneously with a low measuring power adapted to low temperature constraints. The standard $T(R)$ calibration curves (Platinum, diodes, thermocouples) are usually digitally stored in the controller, home-made calibration curves can also be stored. This results in an apparatus given directly the temperature. To control temperature, one or two (or more) control loop are integrated in the Temperature controllers providing a power output (up to 100 W) calculated from a PID (Proportional, Integral, Derivative) process. This output must be connected to a heating resistor located to the stage to be controlled: its temperature will be stable when the available cooling power at this stage is counterbalanced by the heating power provided by the controller. Many recipes exist, more or less successful, depending of the thermal characteristics of the system, to find the appropriate PID coefficients [55] reaching to a fast stabilization of the temperature.

5.6 Optimized heat transmission

5.6.1 Thermal conductivity

Cryogenic systems requires *careful thermal design*. To guarantee uniform chip operation one has to keep control on the thermal fluxes that can lead to non negligible temperature inhomogeneity if too high. Additionally owing to the low cooling power, thermal links to the environment must be minimized. For instance, the coax cable or microwave guide for rf signal transmission to a Josephson array is typically made with a good heat conductor transferring too much heat to the device from room temperature. Thermal anchoring to 1st stage (see Figure 5.4 and Figure 5.5) reduces heat flow and temperature gradients, solving in many cases the problem. Radiation shields around low temperature areas reduces heat from radiated power that would otherwise limit cooling effectiveness and create temperature inhomogeneities.

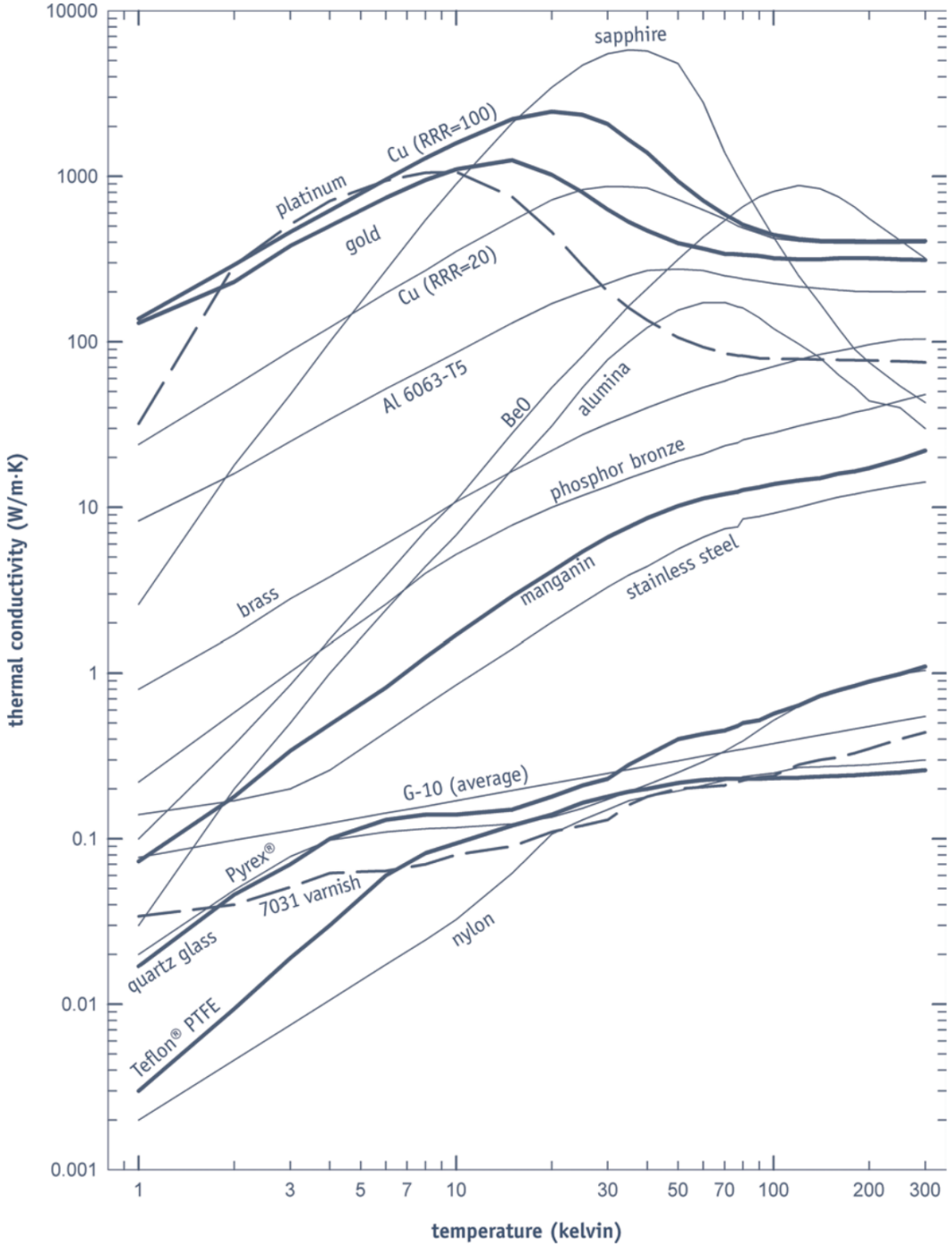

Figure 5.11: Thermal conductivity of the various materials used in cryogenics (from [54]).

5.6.2 Thermal contact & insulation

Owing to the low pressure environment, in our temperature range of interest, thermal conduction is obtained by conduction through solids (tables with temperature of interest in typical cryogenics experiments are available by many ways, See for instance NIST or Lakeshore documents [56]). Note that for pure metal (copper, Au, Al) below ≈ 100 K, the thermal conductivity becomes highly purity dependent.

For *good thermal conductivity* the right choices are Cu (purer is better), Ag (expensive) or Al (but superconductor under 1 K, welding difficult). For thermal insulation the right choices are plastics (Teflon, Nylon, PMMA, etc.), , alumina, thin-walled stainless steel tubes (but welding is not simple) or copper-nickel (easier to weld). In general, amorphous (glass) or materials composed of small crystals and containing a large quantity of defects and impurities are good thermal insulators. At the contrary, very pure crystal (sapphire, for instance) can be used when very high electrical insulation and very high thermal conductivity is required.

All these properties must fit some mechanical requirements. Stainless Steel (series 30(L) and 316(L)) and Titanium are often used when high mechanical constraints are required. These two materials are not good conductors (alloy). Mechanically, copper is not very good. Brass (easily welded) and some family of aluminum (8000, 2000, 7000 depending of the requirements) are sometimes good compromises due to their relatively low cost and their good workability.

As for the wires that carry electrical signals from ambient temperature to low cryogenic temperatures: for low-current terminals, thin threads of constantan or manganin are best for their low thermal conductivity and for the small temperature dependence of their electrical properties. If large electrical currents are to be transported (such as those for powering superconducting magnets) one almost always ends up choosing copper cables as long as they are carefully connected with heat wells on their way to low temperatures. At very low temperatures the best choice is the use of superconducting wires which can be obtained by covering a superconducting solder of thin manganin or constantan wires.

The wires for the measurement of small signals must, of course, always be rolled up on themselves, fixed rigidly and well shielded to reduce electrical noise from the outside.

5.6.3 Contact thermal resistance

Reaching thermal equilibrium and/or homogeneity in a cryogenic system becomes increasingly difficult when the temperature is lowered not only because the thermal conductivity of the materials decreases, but also because the thermal contact between two materials becomes gradually larger when the temperature drops. This "thermal contact resistance" R_K can produce a thermal jump at the interfaces between the materials given by:

$$\Delta T = R_K Q_{\mathrm{p}} \tag{5.3}$$

where Q_{p} is thermal power passing through the contact.

The contact resistances between different types of materials and between cryogenic materials were widely studied. However, this issue is quite complicated and all the data are not completely reliable in the sense that they depend closely of some technical preparation: The devil is in the details. However some basic principles can help to mitigate this problem.

1. R_K is inversely proportional to the effective contact area that can be about 10^{-6} of the apparent contact area due to the microscopic irregularities of the facing metal surfaces. To increase this effective contact, a "filler" material can be used to fill the void space. Due to its low pressure vapor and relatively high thermal conductivity, the vacuum grease is often use for this purpose. Some time, highly deformable pure metals foils are also used (gold or indium for instance).

2. By applying strong pressure/force between surfaces, the effective contact area increases and then the contact resistance can be greatly reduced. In the cryogenic world, it is often said that the contact

resistance is proportional to the applied force more than to the pressure.

3. The contact resistance can be kept reasonably small if the surfaces are clean, possibly gold-plated and pressed against each other with great force. As a matter of fact, the thermal conduction provides by conduction electrons (metal-metal) is rapidly more effective than that due to crystalline vibrations (phonons). Then contact between not oxidized surfaces must be promoted.

4. Most solder alloys are superconducting at low temperature and therefore, on the one hand, they are very good for conducting electrical signals but, on the other hand, their thermal conductivity decreases below superconducting temperature and can be very poor at very low temperatures.

5.7 Sample holder and coldplate

Reliable cryocooler operation requires a very specific thermal design to cope with problems not faced with liquid coolants, like minimization of thermal gradients to guarantee uniform operation of the chip. Moreover, the refrigerator has a reduced cooling power, thus the microwave guide to transmit the RF signal to the chip must be carefully designed in order to limit the heat load on the low temperature stage, while maintaining an effective signal transmission. As mentioned earlier, it is recommended when possible to evacuate part of the heat load coming from room temperature on the cryocooler first stage when exists.

In the INRIM sample holder (Figure 5.12), the chip is pressed tightly by a printed circuit board to a OHFC copper lamina. The PCB has pads for soldering and the chip is bonded to the PCB. Brass screws provide the thermal link between the cold finger and PCT copper sheet that holds the device. The copper laminated is also used as thermal conductive link to the cold plate, interposing and indium sheet for optimal contact.

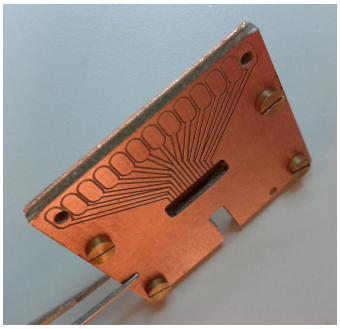

Figure 5.12: INRIM sample holder [49].

The coldfinger surface cannot be generally used to hold directly the chip carrier, to avoid damage and because the metal surface in contact with the cold part of the experiment needs manufacturing to host: thermometer(s) and heater(s) for temperature control, holes for signal wires and temperature control wires, threaded holes for tightly screwing the chip holder to the cooling surface, etc. This is accomplished by an Oxygen-Free-High-Conductivity dish, the "coldplate."

5.8 Security rules

Cryogenics deals with extreme temperature and with liquids, generally not toxic, but can be the cause of oxygen concentration depletion. Then laboratories must follow some important safety constraints. An

example of a non-exhaustive list of some rules that should be implemented in a laboratory using cryogenics and cryogenics liquid in high quantity is given in Appendix A.

5.9 Recomended bibliography

Recomended bibliography is: [48], [51], [57], [58]. For thermometry materials, see for instance Lakeshore Cryogenics documentations. The company provides on line [59] many usefull data and advices about cryogenics (tables and plots of thermal conductivity of various materials, for instance, recommendations about thermometer thermalization and electrical wiring). Pricing is also available on line. Oxford Instruments is another company very active in cryogenic field (turn key solutions) and commercialized many spares useful in cryogenic hardware [60].

Chapter 6

A standard voltmeter referenced to an AC Josephson standard

IPQ

A system setup detailed described in [61] and schematized in figure 6.1 implements a standard voltmeter referenced to an AC Josephson standard. The method has been verified up to 7 V RMS in the frequency range from 50 Hz to 1 kHz with uncertainties in the order of 1.7 µV V^{-1} ($k = 2$). Further tests have been performed to explore the behavior of the setup between 10 Hz and near 5 kHz.

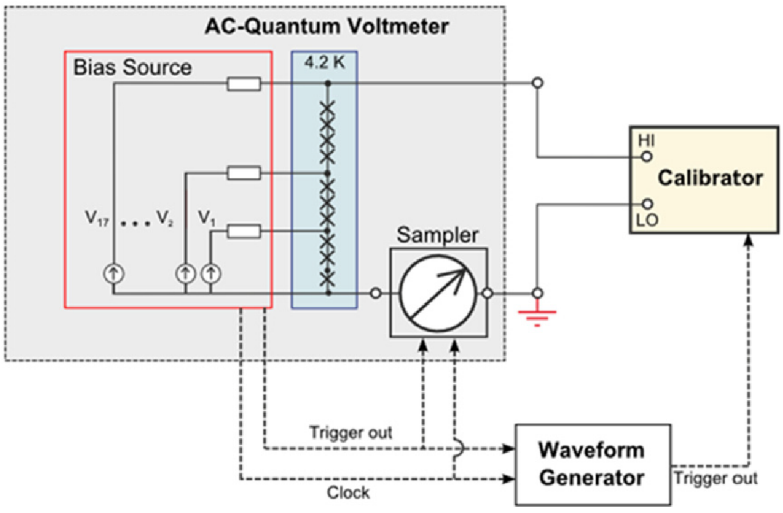

Figure 6.1: System setup.

Example of instrumentation used in the PTB system:

- Array – PTB, SNS 9/4; 10 V with 16 segments,
- Bias Source – Lecroy; 5 units with a total of 16 channels,
- Microwave Generator – Julicher Squid GmbH; 70 GHz,

- Calibrator – Fluke 5720A,
- Sampler – National Instruments, PXI-5922,
- Waveform Generator – Keithley 3390.

The control of the Bias Source allows the generation of a selectable stepwise sine wave in amplitude and frequency by the Josephson array as represented in figure 6.2. The signal generated by the calibrator is compared against the signal from the Josephson array by sampling the differences between both with the ADC PXI-5922. The sum of the differences sampled to the stepwise signal gives a sine wave signal equivalent to the generator signal under measurement from which is calculated the value of the RMS voltage, after removing the points corresponding to the step transitions which are affected by noise (ringing points).

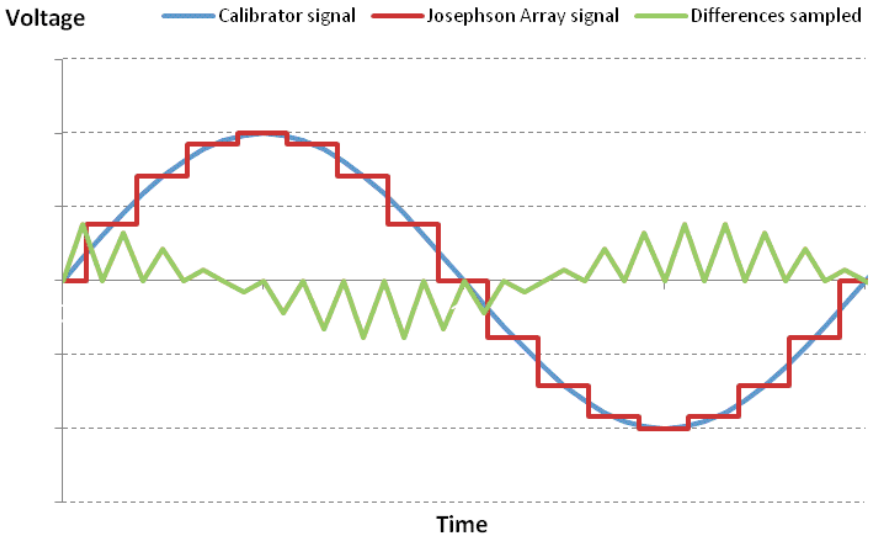

Figure 6.2: Representation of the voltage signals.

The software applications used to control the system have to assure the selection of the relevant parameters of the process:

- Josephson voltage and frequency to the stepwise sine wave.
- Number of steps of each period of the stepwise sine wave.
- Sampling rate of the sampler.
- Number of periods sampled to calculate a mean value for each run.
- Number of mean values averaged to calculate a final value, hereafter called "Loops".
- Number of deleted ringing points, in the begin and end of each voltage step.
- Number of deleted starting points.

Modular applications used to run the system:

- Module to make the selection of the voltage and frequency values of the Josephson Array; the number of steps in which each period of the stepwise wave is divided into and select and apply the microwave frequency to the Josephson array.
- Module to control of the Calibrator selecting the voltage and frequency of its output as well as the control of the Signal Generator to select the delay phase value to be introduced in the Calibrator output related to Josephson signal.
- Module to define the number of periods and loops to be averaged; the number of "Delete Starting Points" and "Delete Ringing Points". Support the calculation of the measured RMS voltage value of the signal being measured and saved n Loops of measurements in a text file.

Example of system configuration parameters:

Number of steps	20
Periods	40
Loops	100
Delete Ringing Points	50
Delete Starting points	0
Sampling Rate	10 MSa/s

The number of periods and loops in the table above could be applied for the frequencies equal or greater than 40 Hz. For lower frequencies, those values have to be reduced to solve the limitation of memory. The experimental standard-deviation of the measurements depends on the frequency value: it can be observed that the lower values, between 1 and $2\,\mu V\,V^{-1}$, were found for the frequency interval of 30 Hz to 100 Hz. For the higher and lower frequencies measured, the standard deviation increases to an order of $10\,\mu V\,V^{-1}$. To handle this, the number of periods could be increased: at 20 Hz, with a sampling rate reduced to 2 MSa/s to free memory and to allow, in that way, the increase of the period number, it was showed that an increase of 20 periods to 80 periods has a consequence of reducing the standard deviation from $9.1\,\mu V\,V^{-1}$ to $3.0\,\mu V\,V^{-1}$. For higher frequencies, the main parameter to reduce the noise is also the number of periods: at 1 kHz at 3 kHz increasing the number of averaged periods from 40 to 320 allows the standard deviation decreases to $1.5\,\mu V\,V^{-1}$. When the number of sampled points per step is reduced at higher frequencies followed by the consequent reduction of time interval of each step, the increase of number of averaging periods works well to reduce the dispersion of the measurements. For frequencies lower than 30 Hz, despite the higher number of sampled points per step, there is a minimum number of periods that are need to characterize the repeatability of the system.

Chapter 7

AC Voltage Measurements using PJVS and Differential Sampling

TUBITAK

For accurate AC voltage measurements with Programmable Josephson Voltage Standard (PJVS) differential sampling method is used. PJVS system output is configured as quantum accurate stepwise voltage for definite frequency (same as DUT output), definite amplitude (the closest value to DUT output) and appropriate step count. PJVS output voltage levels for each step V_j can be calculated as:

$$V_j = V_{\mathrm{p}} \sin \frac{2\pi j}{N} \tag{7.1}$$

where N is total step number, j is step index and V_{p} is peak voltage of DUT output. Because of the limited resolution of the PJVS, it is not possible to obtain exact voltage levels, so the closest voltage levels are selected.

By using differential sampling, non-ideal behaviors of sampler like drift, INL, gain errors are drastically decreased. Besides, transient region effect is eliminated by using proper timing or ignoring samples corresponding to that region. System setup can be seen at Figure 7.1.

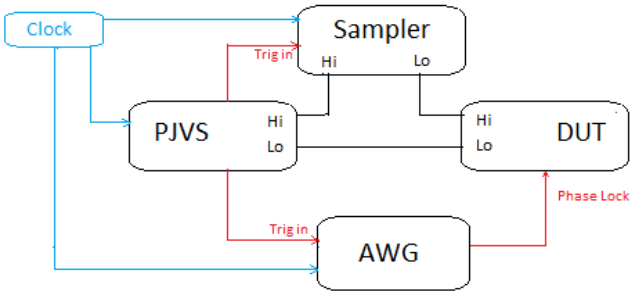

Figure 7.1: Quantum Voltmeter Setup.

In this setup timing is crucial and all devices except DUT are locked with the same clock. PJVS, DUT, AWG and sampler are triggered with the necessary phase. PJVS and DUT are synchronized to

obtain minimum differential signal, for this purpose AWG output signal phase is adjusted. In papers it is shown that small phase shifts between PJVS and DUT triggers do not affect the measurement accuracies. Synchronization scheme is depicted in Figure 7.2.

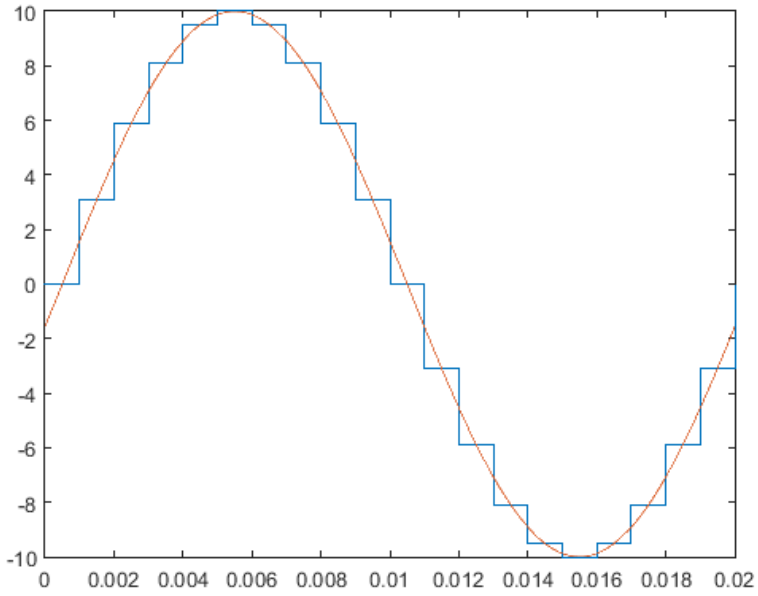

Figure 7.2: Blue line indicates PJVS output and red line indicates DUT output. Simulated output is $20\,\mathrm{V}$ peak-to-peak, frequency is $50\,\mathrm{Hz}$, step count is 20.

As sampler, there are different options like Agilent 3458A integrating ADC [62], [63] and NI PXI-5922 $\Sigma\Delta$-ADC [61]. When 3458A is used, integration time and sampler trigger is set to avoid transition region effect, then one sample is taken for each step of the PJVS output.

Disadvantages of this ADC are low sampling frequency and extra work needed for synchronization because it has no clock in or clock out connector. In latter case high speed sampling is performed and transient region samples are deleted. Although $\Sigma\Delta$-ADC allows for higher sampling rates, its accuracy is worse than Agilent 3458A. Differential voltage is simulated as in Figure 7.3.

It can be seen that peak voltage of the accepted region is about $0.8\,\mathrm{V}$, decreased more than 10 times for 20 step counts and half step integration time. Integration time and the number of steps can be changed if necessary.

To reconstruct the original waveform, samples taken from 3458A are added to exactly known PJVS output step corresponding to related sample.

Because frequency is known, three parameter sine-fit method [64] can be used to get other parameters; amplitude, phase and offset. To obtain parameters of harmonic components or contribution at the power line frequency, iterative three parameters sine-fit can be used. In this method, all the parameters are obtained starting from fundamental component. Then, for second component three parameter sine-fit is again applied to residual signal. This procedure is repeated up to desired frequency component count. Another approach is to create observation matrix D for multi harmonic signal [65].

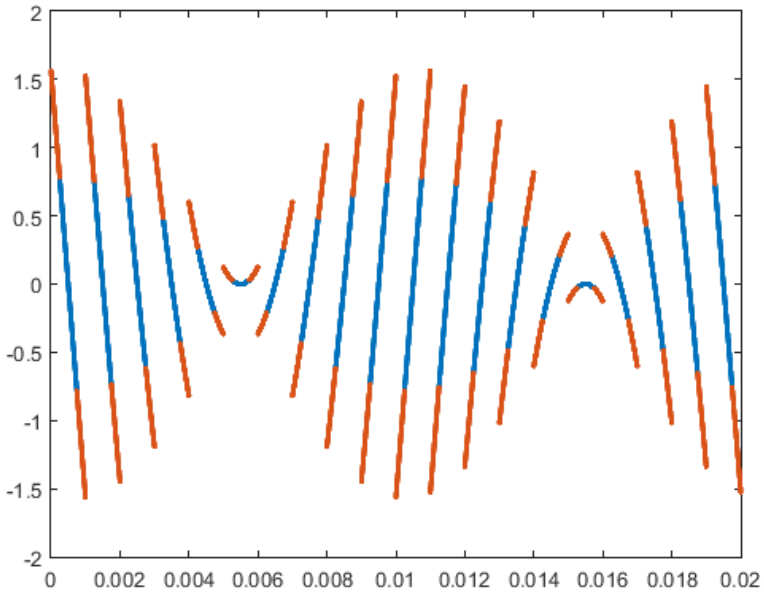

Figure 7.3: Difference voltage pattern. Red regions indicate rejected area and blue ones indicate integrating region for half step integration time.

$$D = \begin{bmatrix} \cos\omega t_1 & \sin\omega t_1 & \cos 2\omega t_1 & \sin 2\omega t_1 & \dots & \cos H\omega t_1 & \sin H\omega t_1 & 1 \\ \cos\omega t_2 & \sin\omega t_2 & \cos 2\omega t_2 & \sin 2\omega t_2 & \dots & \cos H\omega t_2 & \sin H\omega t_2 & 1 \\ \vdots & \vdots & \vdots & \vdots & \ddots & \vdots & \vdots & \vdots \\ \cos\omega t_N & \sin\omega t_N & \cos 2\omega t_N & \sin 2\omega t_N & \dots & \cos H\omega t_N & \sin H\omega t_N & 1 \end{bmatrix} \tag{7.2}$$

Where ω is angular fundamental signal frequency ($2\pi f$), t_i is i^{th} sample time (for uniform sampling $((i-1)/f_{\text{s}})$) and H is total harmonic component number. Then, estimation vector $\hat{x}$ can be obtained via:

$$\hat{x} = \left(D^{\text{T}}D\right)^{-1}\left(D^{\text{T}}y\right) \tag{7.3}$$

In the equation, y is reconstructed signal vector.

$$\hat{x} = \left[Y_1 Z_1 Y_2 Z_2 \dots Y_H Z_H C\right]^{\text{T}}. \tag{7.4}$$

Each harmonic parameter can be estimated as: for amplitude

$$A_h = \sqrt{Y_h^2 + Z_h^2} \tag{7.5}$$

for phase

$$\Theta_h = \begin{cases} \tan^{-1}\left[\frac{-Y_h}{Z_h}\right] + \pi, \wedge Z_h < 0 \\ \tan^{-1}\left[\frac{-Y_h}{Z_h}\right], \wedge Z_h \geq 0 \end{cases} \tag{7.6}$$

Then estimated amplitudes must be corrected with sinc function:

$$\frac{\sin \pi f T_{\text{DVM}}}{\pi f T_{\text{DVM}}}, \tag{7.7}$$

where f is fundamental frequency and T_{DVM} is aperture time of integrating ADC.

C represents the offset. To get contribution at the power line frequency four parameters sine-fit with $50\,\mathrm{Hz}$ starting frequency can be applied to residual.

In the scenario that PXI-5922 is sampler, differential sampling frequency is much higher than 3458A scenario. In this situation the samples corresponding to transient region are deleted and quantum accurate samples are used. Before adding the samples to PJVS output voltage mean of the remained samples are taken. Then, this mean value is added to PJVS output and the reconstructed signal is obtained. After reconstruction the signal corrected by sinc function and then using RMS formula the RMS value of the DUT output can be obtained.

Uncertainty components of the measurement system [61];

- Noise (Type A).
- PJVS (Type B).
- Sampler drift, gain, INL (Type B).
- Sampler bandwith (Type B).
- Calibrator drift (Type B).
- Phase error (Type B).

Chapter 8

Procedure for calibration ac-dc transfer standards using AC quantum voltage standards

TUBITAK

8.1 Scope

The aim of this procedure is to provide general guidelines on the application of AC quantum voltage standards (QVS) for the calibration of the frequency response of the ac-dc transfer standards.

8.2 Method

Ac-dc transfer standards or thermal converters are devices used to compare RMS values of the AC and DC voltages by comparing their heating power on a resistor [66]. Main parameter used to describe thermal converter is ac-dc transfer difference and is defined by:

$$\delta = \frac{V_{\mathrm{AC}} - V_{\mathrm{DC}}}{V_{\mathrm{DC}}} \tag{8.1}$$

where V_{AC} is RMS value of the AC voltage, V_{DC} is the DC voltage which, when reversed, produces the same mean output voltage of the thermal converter as V_{AC}, i.e.

$$V_{\mathrm{DC}} = \frac{|V_{\mathrm{DC+}}| + |V_{\mathrm{DC-}}|}{2} \tag{8.2}$$

Ac-dc transfer difference of a thermal converter is determined by applying known voltages from AC quantum standard and measuring output of thermal converter. Transfer difference can be calculated by:

$$\delta = \frac{V_{\mathrm{ACJ}} - V_{\mathrm{DCJ}}}{V_{\mathrm{DCJ}}} - \frac{E_{\mathrm{AC}} - E_{\mathrm{DC}}}{nE_{\mathrm{DC}}} \tag{8.3}$$

where δ is ac-dc transfer difference, V_{ACJ} is RMS value of the AC voltage produced by AC Quantum standard, V_{DCJ} is average of the absolute values of a DC voltage produced by AC Quantum standard in a

forward and reverse direction, E_{AC} is output voltages of the thermal converter when applied V_{ACJ}, E_{DC} is average of the output voltages of the thermal converter when applied V_{DCJ} in a forward and reverse direction and n is sensitivity parameter of the thermal converter.

8.3 Calibration Procedure

There are two types of quantum voltage standards that can be used for the calibration of the TCs: programmable Josephson Voltage Standards (PJVS) [67], and pulse driven Josephson voltage standards or Josephson Arbitrary Waveform Synthesizers (JAWS) [5].

8.3.1 PJVS, RMS Calibration

PJVS are based on using binary-divided arrays of damped Josephson junctions which can produce stepwise approximated voltages (SAV) when biased by synchronized currents sources [4]. Using stepwise-approximation synthesis, PJVS can generate arbitrary sine waves with calculable (rms) voltage and spectral content. The primary drawback to this synthesis technique is the uncertainty that results from switching between the discrete voltages due to finite rise times and transient signals [68], [69]. When come to the calibration of the thermal converter by using PJVS, another obstacle is the error due to the current that is required to drive the heater of the TC.

The shape and duration of the transients, and therefore the associated error, depend on numerous parameters such as the speed of the bias electronics and the circuit layout, the bias currents used, the microwave power, cabling etc. The error of the PSJV signal due to the transitions between the steps can be decreased by using fast bias electronics and impedance compensation of cabling [9], and by increasing number of steps. It has been shown that measured ac-dc difference linearly dependent on bias current trimming, while shape of the transient is kept constant if other system parameters are not changed. Linear slopes of the ac-dc transfer differences for different bias current trims intersecting at one point, at which, the stepwise-approximated waveform, although not quantized during the transients, will nevertheless have the same rms value as an ideally quantized waveform. This is valid under assumption that ac-dc difference of the test TC has flat response over the frequencies measured, however in reality, this cannot be assumed automatically. Practical approach proposed in [70] is as follows:

1. Calibrate the TC, using conventional methods, at the highest frequency where the JWS voltage can be generated, for example, $5\,\mathrm{kHz}$.
2. Using the set-up from Figure 8.1, sweep the bias trim current at this frequency. Due to its frequency dependence, the curve of the ac-dc difference measurement result has the largest slope compared to other frequencies.
3. Find the bias current that corresponds to the TC error obtained from step 1 above.
4. Use this bias current at lower frequencies.

As stated before, it is necessary to provide an additional electronic circuit to drive the heater of the TC when using PJVS as voltage source. There are different solutions:

- Extra current source synchronized to the bias source [69].
- Buffer amplifier [71].
- Transconductance amplifier [72].

Using an amplifier (Buffer or Transconductance) is less complicated than additional current source, so procedure given here assumes using of the transconductance amplifier.

Briefly calibration procedure is given as follows:

- Connect TC to the PJVS, see Figure 8.1.
- Perform system optimization as described above.
- Apply voltages to TC in the sequence DC+, AC, DC-.
- Calculate ac-dc transfer difference of the TC using 8.3.

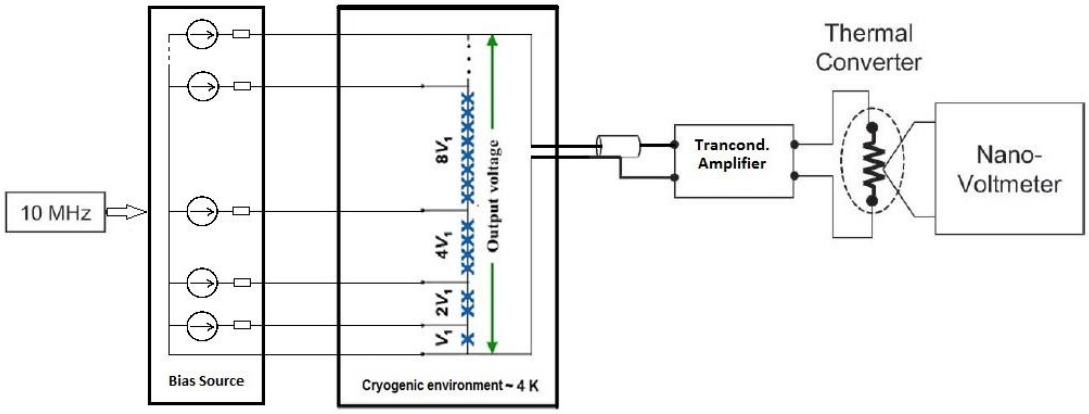

Figure 8.1: Measurement Setup for Calibration TC with PJVS and amplifier.

Explained procedure can be used also for calibration of the AC RMS voltmeters, as Fluke 5790A and Datron 4200.

8.3.2 PJVS, Sampling

The other way to calibrate TC with a PJVS based system is to use an extra calibrator or generator whose ac and dc voltages are directly measured by PJVS using differential sampling [61], [73]. The main advantages of this approach compared to applying the PJVS-generated SAV and dc voltages to the TC are that:

1. the TVC is supplied with a pure sine wave voltage and is in all other respects in the same condition as when used in conventional ac-dc systems,
2. the closeness of the PJVS and the TVC voltages provides a virtually unloaded condition for the PJVS,
3. The transients in the SAV affect its fundamental less than the RMS value of the whole signal.

During the measurement, calibrator and sampler are synchronized to the bias source. Difference of the AC and DC voltages of the calibrator and PJVS are measured by Sampler using differential sampling technique. After AC and DC voltages of the calibrator are measured with PJVS, ac-dc transfer differences of the TC are calculated by (2).

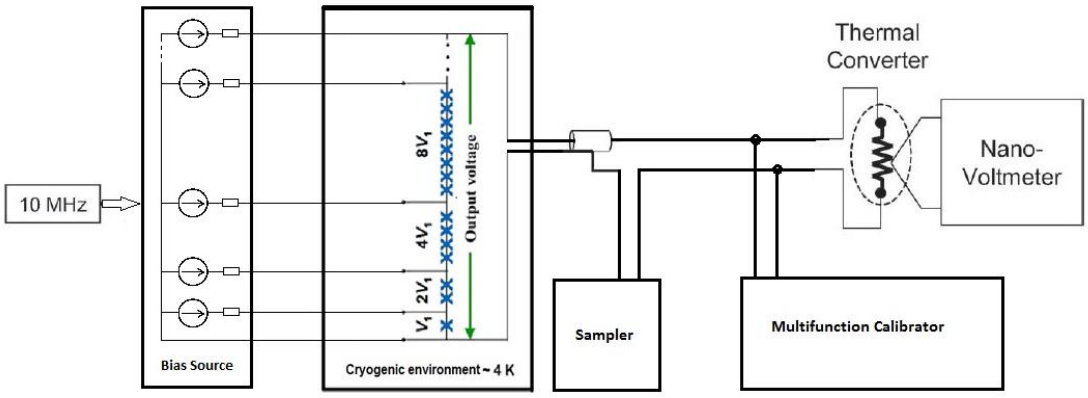

Figure 8.2: Measurement Setup for Calibration TC with PJVS and multifunction calibrator.

8.3.3 JAWS

The JAWSs, based on pulse driven Josephson array are able to generate quantized AC waveforms from DC to Megahertz range, with excellent spectral purity, low noise and no drift. Recent works [13], [74] lead to 1 V level systems, which are suitable for the calibration of the TC. Major drawback of the JAWS is the influence of the connection between the array inside the cryogenic environment and the test instrument. This error can be compensated to some level by properly impedance matching [35]. Special designed transconductance amplifier used to unload PJVS when TC is calibrated can also be used with JAWS so that cabling now does not affect measurement in the first order [75].

8.3.4 Uncertainty

The following parameters have to be considered in the uncertainty budget for the calibration of the TC by using a QVS:

PJVS, RMS

1. Quantization of steps, typically accuracy of the Josephson standard
2. Transient effects, depend on bias electronics and matching
3. Amplifier influence
4. Connections
5. TC calibration at high frequency
6. Type A, standard deviation of the measurements

PJVS, Differential Sampling

1. Quantization of steps, typically accuracy of the Josephson standard
2. Stability and INL of the digitizer
3. Calibrator drift
4. Phase error
5. Type A, standard deviation of the measurements

Chapter 9

Calibrating voltmeters with PJVS

JV

The stepwise approximated sine waves generated by the PJVS can be used directly as an RMS voltage source for low frequencies. As the frequency of the waveform is increased, the transients between the steps becomes dominant, and the quantum accuracy of the signal is lost. By using a DAC generated sine wave U, with the same frequency as the PJVS wave V, it is possible to transfer the quantization at the steps to the DAC generated wave by sampling the difference at the steps.

The readings are taken when the difference U-V is close to zero, by adjusting both the phase, amplitude and frequency of the two waves. The DAC source can then be used as a real-time calibrated voltage source, for calibrating a voltmeter, given that the influence of the difference sampling does not affect the results in a substantial way. A schematic description is shown in Fig.9.1. Two separate difference amplifiers (DA) were compared in [76], showing that two similar DAs give the same result for the calibration of a digital voltmeter, within a few $\mu V\,V^{-1}$. Tests comparing these two DAs with an NI5922 sampler showed that the results differ by more than a few $\mu V\,V^{-1}$. Analysing the FFT of the error signal over several wavelengths, showed that adding a choke (coaxial cable wrapped around a solid ferrite core) reduced the noise of the readings from the ADC substantially, but connecting the NI5922 (parallel to the two other DAs) lead to a similar noise level as without the choke. This indicates that the NI5922 operates in a slightly different way and that the isolation of the device from ground is challenging.

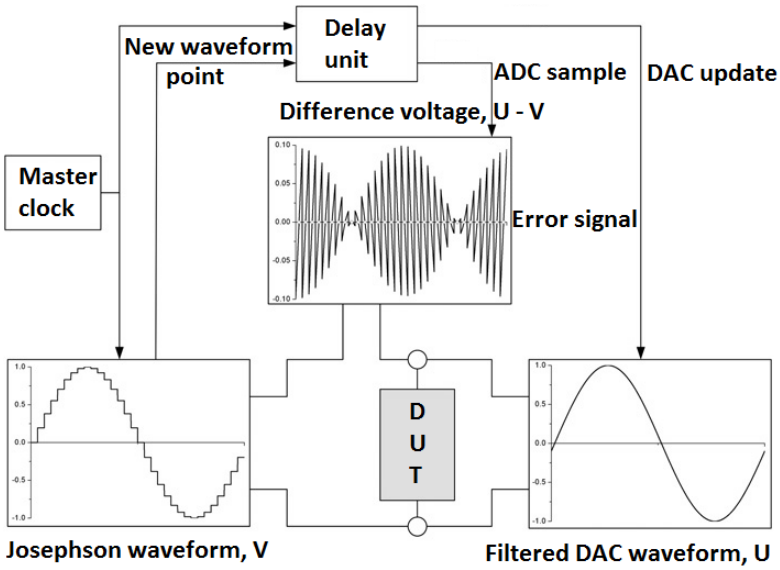

Figure 9.1: Schematic description of the NPL differential sampling setup.

Chapter 10

Procedure for metrology grade characterization of analog-to-digital converters frequency response using ac quantum voltage standards

CEM

10.1 Scope

The aim of this procedure is to provide general guidelines on the application of AC quantum voltage standards for the characterization of the frequency response of Analog-to-Digital Converters (ADC). The frequency characterization is performed up to 20 kHz.

10.2 Method

The proposed method for the frequency response characterization is based on the comparison of the known AC quantum input signal to the values obtained by the ADC sampling.

10.3 Quantum standards

Two different ACQ voltage standards can be used, Programmable Josephson Voltage Standard (PJVS) and a Josephson Arbitrary Waveform Synthesizer (JAWS). The description, characteristics and operation of these standards are defined on the previous chapters of this guide.

10.3.1 PJVS

In these systems the AC voltage is obtained using binary-divided arrays of damped Josephson junctions. Voltage waveforms are synthesised by periodic switching of the binary-divided arrays. It is equivalent to a Digital-to-Analog converter where each step of the wave has the accuracy of a directly traceable quantum standard.

The main limitation of these systems is the transition time from one step to the other. During this time there is a non-calculable oscillation on the signal. The synchronization of the Josephson source and the digitizer so that the signal is sampled only during the quantized part of the wave do not solve the problem, because in this way the digitizer is sampling a DC signal so the AC behaviour is not evaluated.

Several solutions have been investigated to overcome this limitations.

The shape of the transitions is influenced for several parameters, as frequency, power or bias current. These parameters can be adjusted in a way that the transition shape compensates the deviation from an ideal signal, so the RMS of the signal is the same than the ideal. At the end of this chapter there are references to this method.

Another way is to perform differential measurements. An ADC measures the different between a source and the PJVS. The samples are taken during the quantized part of the PJVS. From the samples of the difference the AC source can be reproduced with direct traceability to the Quantum standard. The error on characterization of the AC source depends on the error of the measured samples. The influence of the error of the sampler relative to the signal is divided by the signal reference and samples amplitude relation. There are some limitations of these method, due to the step response of the ADC used to measure the difference, a delay time after the step change and the sampling is necessary. This delay depends also on the magnitude of the voltage change. This limit the number of samples for period of the signal. The PJVS need a time to set each quantum value. As the frequency increases the number of samples for period decreases. This means an increase on the magnitude of the difference limiting the maximum frequency to characterize the ADC in the order of few kHz. At the end of this chapter there are some references on this method application.

10.3.2 JAWS

The JAWS is able to generate pure sine wave at different frequencies. The main limitation of this standard is the need to use long cables from the output of the calculable voltage inside a cryostat to the instrument under test. These leads produce a voltage frequency dependence error. The error is squared with the frequency. At 20 kHz, the error can be in the order of $4\,\mu V\,V^{-1}$. Several methods have been described for this error compensation. References to these publications are listed at the end of this chapter.

10.4 Measurand definition

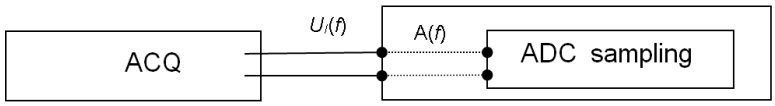

Figure 10.1: Scheme of connection during sampling of ACQ signal by ADC.

To characterize the frequency response, for each frequency the ACQ signal is applied to the digital converter, the signal is sampled and processed to obtain the measured amplitude, see Fig. 10.1. From the direct comparison of the applied and processed signals at several frequencies, the frequency response is obtained.

For each frequency, the calibrated AC source ($U_{\mathrm{I}}(f)$) is applied to the ADC *at some defined operation conditions*. The estimate of the output signal ($A(f)$) is obtained from the taken samples using a convenient algorithm. The $A(f)$ signal is corrected from the error introduced due to the sampling aperture and the corrected signal $A_{\mathrm{c}}(f)$ is used to obtain the error for each particular frequency at defined operation

conditions. In the case that the aperture time can be varied, as in the Keysight 3458A, the frequency response is obtained for several T_a

$$e(f) = A\mathrm{c}(f) - U_\mathrm{I}(f) \tag{10.1}$$

The corrected value $A\mathrm{c}(f)$ arrives from the fact that integrating analog-to-digital converters measure the mean value (A_i) during the integration time and this value is assigned to the mean time of the time aperture t_i.

$$A_i = \frac{1}{T_\mathrm{a}} \int_{t_i - T_\mathrm{a}/2}^{ti + T_\mathrm{a}/2} u(t)\mathrm{d}t \tag{10.2}$$

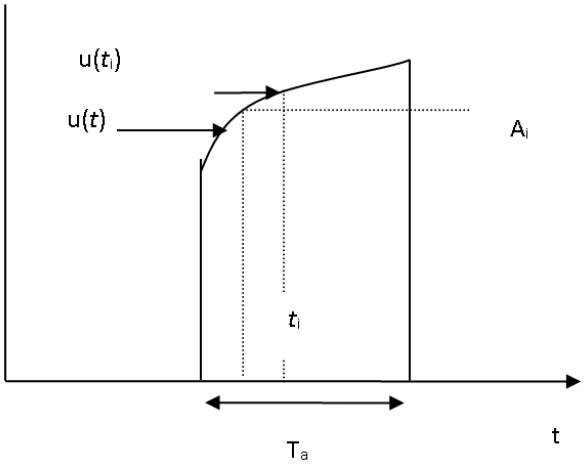

Figure 10.2: Time aperture.

For a sine signal at frequency f there is a difference between the mean value and the signal value at the time t_i (see figure 10.2), the theoretical corrected value can be obtained with the following corrective term:

$$K(f, T_\mathrm{a}) = \frac{\pi f T_\mathrm{a}}{\sin(\pi f T_\mathrm{a})}. \tag{10.3}$$

There is an uncertainty on the ADC time aperture value, the influence of this uncertainty becomes more significant as the product (fT_a) approaches unity and will be considered on the uncertainty estimation.

The time aperture and the temperature, at which the frequency response is measured, need to be included in the definition.

The measurements are performed for a set of frequencies within the ADC working range, and the error and uncertainty for each frequency is obtained ($e(f)$, $U(f)$). From these set of values a transfer function can be fitted to provide the error and uncertainty to any interpolated frequency. The error caused by the fit has to be included in the final uncertainty estimation.

10.5 Configuration

For asynchronous sampling a synchronization signal between the source signal and the Digital-to-Analog converter is not necessary and is the unique option when it is not possible to phase lock the source and the DAC, see figure 10.3. The 10 MHz reference signal phase locks the internal source oscillator of the

AC source. For the below configuration and in case of asynchronous sampling, the time reference will be obtained from the DAC internal clock, or any external clock. If the clock used to trigger the DAC is not locked to a 10 MHz reference it is recommended to measure the frequency error of the clock. This information will be very useful for data processing by means of the four-parameter least-squares sine fit method, to provide a good initial estimate of the frequency f_0. For synchronous sampling the frequency reference will be the external reference.

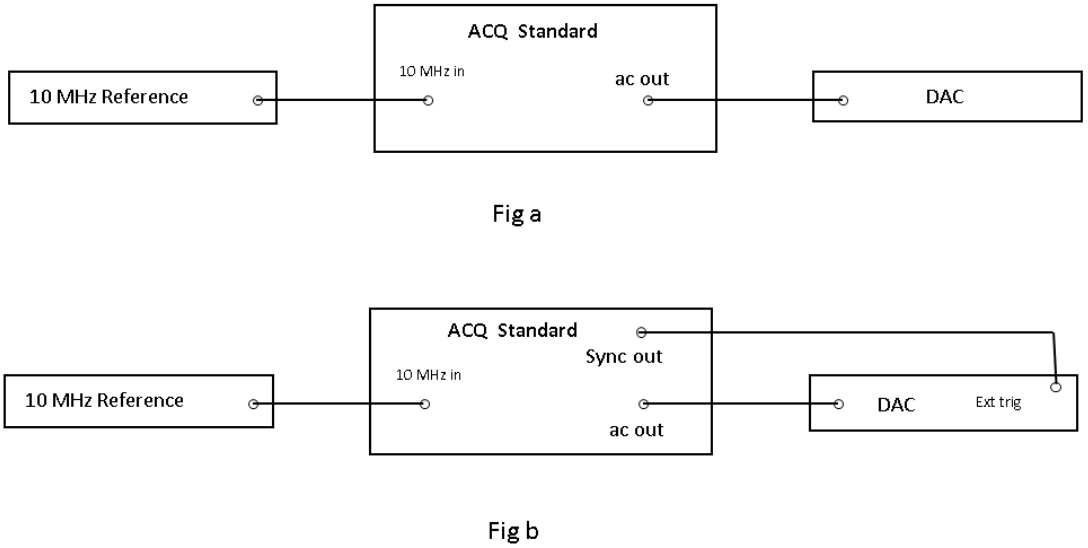

Figure 10.3: Configurations for asynchronous (a) and synchronous (b) sampling.

10.6 Data acquisition

The measurement conditions are configured in the DAC, usually via a computer communications system. The trigger system of the ADC is configured so that internal clock establishes the sampling instants (in an asynchronous sampling scheme). After the set of samples are acquired, it is read and stored.

10.7 Data processing

The processing of the samples can be performed using the "Q-Wave Toolbox" [77] or any other applications. The file containing samples is read as the input of the processing stage. Other information may be required depending on the selected processing method. If FFT is used, a sampling rate needs to be provided as an input via a measurement configuration file. With this information, the spectral analysis of the samples is performed by (windowed) FFT. If a method using least squares sine wave is used, a signal frequency is usually needed to obtain best results.

Results are stored in a sheet in order to easily plot, rearrange and reuse them. The measurement conditions are defined depending on the signal frequency to be measured, the main parameter to be defined are: Coherency of the measurement system, sampling frequency (must meet the Nyquist requirement), time aperture, dead time, (time aperture and dead time must be compatible with the sampling frequency),

number of signal periods to be sampled, DAC range. In case of storing the obtained samples in the internal memory of the DAC, the maximum memory size of the DAC must be considered.

10.8 Uncertainty

The main sources of uncertainty are described according to [78] and is mainly based on [79]. The following section describes the uncertainty estimation corresponding to the DAC error on the amplitude measurement of an ACQ voltage signal. The error and uncertainty are obtained for several frequencies. The DAC error and uncertainty for any other frequency can be obtained from the least-square fit of the error and uncertainty determination at several frequencies within the required frequency range of interest.

The output quantity is the gain error of the DAC at a defined frequency (f_a) and time aperture (T_a).

The input quantities are following:

- The n samples taken:
$$V_1, V_2, \ldots, V_n \ . \tag{10.4}$$
- The n times t when the samples are taken
$$t_1, t_2, \ldots, t_n \ . \tag{10.5}$$
- The time aperture T_a if it can be varied, as the Keysight 3458A.
- The sampling frequency f_s.
- The model relating the output quantity and input quantities is as follows:
$$e(f_\mathrm{a}, T_\mathrm{a}) = A(f_\mathrm{a}) - V_1(f_\mathrm{a}) + C_\mathrm{a}(f_\mathrm{a}) + C_\mathrm{alg} + C_\mathrm{sf} \tag{10.6}$$
Where
  - $e(f_\mathrm{a}, T_\mathrm{a})$ is the DAC gain error for a given frequency and time aperture.
  - $A(f_\mathrm{a})$ is amplitude value obtained from the n taken samples at times t_n.
$$A(f_\mathrm{a}) = f_1(V_1, V_2, \ldots, V_i, t_1, t_2, \ldots, t_i) \tag{10.7}$$
  - f_1 denotes the function used to reproduce the signal from the samples.
  - $V_\mathrm{I}(f_\mathrm{a})$ is the reference applied signal from the Quantum standard, JAWS or in the case of using a PJVS the quantum corrected AC signal.
  - $C_\mathrm{a}(f_\mathrm{a})$: There is an uncertainty on the ADC time aperture value (T_a), the influence of this uncertainty becomes more significant as the product (fT_a) approaches unity.
  - C_alg: Correction due to the performance of the applied data processing method other than $C_\mathrm{a}(f)$.
  - C_sf : Correction due to the sampling frequency. To evaluate this correction several measurements of the same signal must be done at different sampling frequencies.

10.9 Probability density functions (PDFs)

The PDFs for the input quantities of the model are the following:

$V_{\mathrm{I}}(f_{\mathrm{a}})$. It comes from the ACQ reference signal. The error and uncertainty of this component are: Using a filtered DAC corrected with a PJVS the correction. Using a JAWS, the voltage error on the leads from the quantum reference to the DAC. Literature references are provided at the end of this chapter in the way to evaluate and compensate for this error.

$A(f_{\mathrm{a}}) = f(V_i, t_i)\ V_i$: the mean dc measured mean values during the integration time. The errors due to the dc calibration, linearity, and stability of the DAC are intrinsic to the frequency response of the DAC so their uncertainty is not considered. There is a gain variation of V_i with T_{a}. T_{a} is measured internally for the DAC, the systematic error in T_{a} is intrinsic to the DAC and is included in the frequency response. The only V_i uncertainty contribution considered is due to quantization. In fact with the time t_i when the samples are taken, variation of t_i during the measurement (time jitter) contributes to the uncertainty. According to the above, the two uncertainty components for this function are time jitter and quantization. It has been verified that the distribution due to the contribution of time jitter and quantization can be combined as a quadratic sum of the two terms obtained separately. The two components are then evaluated independently. Regarding jitter, a rectangular distribution using the specification of the DAC can be considered, If a specific evaluation of the DAC is not available. The influence of quantization can be represented by the Wagdy equation for the DFT as follows:

$$u_q^2 = \frac{\Delta^2}{6N}; \Delta = \frac{D}{2^n} \tag{10.8}$$

where D is the dynamic range, n is the number of quantization bits and N the number of samples.

$C_{\mathrm{a}}(f_{\mathrm{a}})$: This correction is due to the integrating ADC conversion and is not intrinsic to the DAC. The correction is the following

$$K(f_{\mathrm{ac}}, T_{\mathrm{a}}) = \frac{\pi f_{\mathrm{ac}} T_{\mathrm{a}}}{\sin(\pi f_{\mathrm{ac}} T_{\mathrm{a}})} \tag{10.9}$$

The frequencies of the source, f_{ac}, can be measured using a 10 MHz reference with a negligible uncertainty. It is assumed that the error on T_{a} comes from the error on the DAC internal time reference that needs to be evaluated. The K correction is applied using the measured T_{a} in the equation. C_{alg}. This component can be obtained processing simulated ideal signals by the used algorithms.

10.10 Selected biography

Applications of PJVS

- [10]: A quantum waveform synthesizer directly traceable to the PJVS is described. An NPL designed differential amplifier is used to measure the differences between the PJVS and the synthesizer.
- [80]: This paper describe a method to precisely tune the PJVS bias parameters to produce an AC standard source that can directly synthesize voltage with quantum accuracy. The PJVS is used for the ADC characterization. The corrected ADC is used to tune the parameters. Uncertainties of $0.8\,\mu\mathrm{V\,V}^{-1}$ for 1.2 V RMS amplitude at 1 kHz are reported.

- [61]: In this paper an ac waveform is compared with a PJVS using differential measurement principle. The method has been verified up to 7 V RMS in the frequency range from 50 Hz to 1 kHz, uncertainties are in the order of $1.7\,\mu V\,V^{-1}$.
- [81]: This papers describes the use of a PJVS to obtain the integral nonlinearity of a DAC.
- [82]: A PJVS is used to investigate the influence of device setting of a 3458A Digital multimeter. Influence of delay Time, Aperture time at 53 Hz and at DC, and variation of number of samples per period.
- [83]: A PJVS is used to evaluate, noise performance, step response and integral non linearity of three ADC. The device under test are the NI 5922, NI 4461 from National Instruments and NPL 7767 designed by NPL.
- [84]: A PJVS from 11 Hz to 400 Hz is sued to evaluate RMS values, gain variation with aperture time, Hysteresis, and Nonlinearities of a 3458A.

Applications of JAWS

The JAWS is well described on previous chapters of this guide. The following references describes the evaluation and compensation of the main limitation of this system. The influence of the cables leads over the output of the JAWS.

- [35]: In this paper the reflected wave theory is used to evaluate the lead effect and compensate it by the use of impedance matching. The method is used for device under test with high input impedance. Using this method the uncertainty of the ac quantum source is in the order of 0.5 ppm ppm at 100 kHz.
- [85]: In this paper the effect of the cables is evaluated by comparing the AC-DC difference between two thermal voltage converters with and without the ACJVS wiring connected in between.

Chapter 11

Calibration of thermal converters, voltmeters and AC sources

GUM

11.1 Principles of AC/DC converters

AC/DC converters allows the traceability between AC and DC voltage standards. To precisely provide such transfer the thermal method is used. This concept is the comparison of two voltages: AC RMS and DC. The Input voltage is converted to the nonelectrical quantity such as temperature. It causes the induction of the output electrical quantity such as thermoelectric force or the current of emitter in transistor. The following diagram (see Figure 11.1) illustrates the principle of such measurement.

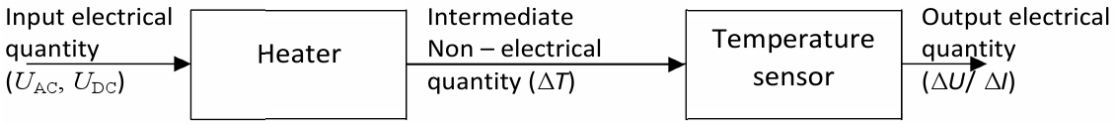

Figure 11.1: Principles of TVC operation.

From the measurement point of view the most important parameter of the thermal voltage converters is AC/DC transfer difference which is given by equation:

$$\sigma_{\text{AC-DC}}(f) = \frac{U_{\text{AC}} - U_{\text{DC}}}{U_{\text{DC}}}, \text{ for } E_{\text{AC}} = E_{\text{DC}} \tag{11.1}$$

$\sigma_{\text{AC-DC}}(f)$ – the transfer difference, U_{AC} – the RMS value of the converter AC input voltage, U_{DC} – the value of the converter's DC input voltage, E_{AC} – the converter output voltage at the AC input signal, E_{DC} – the converter output voltage at the DC input signal.

11.1.1 Single Junction Thermal Voltage Converters (SJTVC)

This is the oldest one and still used AC/DC converter. In the single junction TVC resistance wire under input voltage heats up insulated thermocouple. Heater wire, thermocouple and leads are placed in vacuum glass bulb (see Figures 11.2 and 11.3).

Figure 11.2: Single-junction TVC. Left: schematics, right: photograph.

Under the nominal current heater temperature raises up to about 150 °C. It can cause approx. 7 mV thermal EMF thermocouple junction. Such low voltage is difficult to measure precisely. This kind of the thermal converter is characterized by the quasi quadratic function of the output voltage given by:

$$E = cV_{\mathrm{I}}^{n} \tag{11.2}$$

where c – proportional coefficient, V_{I} – input voltage, n – transfer function exponent ($n \approx 1.7 \div 2$)

Therefore, it practically limits the use of SJTVC with a voltage of less than 50 % of its nominal input value. This type of the voltage converter is sensitive to input overvoltage. Using higher values of the input voltage than its nominal value the converter can be damaged as a result of overheating and burning resistance wire.

11.1.2 Multi Junction Thermal Voltage Converters (MJTVC)

Unlike single-junction TVCs, MJTVC converters contain multiple thermocouples in series. The main advantage of such devices is higher output signal which can be measured more easily and precisely. The output thermoelectrical voltage typically is about 90 mV. It can be manufactured in traditional glass bulb. Currently multi-junction converters are also produced in planar form, using semiconductor fabrication processes and micromachining techniques. Such TVCs have planar or thin-film form on substrate material like silicon or quartz crystal.

11.1.3 Semiconductor TVC

It can be manufactured in the form of two monolithic integrated circuit boards. They are placed in a vacuum casing for thermal insulation. With the bipolar transistor integrated circuit consists diffusion resistor as a heater. Both converter boards are connected to the differential amplifier. The advantage of such setup is elimination of the temperature influence. Another benefits of semiconductor TVC are higher sensitivity and time stability. For example Fluke 792A or Fluke 5790A (Figure 11.4). Using Semiconductor TVC is easier to operate because the higher output voltage (about 2 V) at the nominal input voltage. Another difference in this type of converters is linear output voltage characteristics. Unlike junction thermal converters it has overload protection. Semiconductor converters typically operates using battery power.

Figure 11.3: Holt model 11 SJTVCs.

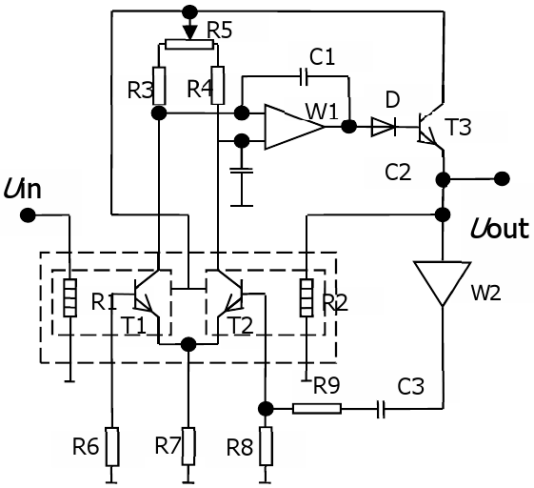

Figure 11.4: Semiconductor TVC Fluke 792A. Left: photo, right: schematics.

11.2 Measurement system of the thermal converter based AC voltage standard

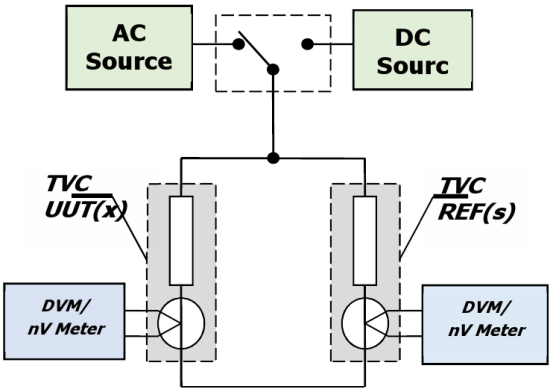

Figure 11.5: Schematic diagram of an AC-DC difference comparator system.

11.2.1 AC/DC converters

Practically AC/DC converters are enclosed in electrostatically screened chassis. Additional resistor is connected to thermal converter for current adjustment. Typical to connect converters type N or General Radio GR874 connectors are used with coaxial cables. Wrapping wires around ferrite ring favors better performance.

11.2.2 Voltmeters

The best performance of the measurement could be obtained by using nanovoltmeters. Currently, industry standard is the choice between Keithley 2182 and Keysight (formerly Agilent) 34420A. Instead nanovoltmeters reference 8½ digits voltmeters like Fluke 8508A of Keysight 3458A can be used.

11.2.3 Voltage sources

The High accuracy multifunction calibrators such Fluke 5720 can be used as the AC and DC source. As DC source can be used semiconductor voltage reference Fluke 732B.

11.2.4 AC/DC switching and timing

AC/DC switching have significant role in measurement process. Best performance can be obtained using reliable switches that allows to switch as quickly as possible and have negligible influence on frequency response of thermal converter. It is necessary to maintain an appropriate sequence of measurements (for example: AC, DC+, AC, DC−, AC). It is important DC voltage should be applied to converter in both polarities. It minimizes reversion error.

After applying DC voltage in both polarities input is switched to AC. Typically after switching settle time between 30 and 90 seconds is needed. It is necessary because resistance wire needs time to heat up and to be stabilized. From the practical point of view twelve measurements in series gives the best

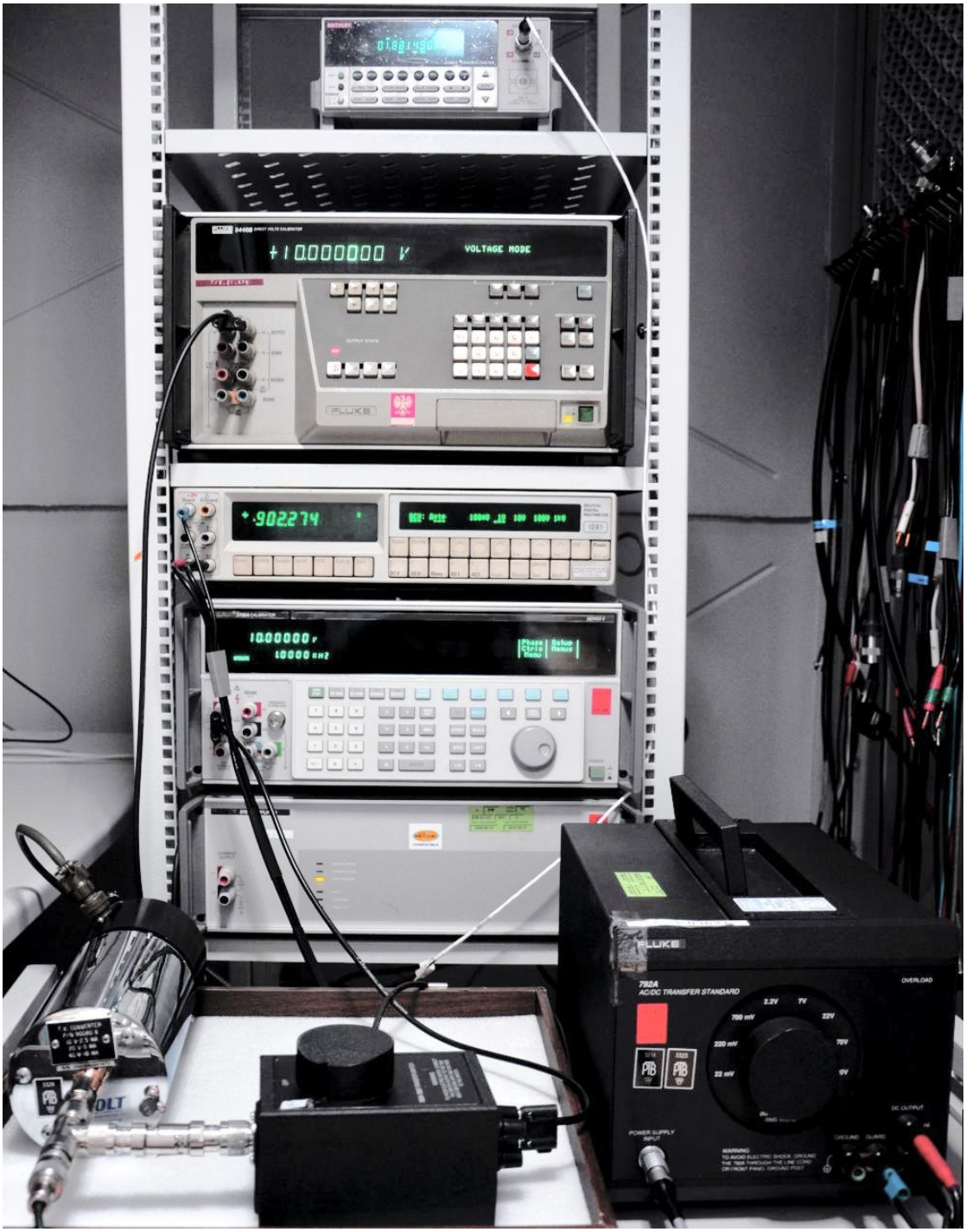

Figure 11.6: AC-DC difference comparator system placed in GUM. The measuring station consists: DC voltage sources FLUKE 5440B calibrator, AC voltage sources FLUKE 5720A/5700A calibrator, Keithley 2182A nanovoltmeter, AC-DC Voltage Tee, reference converter HOLT model 11, UUT Fluke 792A.

Figure 11.7: Left: male (upper) and female (lower) N connector. Right: GR874 hermaphroditic connector.

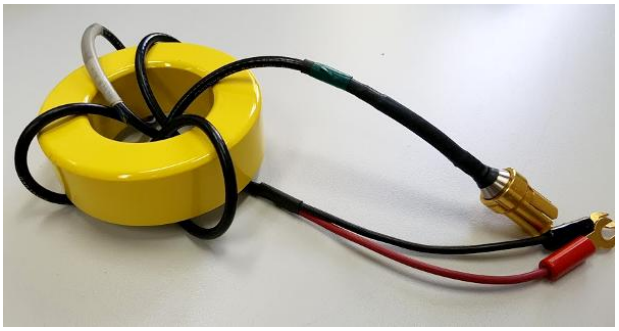

Figure 11.8: Connection wires wounded around ferrite choke toroidal core.

Figure 11.9: AC-DC Voltage Tee used in difference comparator system.

trade-off between time of measurement and accuracy. Typical one series of measurements time is about 40 minutes.

11.3 Comparison of thermal voltage converters

Possession of voltage thermal converters with known AC/DC transfer difference can be used to calibration of another thermal voltage converters involving measurement system described in chapter 11.2.

11.3.1 Comparison principle

To compare thermal voltage converters to channel method can be used. Input of reference TVC with known AC/DC transfer difference (REF) is connected to power selection switch parallel to calibrated converter (UUT). As described in chapter 11.2.4, first DC voltage is applied in positive and negative polarization and output voltage is measured for both TVCs. Its mean value is given by:

$$E_{\mathrm{DC}} = \frac{E_{\mathrm{DC+}} + E_{\mathrm{DC\text{-}}}}{2} \tag{11.3}$$

Next input voltage is switched to AC and E_{AC} output voltage is measured for REF and UUT thermal converters.

Measurement difference is given by:

$$\Delta_{\mathrm{B}} = \frac{E_{\mathrm{SAC}} - E_{\mathrm{SDC}}}{n_{\mathrm{S}} E_{\mathrm{SDC}}} - \frac{E_{\mathrm{XAC}} - E_{\mathrm{XDC}}}{n_{\mathrm{X}} E_{\mathrm{XDC}}} \tag{11.4}$$

where: E_{XAC}, E_{XDC} – value of the output voltage of the UUT converter at AC and DC input signals, E_{SAC}, E_{SDC} – value of the output voltage of the reference converter at AC and DC input signals, n_{x} – exponent of the processing function of the UUT converter, n_{s} – exponent of the processing function of the reference converter, Transfer difference measurement equation is given by:

$$\Delta_{\mathrm{X}} = \Delta_{\mathrm{B}} + \Delta_{\mathrm{A}} + \Delta_{\mathrm{S}} \tag{11.5}$$

Where: Δ_{s} – correction of the reference converter (parameter from the certificate calibration of the reference converter)

11.3.2 Sources of inaccuracies

Uncertainty of such transfer can be expressed as:

$$u^2(\Delta_{\mathrm{X}}) = u^2(\Delta_{\mathrm{B}}) + u^2(\Delta_{\mathrm{A}}) + u^2(\Delta_{\mathrm{S}}) \tag{11.6}$$

were: $u(\Delta_{\mathrm{A}})$ – uncertainty of the correction due to lack of repeatability of results, calculated using a A method, $u(\Delta_{\mathrm{S}})$ – uncertainty of the transfer difference of the standard converter (from the calibration certificate of the template), calculated using a B method, $u(\Delta_{\mathrm{B}})$ – uncertainty arising from the measurement system, calculated using a B method.

Measurement difference uncertainty is type B uncertainty and is expressed as:

$$\begin{aligned} u^2(\Delta_{\mathrm{B}}) = {} & c_1^2 u^2(E_{\mathrm{SAC}}) + c_2^2 u^2(E_{\mathrm{SDC}}) + c_3^2 u^2(n_{\mathrm{S}}) \\ & + c_4^2 u^2(E_{\mathrm{XAC}}) + c_5^2 u^2(E_{\mathrm{XDC}}) + c_6^2 u^2(n_{\mathrm{X}}) \end{aligned} \tag{11.7}$$

where $u(E)$, $u(n)$ - the uncertainty of quantity on which Δ_{B} depends, c - the corresponding sensitivity coefficients.

Sensitivity coefficients are given by:

$$c_1 = \frac{\mathrm{d}\Delta_{\mathrm{X}}}{\mathrm{d}E_{\mathrm{SAC}}} = \frac{1}{n_{\mathrm{S}} E_{\mathrm{SDC}}} \tag{11.8}$$

$$c_2 = \frac{\mathrm{d}\Delta_{\mathrm{X}}}{\mathrm{d}E_{\mathrm{SDC}}} = \frac{E_{\mathrm{SAC}}}{n_{\mathrm{S}}} \left(\frac{-1}{E_{\mathrm{SDC}}^2} \right) \tag{11.9}$$

$$c_3 = \frac{\mathrm{d}\Delta_{\mathrm{X}}}{\mathrm{d}n_{\mathrm{S}}} = \frac{E_{\mathrm{SAC}} - E_{\mathrm{SDC}}}{E_{\mathrm{SDC}}} \left(\frac{1}{n_{\mathrm{S}}^2} \right) \tag{11.10}$$

$$c_4 = \frac{\mathrm{d}\Delta_{\mathrm{X}}}{\mathrm{d}E_{\mathrm{XAC}}} = \frac{1}{n_{\mathrm{X}} E_{\mathrm{XDC}}} \tag{11.11}$$

$$c_5 = \frac{\mathrm{d}\Delta_{\mathrm{X}}}{\mathrm{d}E_{\mathrm{XDC}}} = \frac{E_{\mathrm{XAC}}}{n_{\mathrm{X}}} \left(\frac{-1}{E_{\mathrm{XDC}}^2} \right) \tag{11.12}$$

$$c_6 = \frac{\mathrm{d}\Delta_{\mathrm{X}}}{\mathrm{d}n_{\mathrm{X}}} = \frac{E_{\mathrm{XAC}} - E_{\mathrm{XDC}}}{E_{\mathrm{XDC}}} \left(\frac{1}{n_{\mathrm{X}}^2} \right) \tag{11.13}$$

11.4 Literature

Most important references for this chapter are [86]–[95].

Chapter 12

Software

CMI

12.1 Array characterisation and optimisation

Biasing the segment in the middle of the step maximises operating margins during measurement. Because each segment of the array has slightly different step width for different quantum number, the task is to find out step width and middle of the step for every segment. The characterisation can be done by measuring I-V curve of particular segment with microwave power on. Next a flat part of the step and middle points has to be identified. Because step width can change for different temperature, it is beneficial to characterise array often [96].

12.2 Binary array waveform synthesis

To generate a waveform using PJVS, one have to convert the required waveform into step waveform and for every step a quantum numbers have to be found for each segment, see figure 12.1. The sum of quantum numbers of all segments Q have to be equal (or as near as possible) to $VK_{\text{J-90}}/f$. This can be done in two ways: binary or ternary. Binary means only -1 or $+1$ quantum states of Josephson junctions are used. Ternary means -1, 0, $+1$ quantum states are used. Usually Josephson junctions on the array are divided into segments according powers of 2 series. Thus finding which segments will be used is analogous to converting Q to binary number. It gets complicated because on particular chips some segments can be faulty and cannot be used. Generally this is Subset sum problem (special case of Knapsack problem). The problem is NP-complete. This problem was solved many times and is easy to find out algorithms in literature [97].

12.3 Binary array waveform synthesis – source voltages

A segment is biased to specified quantum number by a bias current. The current is usually produced by a voltage source loaded by the resistance of the connecting cable and the segment. The segment voltage U_{s_n} that have to be applied to a segment n to get a proper current I_{b_n} to obtain quantum state $+1$ can be calculated as:

$$I_n = I_{\text{b}_n} - I_{\text{b}_{n+1}} U_{\text{s}_n} = I_n(R_n + R_{\text{l}_n}) + (U_0 + \cdots + U_n) + I_0 R_{\text{Lo}} \tag{12.1}$$

where R_n is output resistance of source channel n, R_n is the resistance of the connecting cable of channel n on the high potential wire, R_{Lo} is the resistance of the connecting cable at low potential side of chip, U_n and I_{b_n} are the voltage and bias current of segment n.

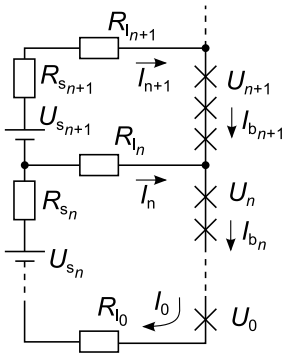

Figure 12.1: Scheme of bias currents flowing in PJVS chip.

12.4 Null detector data collection and processing

Due to number of measured points, data have to be streamed from null detector. This is easy when using digitizers with proper drivers (as National Instruments 5922). When Hewlett Packard/Agilent/Keysight 3458 is used as null detector, proper settings have to be found. The very detailed and best source for informations on this topic is [98]. The book contains full examples for short and long term sampling. A PC-GPIB interface dedicated only for reading data from 3458 should be used to prevent loss of data or synchronization.

The null detector is used to measure only small voltage difference, thus simple correction of offset and gain should sufficient.

12.5 Device control

Large number of devices have to be controlled for PJVS operation. The key to keep software viable and sustainable is to have the software hardware agnostic and modular. This can be achieved to use a hardware abstraction layer between device drivers and core part of software. This will help also to easily add new types of devices into existing software.

12.6 System control, automated measurements and calibrations

The efficient way to keep software simple and easy to maintain is to keep it modular. It means the basic tasks are identified and a measurement is composed of these tasks. In CMI we found the best way is to use a simple excel file with list of measurement points for automated measurements. The software reads every row, sets properties defined in columns and makes a reading.

12.7 Interoperability of software components

The similar case as for hardware, the best way to keep small dependence on other software is by using abstraction layers. For example report can be sent to Microsoft Word or a simple text file. If abstraction layer has defined inputs, it is easy to replace a function writing to report to a Word with a function writing a report to a text file.

12.8 Data storage: content and format

Two kinds of data can be identified in measurement software: 1, samples: typically large volume data of single data type; 2, properties: typically small data with various data types. Due to size, it is usually needed to save samples as binary data. Contrary the properties of measurement, settings etc. can and should be saved as human readable data (INI, YAML etc.) for easy review by users and debugging. It is advantageous to store not only results but all possible data related to the measurement thus any time in the future results can be reviewed, recalculated or analysed using different method.

12.9 Data analysis, measurement parameters, measurement uncertainty

An algorithm have to be applied to obtain quantities (amplitude, frequency, signal spectrum) from sampled data. Useful algorithms can be found in [77].

The errors one have to compensate comes mostly from the stepwise generated waveform [69] and the null meter. Number of steps per period of the waveform determines width of the flat part of the single step. For smaller number of steps the null meter have to measure larger differences, however number of samples in one step is higher.

If the PJVS is used to generate step waveform and null meter measures difference between PJVS and DUT, a signal of DUT cannot be fully reconstructed because of the dead time when PJVS is transitioning to a new step. This is the same as applying series of rectangular (box car) filters to a signal. The impulse response of such a filter is sinc function. However one can suppose the signal of the DUT is repeating and the waveform can be reconstructed by measuring two periods. In the second period the phase of the PJVS stepwise waveform is shifted thus the flat part of the steps covers the parts of waveform where the transition occurred previously.

The quantum standard can be used to measure quantity repeatedly. A view on the noise and stability can be obtained using (overlapped) Allan deviation for different observation times (for good example on the use see [99]). Thus a best number of measurement repetitions can be estimated and lowest uncertainty obtained.

Bibliography

[1] S. P. Benz and C. A. Hamilton, "Application of the josephson effect to voltage metrology," *Proceedings of the IEEE*, vol. 92, no. 10, pp. 1617–1629, Oct. 2004, ISSN: 0018-9219. DOI: 10.1109/JPROC.2004.833671.

[2] J. Kohlmann, R. Behr, and T. Funck, "Josephson voltage standards," *Measurement Science and Technology*, vol. 14, no. 8, p. 1216, 2003. [Online]. Available: http://stacks.iop.org/0957-0233/14/i=8/a=305.

[3] B. Jeanneret and S. P. Benz, "Application of the josephson effect in electrical metrology," *The European Physical Journal Special Topics*, vol. 172, no. 1, pp. 181–206, Jun. 1, 2009, ISSN: 1951-6401. DOI: 10.1140/epjst/e2009-01050-6. [Online]. Available: https://doi.org/10.1140/epjst/e2009-01050-6.

[4] R. Behr, J. M. Williams, P. Patel, T. J. B. M. Janssen, T. Funck, and M. Klonz, "Synthesis of precision waveforms using a sinis josephson junction array," *IEEE Transactions on Instrumentation and Measurement*, vol. 54, no. 2, pp. 612–615, Apr. 2005, ISSN: 0018-9456. DOI: 10.1109/TIM.2004.843084.

[5] S. P. Benz and C. A. Hamilton, "A pulse-driven programmable josephson voltage standard," *Applied Physics Letters*, vol. 68, no. 22, pp. 3171–3173, 1996. DOI: 10.1063/1.115814. eprint: http://dx.doi.org/10.1063/1.115814. [Online]. Available: http://dx.doi.org/10.1063/1.115814.

[6] C. A. Hamilton, C. J. Burroughs, S. L. Kupferman, G. A. Naujoks, and A. Vickery, "A compact transportable josephson voltage standard," *IEEE Transactions on Instrumentation and Measurement*, vol. 46, no. 2, pp. 237–241, Apr. 1997, ISSN: 0018-9456. DOI: 10.1109/19.571821.

[7] M. Schubert, G. Wende, T. May, L. Fritzsch, and H.-G. Meyer, "A new microwave circuit and a new cryoprobe for josephson voltage standards," *Superconductor Science and Technology*, vol. 15, no. 1, p. 116, 2002. [Online]. Available: http://stacks.iop.org/0953-2048/15/i=1/a=320.

[8] P. Kleinschmidt, P. D. Patel, J. M. Williams, and T. J. B. M. Janssen, "Investigation of binary josephson arrays for arbitrary waveform synthesis," *IEE Proceedings - Science, Measurement and Technology*, vol. 149, no. 6, pp. 313–319, Nov. 2002, ISSN: 1350-2344. DOI: 10.1049/ip-smt:20020759.

[9] J. M. Williams, D. Henderson, P. Patel, R. Behr, and L. Palafox, "Achieving sub-100-ns switching of programmable josephson arrays," *IEEE Transactions on Instrumentation and Measurement*, vol. 56, no. 2, pp. 651–654, Apr. 2007, ISSN: 0018-9456. DOI: 10.1109/TIM.2007.891155.

[10] J. M. Williams, D. Henderson, J. Pickering, R. Behr, F. Muller, and P. Scheibenreiter, "Quantum-referenced voltage waveform synthesiser," *IET Science, Measurement Technology*, vol. 5, no. 5, pp. 163–174, Sep. 2011, ISSN: 1751-8822. DOI: 10.1049/iet-smt.2010.0168.

[11] S. Benz, C. Hamilton, C. J. Burroughs, T. Harvey, L. Christian, and J. Przybysz, "Pulse-driven Josephson digital/analog converter," *IEEE Transactions on Appiled Superconductivity*, vol. 8, no. 2, pp. 42–47, Jun. 1998, ISSN: 10518223. [Online]. Available: http://ieeexplore.ieee.org/xpl/articleDetails.jsp?tp=&arnumber=678440&contentType=Journals+&+Magazines&refinements=4291944246&sortType=desc_p_Citation_Count&ranges=1990_2012_p_Publication_Year&queryText=AC+Josephson+Voltage+Standard.

[12] S. P. Benz, S. B. Waltman, A. E. Fox, P. D. Dresselhaus, A. Rüfenacht, L. Howe, R. E. Schwall, and N. E. Flowers-Jacobs, "Performance Improvements for the NIST 1 V Josephson Arbitrary Waveform Synthesizer," *IEEE Transactions on Applied Superconductivity*, vol. 25, no. 3, pp. 1–5, Jun. 2015, ISSN: 1051-8223. DOI: 10.1109/TASC.2014.2364137.

[13] O. F. Kieler, R. Behr, R. Wendisch, S. Bauer, L. Palafox, and J. Kohlmann, "Towards a 1 V Josephson Arbitrary Waveform Synthesizer," *IEEE Transactions on Applied Superconductivity*, vol. 25, no. 3, pp. 1–5, Jun. 2015, ISSN: 1051-8223. DOI: 10.1109/TASC.2014.2366916.

[14] N. E. Flowers-Jacobs, A. E. Fox, P. D. Dresselhaus, R. E. Schwall, and S. P. Benz, "Two-volt josephson arbitrary waveform synthesizer using wilkinson dividers," *IEEE Transactions on Applied Superconductivity*, vol. 26, no. 6, pp. 1–7, Sep. 2016, ISSN: 1051-8223. DOI: 10.1109/TASC.2016.2532798.

[15] N. E. Flowers-Jacobs, S. B. Waltman, A. E. Fox, P. D. Dresselhaus, and S. P. Benz, "Josephson Arbitrary Waveform Synthesizer With Two Layers of Wilkinson Dividers and an FIR Filter," *IEEE Transactions on Applied Superconductivity*, vol. 26, no. 6, pp. 1–7, Sep. 2016, ISSN: 1051-8223. DOI: 10.1109/TASC.2016.2582800.

[16] S. Benz, C. J. Burroughs, P. D. Dresselhaus, N. Bergren, T. Lipe, J. Kinard, and Y.-h. Tang, "An AC Josephson Voltage Standard for AC–DC Transfer-Standard Measurements," *IEEE Transactions on Instrumentation and Measurement*, vol. 56, no. 2, pp. 239–243, Apr. 2007, ISSN: 0018-9456. DOI: 10.1109/TIM.2007.891153. [Online]. Available: http://ieeexplore.ieee.org/xpl/articleDetails.jsp?tp=&arnumber=4126830&contentType=Journals+&+Magazines&refinements=4291944246&sortType=desc_p_Citation_Count&ranges=1990_2012_p_Publication_Year&pageNumber=2&queryText=AC+Josephson+Voltage+Standard%20http://ieeexplore.ieee.org/lpdocs/epic03/wrapper.htm?arnumber=4126830.

[17] S. Benz, P. D. Dresselhaus, C. J. Burroughs, and N. Bergren, "Precision Measurements Using a 300 mV Josephson Arbitrary Waveform Synthesizer," *IEEE Transactions on Applied Superconductivity*, vol. 17, no. 2, pp. 864–869, Jun. 2007, ISSN: 1051-8223. [Online]. Available: http://ieeexplore.ieee.org/xpl/articleDetails.jsp?tp=&arnumber=4277293&contentType=Journals+&+Magazines&refinements=4291944246&sortType=desc_p_Citation_Count&ranges=1990_2012_p_Publication_Year&queryText=AC+Josephson+Voltage+Standard.

[18] O. Kieler, R. Landim, S. Benz, P. D. Dresselhaus, and C. J. Burroughs, "AC–DC Transfer Standard Measurements and Generalized Compensation With the AC Josephson Voltage Standard," *IEEE Transactions on Instrumentation and Measurement*, vol. 57, no. 4, pp. 791–796, Apr. 2008, ISSN: 0018-9456. [Online]. Available: http://ieeexplore.ieee.org/xpl/articleDetails.jsp?tp=&arnumber=4429184&contentType=Journals+&+Magazines&refinements=4291944246&sortType=desc_p_Citation_Count&ranges=1990_2012_p_Publication_Year&pageNumber=2&queryText=AC+Josephson+Voltage+Standard.

[19] H. E. v. d. Brom and E. Houtzager, "Minimizing voltage lead corrections for a pulse-driven josephson voltage standard," in *CPEM 2010*, Jun. 2010, pp. 6–7. DOI: 10.1109/CPEM.2010.5544558.

[20] R. Behr, O. Kieler, J. Kohlmann, F. Müller, and L. Palafox, "Development and metrological applications of josephson arrays at ptb," *Measurement Science and Technology*, vol. 23, no. 12, p. 124 002, 2012. [Online]. Available: http://stacks.iop.org/0957-0233/23/i=12/a=124002.

[21] F. Overney, N. E. Flowers-Jacobs, B. Jeanneret, A. Rüfenacht, A. E. Fox, J. M. Underwood, A. D. Koffman, and S. P. Benz, "Josephson-based full digital bridge for high-accuracy impedance comparisons," en, *Metrologia*, vol. 53, no. 4, p. 1045, 2016, ISSN: 0026-1394. DOI: 10.1088/0026-1394/53/4/1045. [Online]. Available: http://stacks.iop.org/0026-1394/53/i=4/a=1045 (visited on 03/27/2018).

[22] S. Bauer, R. Behr, T. Hagen, O. Kieler, L. Palafox, and J. Schurr, "Implementation of an impedance bridge based on pulse-driven Josephson arrays for arbitrary impedance ratios and phase angles," in *2016 Conference on Precision Electromagnetic Measurements (CPEM 2016)*, Jul. 2016, pp. 1–2. DOI: 10.1109/CPEM.2016.7540626.

[23] S. Bauer, R. Behr, T. Hagen, O. Kieler, J. Lee, L. Palafox, and J. Schurr, "A novel two-terminal-pair pulse-driven josephson impedance bridge linking a 10 nf capacitance standard to the quantized hall resistance," *Metrologia*, vol. 54, no. 2, p. 152, 2017. [Online]. Available: http://stacks.iop.org/0026-1394/54/i=2/a=152.

[24] M. Šíra, O. Kieler, and R. Behr, "A novel method for calibration of adc using jaws," in *CPEM 2018, submitted*, Jun. 2018.

[25] O. F. Kieler, R. Behr, D. Schleussner, L. Palafox, and J. Kohlmann, "Precision Comparison of Sine Waveforms With Pulse-Driven Josephson Arrays," *IEEE Transactions on Applied Superconductivity*, vol. 23, no. 3, pp. 1 301 404–1 301 404, Jun. 2013, ISSN: 1051-8223. DOI: 10.1109/TASC.2013.2237817.

[26] R. Behr, O. Kieler, J. Lee, S. Bauer, L. Palafox, and J. Kohlmann, "Direct comparison of a 1 v josephson arbitrary waveform synthesizer and an ac quantum voltmeter," *Metrologia*, vol. 52, no. 4, p. 528, 2015. [Online]. Available: http://stacks.iop.org/0026-1394/52/i=4/a=528.

[27] P. D. Dresselhaus, M. M. Elsbury, and S. P. Benz, "Tapered Transmission Lines With Dissipative Junctions," *IEEE Transactions on Applied Superconductivity*, vol. 19, no. 3, pp. 993–998, Jun. 2009, ISSN: 1051-8223. DOI: 10.1109/TASC.2009.2019245.

[28] M. Watanabe, P. D. Dresselhaus, and S. Benz, "Resonance-Free Low-Pass Filters for the AC Josephson Voltage Standard," *IEEE Transactions on Applied Superconductivity*, vol. 16, no. 1, pp. 49–53, Mar. 2006, ISSN: 1051-8223. [Online]. Available: http://ieeexplore.ieee.org/xpl/articleDetails.jsp?tp=&arnumber=1603609&contentType=Journals+&+Magazines&refinements=4291944246&sortType=desc_p_Citation_Count&ranges=1990_2012_p_Publication_Year&pageNumber=2&queryText=AC+Josephson+Voltage+Standard.

[29] J. A. Brevik, N. E. Flowers-Jacobs, A. E. Fox, E. B. Golden, P. D. Dresselhaus, and S. P. Benz, "Josephson Arbitrary Waveform Synthesis With Multilevel Pulse Biasing," *IEEE Transactions on Applied Superconductivity*, vol. 27, no. 3, pp. 1–7, Apr. 2017, ISSN: 1051-8223. DOI: 10.1109/TASC.2017.2662708.

[30] O. F. O. Kieler, T. Scheller, and J. Kohlmann, "Cryocooler Operation of a Pulse-Driven AC Josephson Voltage Standard at PTB," en, *World Journal of Condensed Matter Physics*, vol. 03, no. 04, p. 189, Oct. 2013. DOI: 10.4236/wjcmp.2013.34031. [Online]. Available: http://www.scirp.org/journal/PaperInformation.aspx?PaperID=38949&#abstract (visited on 03/27/2018).

[31] O. F. Kieler, J. Kohlmann, and F. M?ller, "Improved design of superconductor/normal conductor/superconductor Josephson junction series arrays for an ac Josephson voltage standard," en, *Superconductor Science and Technology*, vol. 20, no. 11, S318, 2007, ISSN: 0953-2048. DOI: 10.1088/0953-2048/20/11/S04. [Online]. Available: http://stacks.iop.org/0953-2048/20/i=11/a=S04 (visited on 10/21/2016).

[32] S. Benz, C. J. Burroughs, and P. D. Dresselhaus, "AC coupling technique for Josephson waveform synthesis," *IEEE Transactions on Appiled Superconductivity*, vol. 11, no. 1, pp. 612–616, Mar. 2001, ISSN: 10518223. [Online]. Available: http://ieeexplore.ieee.org/xpl/articleDetails.jsp?tp=&arnumber=919419&contentType=Journals+&+Magazines&refinements=4291944246&sortType=desc_p_Citation_Count&ranges=1990_2012_p_Publication_Year&queryText=AC+Josephson+Voltage+Standard.

[33] R. Pinheiro Landim, S. Benz, P. D. Dresselhaus, and C. J. Burroughs, "Systematic-Error Signals in the AC Josephson Voltage Standard: Measurement and Reduction," *IEEE Transactions on Instrumentation and Measurement*, vol. 57, no. 6, pp. 1215–1220, Jun. 2008, ISSN: 0018-9456. [Online]. Available: http://ieeexplore.ieee.org/xpl/articleDetails.jsp?tp=&arnumber=4443860&contentType=Journals+&+Magazines&refinements=4291944246&sortType=desc_p_Citation_Count&ranges=1990_2012_p_Publication_Year&pageNumber=3&queryText=AC+Josephson+Voltage+Standard.

[34] P. Filipski, J. Kinard, T. Lipe, and S. Benz, "Correction of Systematic Errors Due to the Voltage Leads in an AC Josephson Voltage Standard," *IEEE Transactions on Instrumentation and Measurement*, vol. 58, no. 4, pp. 853–858, Apr. 2009, ISSN: 0018-9456. [Online]. Available: http://ieeexplore.ieee.org/xpl/articleDetails.jsp?tp=&arnumber=4685867&contentType=Journals+&+Magazines&refinements=4291944246&sortType=desc_p_Citation_Count&ranges=1990_2012_p_Publication_Year&pageNumber=3&queryText=AC+Josephson+Voltage+Standard.

[35] D. Zhao, H. E. van den Brom, and E. Houtzager, "Mitigating voltage lead errors of an AC Josephson voltage standard by impedance matching," *Measurement Science and Technology*, vol. 28, no. 9, p. 095 004, Sep. 2017, ISSN: 0957-0233, 1361-6501. DOI: 10.1088/1361-6501/aa7aba. [Online]. Available: http://stacks.iop.org/0957-0233/28/i=9/a=095004?key=crossref.c16f14d6fe7d33addcc78ea80dd9fa0a (visited on 08/18/2017).

[36] J. M. Williams, T. J. B. M. Janssen, L. Palafox, D. A. Humphreys, R. Behr, J. Kohlmann, and F. M?ller, "The simulation and measurement of the response of Josephson junctions to optoelectronically generated short pulses," en, *Superconductor Science and Technology*, vol. 17, no. 6, p. 815, 2004, ISSN: 0953-2048. DOI: 10.1088/0953-2048/17/6/014. [Online]. Available: http://stacks.iop.org/0953-2048/17/i=6/a=014 (visited on 03/27/2018).

[37] C. Urano, N. Kaneko, M. Maezawa, T. Itatani, and S. Kiryu, "Pulse driven Josephson voltage standard using modulated optical comb," en, *Journal of Physics: Conference Series*, vol. 97, no. 1, p. 012 269, 2008, ISSN: 1742-6596. DOI: 10.1088/1742-6596/97/1/012269. [Online]. Available: http://stacks.iop.org/1742-6596/97/i=1/a=012269 (visited on 03/27/2018).

[38] E. Bardalen, B. Karlsen, H. Malmbekk, O. Kieler, M. N. Akram, and P. Ohlckers, "Packaging and Demonstration of Optical-Fiber-Coupled Photodiode Array for Operation at 4 K," *IEEE Transactions on Components, Packaging and Manufacturing Technology*, vol. 7, no. 9, pp. 1395–1401, Sep. 2017, ISSN: 2156-3950. DOI: 10.1109/TCPMT.2017.2699485.

[39] J. Nissilä, T. Fordell, O. Kieler, and R. Behr, "Driving a josephson junction array with a mode-locked laser and a photodiode," in *CPEM 2018, submitted*, Jun. 2018.

[40] J. Qu, S. P. Benz, K. Coakley, H. Rogalla, W. L. Tew, R. White, K. Zhou, and Z. Zhou, "An improved electronic determination of the Boltzmann constant by Johnson noise thermometry," en, *Metrologia*, vol. 54, no. 4, p. 549, 2017, ISSN: 0026-1394. DOI: 10.1088/1681-7575/aa781e. [Online]. Available: http://stacks.iop.org/0026-1394/54/i=4/a=549 (visited on 03/27/2018).

[41] F. Overney and B. Jeanneret, *QuADC project: Cable correction and load compensation*, Euramet Expert Meeting on DC and Quantum standards, VTT, Espoo, Finland, Jun. 2017.

[42] May 30, 2018. [Online]. Available: en.wikipedia.org/wiki/Cryocooler.

[43] L. Duband and A. Ravex, "Small cryocoolers," in *Handbook of cryogenic engineering*, J. G. Weisend, Ed., Philadelphia, PA: Taylor and Francis, 1998.

[44] [Online]. Available: www.shicryogenics.com.

[45] [Online]. Available: www.cryomech.com.

[46] May 30, 2018. [Online]. Available: http://en.wikipedia.org/wiki/Pulse_tube_refrigerator.

[47] S. Yuan, *Pulse tube coolers (cycle, engines, cryogenics refrigerators, cryocoolers)*, May 30, 2018. [Online]. Available: http://www.yutopian.com/Yuan/PT.html.

[48] R. Radebaugh, "Cryocoolers: the state of the art and recent developments," *Journal of Physics: Condensed Matter*, vol. 21, no. 16, p. 164 219, 2009. [Online]. Available: http://stacks.iop.org/0953-8984/21/i=16/a=164219.

[49] *Courtesy of A. Sosso, INRIM, Strada delle cacce 91, 10135 Torino, Italy*, May 30, 2018.

[50] [Online]. Available: www.edwardsvacuum.com.

[51] G. Ventura and L. Risegari, *The Art of Cryogenics, Low-Temperature Experimental Techniques*, English, 1st. Elsevier Science, Oct. 2007, p. 378, ISBN: 9780080444796. DOI: 10.1016/B978-0-08-044479-6.X5001-8.

[52] [Online]. Available: www.mtm-inc.com/ac-20100923-cryogenic-thermometers-ndash-an-introduction.html.

[53] S. S. Courts and P. R. Swinehart, "Review of cernox^{TM} (zirconium oxy-nitride) thin-film resistance temperature sensors," *AIP Conference Proceedings*, vol. 684, no. 1, pp. 393–398, 2003. DOI: 10.1063/1.1627157. eprint: https://aip.scitation.org/doi/pdf/10.1063/1.1627157. [Online]. Available: https://aip.scitation.org/doi/abs/10.1063/1.1627157.

[54] [Online]. Available: www.lakeshore.com/Products/Cryogenic-Temperature-Sensors/Pages/default.aspx.

[55] [Online]. Available: http://blog.opticontrols.com.

[56] [Online]. Available: https://www.lakeshore.com/Documents/LSTC_appendixI_1.pdf.

[57] G. K. White and P. J. Meeson, *Experimental Techniques in Low-Temperature Physics*, English, 4th. Clarendon: Oxford Science Publications, Apr. 25, 2002, p. 296, ISBN: 9780198514275.

[58] F. Pobell, *Matter and Methods at Low Temperatures*, English, 3rd. Springer-Verlag Berlin Heidelberg, 2007, p. 461, ISBN: 978-3-540-46360-3. DOI: 10.1007/978-3-540-46360-3.

[59] [Online]. Available: www.lakeshore.com.

[60] [Online]. Available: www.cryospares.de.

[61] J. Lee, R. Behr, L. Palafox, A. Katkov, M. Schubert, M. Starkloff, and A. C. Böck, "An ac quantum voltmeter based on a 10 V programmable josephson array," *Metrologia*, vol. 50, no. 6, p. 612, 2013. [Online]. Available: http://stacks.iop.org/0026-1394/50/i=6/a=612.

[62] A. Rüfenacht, C. J. Burroughs, P. D. Dresselhaus, and S. P. Benz, "Differential sampling measurement of a 7 v rms sine wave with a programmable josephson voltage standard," *IEEE Transactions on Instrumentation and Measurement*, vol. 62, no. 6, pp. 1587–1593, Jun. 2013, ISSN: 0018-9456. DOI: 10.1109/TIM.2013.2237993.

[63] A. Rüfenacht, C. J. Burroughs, S. P. Benz, P. D. Dresselhaus, B. C. Waltrip, and T. L. Nelson, "Precision differential sampling measurements of low-frequency synthesized sine waves with an ac programmable josephson voltage standard," *IEEE Transactions on Instrumentation and Measurement*, vol. 58, no. 4, pp. 809–815, Apr. 2009, ISSN: 0018-9456. DOI: 10.1109/TIM.2008.2008087.

[64] IEEE Instrumentation and Measurement Society, Waveform Measurements and Analysis Committee, Institute of Electrical and Electronics Engineers, and American National Standards Institute, *IEEE Standard for Digitizing Waveform Recorders*, English. New York, N.Y.: Institute of Electrical and Electronics Engineers, 2008, ISBN: 978-0-7381-5350-6 0-7381-5350-8 978-0-7381-5351-3 0-7381-5351-6.

[65] P. M. Ramos and A. C. Serra, "Least squares multiharmonic fitting: convergence improvements," *IEEE Transactions on Instrumentation and Measurement*, vol. 56, no. 4, pp. 1412–1418, Aug. 2007, ISSN: 0018-9456. DOI: 10.1109/TIM.2007.899873.

[66] M. Klonz, "Current developments in accurate AC-DC transfer measurements," *IEEE Transactions on Instrumentation and Measurement*, vol. 44, no. 2, pp. 363–366, Apr. 1995, ISSN: 0018-9456. DOI: 10.1109/19.377853.

[67] C. A. Hamilton, C. J. Burroughs, and R. L. Kautz, "Josephson d/a converter with fundamental accuracy," *IEEE Transactions on Instrumentation and Measurement*, vol. 44, no. 2, pp. 223–225, Apr. 1995, ISSN: 0018-9456. DOI: 10.1109/19.377816.

[68] C. J. Burroughs, A. Rüfenacht, S. P. Benz, P. D. Dresselhaus, B. C. Waltrip, and T. L. Nelson, "Error and transient analysis of stepwise-approximated sine waves generated by programmable josephson voltage standards," *IEEE Transactions on Instrumentation and Measurement*, vol. 57, no. 7, pp. 1322–1329, Jul. 2008, ISSN: 0018-9456. DOI: 10.1109/TIM.2008.917260.

[69] J. Lee, R. Behr, A. S. Katkov, and L. Palafox, "Modeling and Measuring Error Contributions in Stepwise Synthesized Josephson Sine Waves," *IEEE Transactions on Instrumentation and Measurement*, vol. 58, no. 4, pp. 803–808, Apr. 2009, ISSN: 0018-9456. DOI: 10.1109/TIM.2008.2011099.

[70] I. Budovsky, R. Behr, L. Palafox, S. Djordjevic, and T. Hagen, "Technique for the calibration of thermal voltage converters using a josephson waveform synthesizer and a transconductance amplifier," *Measurement Science and Technology*, vol. 23, no. 12, p. 124 005, 2012. [Online]. Available: http://stacks.iop.org/0957-0233/23/i=12/a=124005.

[71] O. Seron, S. Djordjevic, I. Budovsky, T. Hagen, R. Behr, and L. Palafox, "Precision AC-DC transfer measurements with a josephson waveform synthesizer and a buffer amplifier," *IEEE Transactions on Instrumentation and Measurement*, vol. 61, no. 1, pp. 198–204, Jan. 2012, ISSN: 0018-9456. DOI: 10.1109/TIM.2011.2157429.

[72] I. Budovsky and T. Hagen, "A precision buffer amplifier for low-frequency metrology applications," in *CPEM 2010*, Jun. 2010, pp. 28–29. DOI: 10.1109/CPEM.2010.5544183.

[73] I. Budovsky, D. Georgakopoulos, and T. Hagen, "System for precision ac-dc difference measurements based on a programmable josephson voltage standard," in *CPEM 2010*, Jun. 2010, pp. 50–51. DOI: 10.1109/CPEM.2010.5543405.

[74] S. P. Benz, S. B. Waltman, A. E. Fox, P. D. Dresselhaus, A. Rüfenacht, J. M. Underwood, L. A. Howe, R. E. Schwall, and C. J. Burroughs, "One-volt josephson arbitrary waveform synthesizer," *IEEE Transactions on Applied Superconductivity*, vol. 25, no. 1, pp. 1–8, Feb. 2015, ISSN: 1051-8223. DOI: 10.1109/TASC.2014.2357760.

[75] L. Palafox, R. Behr, O. Kieler, J. Lee, I. Budovsky, S. Bauer, and T. Hagen, "First metrological applications of the ptb 1 v josephson arbitrary waveform synthesizer," in *2016 Conference on Precision Electromagnetic Measurements (CPEM 2016)*, Jul. 2016, pp. 1–2. DOI: 10.1109/CPEM.2016.7540602.

[76] H. Malmbekk, C. D. Shelly, and J. M. Williams, "Calibrating a voltmeter with a PJVS using a DAC as a real-time calibrated transfer standard," in *CPEM 2018, submitted*, Jun. 2018.

[77] M. Šíra, S. Mašláň, and V. Nováková Zachovalová, "QWTB – Software Tool Box for Sampling Measurements," in *Conference on Precision Electromagnetic Measurements Digest*, Ottawa, Canada: IEEE, Jul. 2016, p. 2, ISBN: 978-1-4673-9133-7. DOI: 10.1109/CPEM.2016.7540599. [Online]. Available: http://ieeexplore.ieee.org/document/7540599/?reload=true.

[78] JCGM., *Evaluation of Measurement Data - Guide to the Expression of Uncertainty in Measurement*, JCGM, Ed. Bureau International des Poids et Measures, 1995, ISBN: 92-67-10188-9.

[79] JCGM, *Evaluation of Measurement Data - Supplement 1 to the "Guide to the Expression of Uncertainty in Measurement" - Propagation of Distributions Using a Monte Carlo Method*, JCGM, Ed. Bureau International des Poids et Measures, 2008.

[80] C. J. Burroughs, A. Rüfenacht, S. P. Benz, and P. D. Dresselhaus, "Method for Ensuring Accurate AC Waveforms With Programmable Josephson Voltage Standards," *IEEE Transactions on Instrumentation and Measurement*, vol. 62, no. 6, pp. 1627–1633, Jun. 2013, ISSN: 0018-9456. DOI: 10.1109/TIM.2013.2250192.

[81] F. Overney, A. Rüfenacht, J. P. Braun, and B. Jeanneret, "Josephson-based test bench for ac characterization of analog-to-digital converters," in *CPEM 2010*, Jun. 2010, pp. 215–216. DOI: 10.1109/CPEM.2010.5544779.

[82] H. van den Brom, E. Houtzager, S. Verhoeckx, Q. Martina, and G. Rietveld, "Influence of Sampling Voltmeter Parameters on RMS Measurements of Josephson Stepwise-Approximated Sine Waves," *IEEE Transactions on Instrumentation and Measurement*, vol. 58, no. 10, pp. 3806–3812, Oct. 2009, bibtex: vandenBrom2009, ISSN: 0018-9456. [Online]. Available: http://ieeexplore.ieee.org/xpl/articleDetails.jsp?tp=&arnumber=5232868&contentType=Journals+&+Magazines&refinements=4291944246&sortType=desc_p_Citation_Count&ranges=1990_2012_p_Publication_Year&pageNumber=4&queryText=AC+Josephson+Voltage+Standard.

[83] F. Overney, A. Rüfenacht, J. P. Braun, B. Jeanneret, and P. S. Wright, "Characterization of Metrological Grade Analog-to-Digital Converters Using a Programmable Josephson Voltage Standard," *IEEE Transactions on Instrumentation and Measurement*, vol. 60, no. 7, pp. 2172–2177, Jul. 2011, ISSN: 0018-9456. DOI: 10.1109/TIM.2011.2113950.

[84] W. K. Ihlenfeld, E. Mohns, R. Behr, J. Williams, P. Patel, G. Ramm, and H. Bachmair, "Characterization of a High-Resolution Analog-to-Digital Converter with an Ac Josephson Voltage Source," in *Precision Electromagnetic Measurements Digest, 2004 Conference on*, bibtex: Ihlenfeld2004, IEEE, 2004, pp. 662–663. [Online]. Available: http://ieeexplore.ieee.org/xpls/abs_all.jsp?arnumber=4097424 (visited on 03/09/2015).

[85] P. S. Filipski, M. Boecker, S. Benz, and C. J. Burroughs, "Experimental Determination of the Voltage Lead Error in an AC Josephson Voltage Standard," *IEEE Transactions on Instrumentation and Measurement*, vol. 60, no. 7, pp. 2387–2392, Jul. 2011, bibtex: Filipski2011, ISSN: 0018-9456. [Online]. Available: http://ieeexplore.ieee.org/xpl/articleDetails.jsp?tp=&arnumber=5727951&contentType=Journals+&+Magazines&refinements=4291944246&sortType=desc_p_Citation_Count&ranges=1990_2012_p_Publication_Year&pageNumber=3&queryText=AC+Josephson+Voltage+Standard.

[86] M. Klonz, "CCE comparison of AC-DC voltage transfer standards at the lowest attainable level of uncertainty," *IEEE Transactions on Instrumentation and Measurement*, vol. 46, no. 2, pp. 342–346, Apr. 1997, ISSN: 0018-9456. DOI: 10.1109/19.571852.

[87] H. Laiz, M. Klonz, E. Kessler, M. Kampik, and R. Lapuh, "Low-frequency AC-DC voltage transfer standards with new high-sensitivity and low-power-coefficient thin-film multijunction thermal converters," *IEEE Transactions on Instrumentation and Measurement*, vol. 52, no. 2, pp. 350–354, Apr. 2003, ISSN: 0018-9456. DOI: 10.1109/TIM.2003.810037.

[88] F. L. Hermach, "Thermal converters as AC-DC transfer standards for current and voltage measurements at audio frequencies," *Journal of Research of the National Bureau of Standards*, vol. 48, no. 2, pp. 122–138, Feb. 1952. DOI: 10.6028/jres.048.018.

[89] A. Barański and A. Podemski, "Etalon napięcia przemiennego w zakresie do 1000 V i częstotliwo ci do 100 kHz," *Przegl. Elektrotech.*, pp. 68–71, 1991.

[90] P. S. Filipski, C. J. van Mullem, D. Janik, M. Klonz, J. R. Kinard, T. E. Lipe, and B. C. Waltrip, "Comparison of high-frequency AC-DC voltage transfer standards at NRC, VSL, PTB, and NIST," *IEEE Transactions on Instrumentation and Measurement*, vol. 50, no. 2, pp. 349–352, Apr. 2001, ISSN: 0018-9456. DOI: 10.1109/19.918139.

[91] W. G. K. Ihlenfeld and E. Mohns, "Ac-dc transfer measurements of highest accuracy with synchronous analogue-to-digital conversion," *Metrologia*, vol. 41, no. 3, p. 111, 2004. [Online]. Available: http://stacks.iop.org/0026-1394/41/i=3/a=001.

[92] *EA interlaboratory comparison EL25, AC-DC voltage transfer difference, COFRAC/LCIE paris*, 2002.

[93] *792A AC/DC transfer standard instruction manual*, rev. 1 12/92.

[94] [Online]. Available: www.fluke.com.

[95] A. Barański, J. Ratajczak, and P. Zawadzki, "Przetworniki termoelektryczne AC/DC jako wzorce napięcia przemiennego," *PAK*, vol. 9bis, pp. 38–41, 2007.

[96] M. Schubert, M. Starkloff, K. Peiselt, S. Anders, R. Knipper, J. Lee, R. Behr, L. Palafox, A. C. Böck, L. Schaidhammer, P. M. Fleischmann, and H.-G. Meyer, "A dry-cooled ac quantum voltmeter," *Superconductor Science and Technology*, vol. 29, no. 10, p. 105 014, 2016. [Online]. Available: http://stacks.iop.org/0953-2048/29/i=10/a=105014.

[97] T. H. Cormen, C. E. Leiserson, R. L. Rivest, and C. Stein, *Introduction to Algorithms, 3rd Edition*, English, 3rd. Cambridge, Mass: The MIT Press, Jul. 2009, ISBN: 978-0-262-03384-8.

[98] R. Lapuh, *Sampling with 3458A*. to be published, 2018.

[99] T. Witt, "Using the Allan variance and power spectral density to characterize dc nanovoltmeters," in *Conference on Precision Electromagnetic Measurements. Conference Digest. CPEM 2000 (Cat. No.00CH37031)*, bibtex: Witt2000, vol. 50, Sydney, Australia: IEEE, Apr. 2000, pp. 667–668, ISBN: 0-7803-5744-2. DOI: 10.1109/CPEM.2000.851188. [Online]. Available: http://ieeexplore.ieee.org/lpdocs/epic03/wrapper.htm?arnumber=851188%20http://ieeexplore.ieee.org/lpdocs/epic03/wrapper.htm?arnumber=918162.

Appendices

Appendix A

Safety rules in cryogenics

INRIM, FCT

A.1 Disclaimer

These following rules *are just an indication, guidelines and examples* of some precautions to be used or implemented in laboratories dealing with cryogenics. Following these – or some of these - indications does not imply any responsibilities of the authors of this text for any damage or injuries or expenses.

A.2 Generalities

Cryogenic liquids (liquefied cryogenic gases) are defined as substances with boiling points lower than $\approx -100\,\mathrm{K}$ ($\approx -173\,^{\circ}\mathrm{C}$). These operational instructions regulate the general aspects concerning the use, transport and storage of cryogenic liquids, in this case liquid nitrogen (LN_2, boiling point $-195\,^{\circ}\mathrm{C}$) and liquid helium (LHe, boiling point $-269\,^{\circ}\mathrm{C}$), and access to the laboratories in which they are used. Regarding any other cryogenic liquids, which may involve additional safety problems compared to those covered here (explosion, fire, toxicity, etc.), the information herein must be adequately integrated.

It is the duty of the supervisors/responsibles to take care of their application and to instruct the workers according to the information, training and training methods provided. In rooms where it is necessary, additional security procedures may be applied to supplement, but not to replace, this.

A.3 Security risks

The two main risks related to safety in the presence of cryogenic liquids are:

- damage to fabrics due to freezing due to direct contact with the liquid or with its vapor;
- asphyxia in the event of spills or inadequate evaporation of liquids (The evaporation of one liter of cryogenic liquid leads to $\approx 700\,\mathrm{l}$ of gas at room temperature), or excessive condensation of atmospheric oxygen in poorly ventilated areas. In these three cases the risk is connected to the inhalation of low quantities of oxygen.

Particular attention must be paid to protecting from cryogenic liquid particularly sensitive mucous membranes and tissues or the eyes. The anesthetizing action of the cold sometimes causes frostbite without being aware of what is happening. You can then also have, important effects of cold on the lungs:

a short exposure can cause feelings of malaise, while prolonged inhalation of cold gas vapors can produce serious effects on lung tissue. It should also be remembered that in case of suffocation the event is totally asymptomatic, you do not perceive any sensation of breathlessness (which instead it is typical of an excessive concentration of CO_2).

Two other risks that should not be underestimated are:

- the embrittlement of the structures, by accidental or intentional contact, caused by a "Crystallization" or from a drop below the glass transition temperature of the materials, even the most flexible ones, at cryogenic temperatures;
- the increase of pressure in dewars or cryostat (isolated recipient used to store the cryogenic liquids in the laboratories) due to the formation of ice near the access ports or vent valves, limiting their correctness operation or even causing it to block with the risk of explosion of the dewar.

The increase in pressure can also be particularly dangerous when liquids come exposed to heat sources, this is why liquids should only be stored in specific areas designated. Explosion risks due to enrichment may also develop oxygen in particular conditions.

The low temperatures reached by cryogenic liquids require particular attention during handling, the vapor released from a liquid can cause the same problems as the liquid. The vapors of liquid helium, liquid nitrogen and liquid oxygen are also not to be underestimated because odorless and colorless and therefore imperceptible to our senses.

Events that can indicate the onset of a problem that can lead to an accident:

1. Evaporation rates of the abnormal cryogenic liquid, both too high and too low.
2. Condensation or freezing of atmospheric humidity at unusual levels in places where normally this effect should not be observed.
3. Difficulty in opening or closing valves.
4. Abnormal development of jets or steam feathers.
5. Increasing pressure in the dewar.
6. Whistles or whistles indicating the forced expulsion of quantities of cold steam significantly more high standards.

A.3.1 Levels of oxygen

The cryogenic liquids, when brought back to room temperature, are in the gaseous state, therefore, in case of evaporation they are subject to a volume expansion, in the ratio of one factor that depends on substance to substance (694 for LN_2, 750 for LHe (see section A.3.12, reference [3]), but for simplicity it is assumed to be equal to about 1000. Therefore, by evaporating, 1 liter of cryogenic liquid becomes 1000 liters ($1\ m^3$) of gas.

Evaporation of an excessive amount of cryogenic liquid can cause severe reduction of the oxygen concentration in the laboratory, and is therefore extremely dangerous.

The laboratories where large quantities of cryogenic liquids are used (see below for indications how to evaluate these quantities) must be equipped with an oxygen level monitoring system (fixed or portable). Follow the instructions given in the procedures which regulates access to premises to the armed for the risk of hypo and hyper-oxygenation tightly. In the table a following, different levels of oxygen are reported with the associated indicative effects and symptoms, which may vary from person to person and depending on individual health conditions.

% O_2 (volume)	Effects and symptoms at room pressure (see section A.3.12, ref. [4])
> 23.5	Extreme danger of combustion and fire.
20.9	Normal concentration of oxygen in the air.
19.5	Level of minimum allowable oxygen.
From 15 to 19	Reduced work capacity and concentration. Reduced motor coordination capacity Malaise. Possible loss of knowledge.
From 10 to 12	Increased breathing rhythm. Lips cyanotic. Possible loss of knowledge.
From 8 to 10	Loss of knowledge, nausea, vomit.
From 6 to 8	Possible recovery of and vital functions within 4 – 5 minutes. Probability of death close to 50 % after 6 minutes. Probability of death close to 100 % after 8 minutes.
From 4 to 6	Coma in 40 seconds, convulsions, respiratory arrest, death.

An atmospheric oxygen level of 19.5 % is considered the minimum allowable. Nobody is allowed to operate in an environment containing less oxygen. Any monitoring stations of the level of oxygen or in the rooms, or portable oxygen sensors, must have an armed level adjusted to 19.5 % or higher. Remember that in case of reduced oxygen concentration does not perceive any sensation of shortness of breath: asphyxia is therefore asymptomatic.

A.3.2 Cold burn hazards

A particular risk for the personnel using cryogenic liquids is the contact of the latter with skin and eyes. Given that these liquids are prone to splash due to the 'high ratio of expansion between the volume of liquid and that of gas when handling fluids cryogenic is mandatory to wear visors of protection for eyes and face, gloves for the low adequate temperatures and footwear. Avoid that the unprotected parts of the body come into contact with areas that are not adequately insulated or tubes containing cryogenic liquids. The low temperature of a material can provoke its firm attachment of the skin and result in a sever lesion of the skin in the "natural" attempt at fast separation. Even a very short contact of the skin and the cryogenic liquid can cause tissue damage similar to that caused by burns due to high temperatures. Prolonged contact can cause blood clots that can potentially have very serious consequences.

A.3.3 Collective protection devices

It is forbidden to introduce large quantities of cryogenic liquids in a room or in a laboratory, unless the environment is equipped for monitoring of the level of oxygen with appropriate sensors. Therefore it is necessary:

- to identify the maximum total quantity, V_{liquid} of cryogenic liquid that may be present at a given moment inside the laboratory.
- hypothesize that the entire quantity of cryogenic liquid can evaporate (due to a failure or an accident) in a short time. It is therefore necessary to multiply V_{liquid} per 1000 (factor of expansion of the cryogenic liquid when it evaporates) obtaining the total volume of gas $V_{\text{gas}} = 1000 \cdot V_{\text{liquid}}$.
- compare V_{gas} with the total volume of the V_{room} of the room.

One can then apply the following table (the number in parentheses are calculated for a laboratory of $\approx 250\,\text{m}^3$, for instance $50\,\text{m}^2$ and $5\,\text{m}$ high):

$V_{\text{liquid}}/V_{\text{room}}$	$V_{\text{gas}}/V_{\text{room}}$	Action
< 0.00007 ($< 20\,\text{l}$)	< 0.07 ($< 20\,\text{m}^3$)	No action required
$0.00007 < 0.00028$ ($20\,\text{l} < 80\,\text{l}$)	$0.07 < 0.28$ ($20\,\text{m}^3 << 80\,\text{m}^3$)	Laboratory must be provided with oxygen sensors and monitor unit or All workers must be provided with a portable oxygen sensor
≥ 0.00028 ($\geq 80\,\text{l}$) (Dewars with $100\,\text{l}$ and more are frequent)	≥ 0.28 ($\geq 320\,\text{m}^3$)	Laboratory must be provided with oxygen sensors and monitor unit.

Laboratories equipped with oxygen sensors and monitoring unit for the use of portable oxygen sensors must be equipped with a special safety procedure that regulates access to the premises. It will be the responsibility of the person in charge to request ordinary maintenance or extraordinary oxygen detection system or portable sensors according to the indications supplied by the manufacturer and reported in the user and maintenance manual, taking into account the status of plant efficiency, number of working hours, etc.

If it is deemed opportune, in the face of a careful evaluation process, the control units of oxygen level monitoring can automatically activate, in case of alarm, a forced extraction system that expels the oxygen-impoverished atmosphere and forces its replacement with air taken from outside the laboratory.

The positioning of permanent oxygen sensors must be chosen based on the location of the dewar, containers, tanks and cryostats, and of the cryogenic liquid used. Remember that liquid nitrogen vapors are heavier than air, therefore in a laboratory where it is used only liquid nitrogen the oxygen sensors will be positioned at little distance from the floor ($50\,\text{cm}$ to $70\,\text{cm}$ from the ground). Instead, the liquid helium vapors are lighter than air, so in a laboratory where only liquid helium is used the sensors of oxygen will be placed a short distance from the ceiling ($10\,\text{cm}$ to $30\,\text{cm}$ from the ceiling, provided that there are no aeration devices that could distort the sensor reading).

If both cryogenic liquids are used, the sensors should be placed approximately at a height corresponding to the head of people or, if possible, install two sets of sensors, one near the floor and the other near the ceiling.

On the other hand, portable oxygen sensors, if they have been chosen, in the case described above, in alternative to sensors with relative oxygen monitoring unit, they must always be worn from all the workers present in the laboratory.

A.3.4 Clothing and personal protective equipment

Depending on the use made of the liquid cryogenic, of the type of tank or dewar, and the risk of contact with the liquid, with its own spray or with its vapor, the use of one or more devices below listed is necessary for personal protection. Regardless of the need to wear one or more protection devices, when cryogenics liquid have to be manipulated is mandatory to stick to some rules concerning clothing. In particular, clothing must be worn covering the upper and lower limbs and closed shoes. The use of t-shirts or shirts with short sleeves, trousers or skirts that leave discovered part of the legs, or sandals is not permitted.

Personal protection for cryogenics:

Gloves

The cryogenic gloves (EN 511) are thermally insulated and waterproof. They are equipped of long sleeves covering most of the forearm. They do not allow immersion of the hand in LHe, and allow it and in LN_2

only for very short times. Are therefore prohibited the operations, routine or exceptional, that involve the immersion of the hand in LHe and from limit only those in LN_2 to exceptional cases. The gloves allow you to touch cold objects come in contact with cryogenic liquids or stay in contact with them for some time vapors. However, when you start feeling cold or you feel the glove becomes stiff, remove immediately from the cold side and remove the gloves, which they must be able to slip out easily even just by shaking the arm to the floor.

Visor

The visor protects the face and eyes from both splashes and cold vapor. It must cover the face well. For all the devices listed above, the worker must scrupulously observe the indications of use indicated in the respective manuals. It will be the responsibility of the person in charge of laboratory deliver personal protective equipment, using the appropriate forms and carry out information, training and possibly training for use.

A.3.5 Rules of conduct for the use of cryogenic liquids

Use only containers designed and certified specifically for the required use. It is forbidden the use of inadequate containers such as pots, bottles, polystyrene foam trays, etc. that are not expressly designed to contain cryogenic liquids of the type employed.

The operator must always wear gloves, visor, apron, protective overshoes supplied in the laboratory, in accordance with this safety procedure and with any specific safety procedures for the laboratory or activity.

When loading a "hot" container, stay away from liquids that evaporate or leak out and from the gas that develops. Proceed slowly with the filling process in order to limit the increase of pressure or splashes.

The operator must work interposing between the cryogenic liquid container and the escape route, that should not be obstructed. The safety or vent valves of cryogenic liquid containers must point towards areas that are not passing through. It is forbidden to pass or stop along their direction drain.

Make sure that the transfer tubes are in the correct use conditions: if they are double wall, must have insulation according to specifications and no obvious damage that can put the operator at risk during the transfer process.

Make sure that any vacuum insulation systems of the transfer pipes (cavities, insulation jackets, etc.) or cryogenic liquid containers are efficient, checking the vacuum level and, if necessary, restore it with appropriate pumping.

If it is necessary to pressurize a container for cryogenic liquids, always leave it open with at least one pressure relief valve and in any case keep this container within the overpressure limit indicated by the container manufacturer. The explosion or implosion of a cryogenic container is one of the more dangerous accident caused by cryogenics liquids.

A.3.6 Transfer of cryogenic liquids

Do not transfer liquefied gas from one container to another for the first time without direct supervision and instructions of someone who has already done this operation. If the racking is done without the special "transfer tube", or to an open container, it must be carried out very slowly (especially at the beginning) to minimize boiling and splashing.

As a rule, the transfer of cryogenic liquids from one container to another is carried out by pressurizing slightly the starting dewar (refer to the specific procedures for each laboratory or to the manual of the equipment in use for any precise pressure indications required), using the vapors of the same cryogenic liquid, or an external source of gas thereof type (gaseous helium for LHe, gaseous nitrogen for LN_2). It is possible to use gaseous helium for pressurize dewar of LN_2, while it is impossible to use gaseous nitrogen

to pressurize dewar of LHe in terms of the temperature of LHe and nitrogen solidifies, therefore pay close attention to the indications of gas recognition available to the laboratory, especially when these they are provided through specific lines. The use of compressed air to pressurize is prohibited for dewars of both LN_2 and LHe, as the oxygen present in the air would become liquid going to constitute a mixture at risk of explosion and fire.

The slight overpressure of the starting dewar allows the cryogenic liquid to be poured into the destination dewar (a real dewar or a cryostat that constitutes the measurement or temperature control system), through the transfer tube, that is specifically designed for this kind of operations. Transfer tubes differ between LHe (have a vacuum insulation jacket) and LN_2 (they are usually shirtless isolation and more flexible), and should not be exchanged between them. Only where expressly indicated from the manufacturer, a transfer tube can be used interchangeably for both types of cryogenic liquid (typically an insulated tube suitable for LHe is also suitable for LN_2 but not the other way around).

During the operations of decanting of cryogenic liquids, the oxygen can be liquefied from the air to contact with cold surfaces. Drops of liquid air usually seep from pipes, joints, valves are usually visible or cold fillets during pouring operations. These drops are extremely rich in oxygen (about 50 %), and therefore present a high risk of fire or explosion. It must therefore be payed the utmost attention so that these drops cannot run on possible ignition sources (hot materials, live electrical conductors, etc.), or on materials easily flammable (including vacuum seals or greases or oils used for lubrication or sealing).

For the LHe, the use of suitable transfer tubes is mandatory and is the only permitted way to transfer the cryogenic liquid. In fact, liquid helium has a very low latent heat of evaporation, and just 1 W of power is enough to evaporate 1.4 liter of liquid helium per hour. On the contrary, it has a high enthalpy, so it takes a lot of energy to heat the steam.

Therefore, it is mandatory to use transfer pipes specifically designed for the transfer they offer adequate forms of thermal insulation towards the outside. Both the starting and the destination dewar must not allow accidental contact with the cryogenic liquid, or expose it to air. The starting dewar, in order to be pressurized, must have the air valves intercepted, except for the valves security, which by design are not interceptable and which absolutely must not be tampered with. The safety valves are designed to avoid pressures higher than those necessary for decanting, therefore they do not interfere with the transfer operations.

For LN_2 the use of suitable transfer tubes is strongly recommended, but in circumstances particular other means for transferring the cryogenic liquid may be permitted. In particular, it is possible to use different tubes (for example in polymer), provided the pressures to which it is transferred the cryogenic liquid is very low. In fact, these pipes must be previously tested to insure that the passage of liquid nitrogen does not lead to its break that can result in a jet of liquid cryogenic very dangerous. One must also pay attention to the fact that it could be created enrichment of oxygen near the tube, with consequent risk of fire or explosion.

It is also possible to transfer LN_2 from non-pressurized containers by simple deposit or fall, provided that weight and encumbrance of the starting container allow an easy handling, and also towards open containers, provided they are stable and have sufficient mouth large enough to avoid the risk of spilling outwards or toppling over the container.

In these cases it is mandatory to wear all the protective devices indicated above, proceed with extreme caution, and make sure that the flow of LN_2, in case of accidental leakage, does not affect any person. When transferring LN_2 for deposit, the quantities involved must be obligatorily very reduced, also to avoid the accumulation of liquid oxygen in the mixture, with consequent risks of fire and explosion.

Normally, it is mandatory that the operations of decanting of cryogenic liquid be controlled by expert personnel during their entire operation; indicatively, the presence of at least two people, of which at least one expert. This is to intervene promptly in case of malfunctions, breakdowns, leaks, spills, sprays, or to stop the transfer if the recipient of the destination is no longer able to receive further liquid.

Only in specific cases, indicated by appropriate safety procedures related to individual laboratories

or activities, it is allowed to leave the room in which a transfer operation is in progress. In these cases (typically during vapor pre-cooling operations, or operation of open-flow cryostat), the dewar containing the cryogenic liquid must be visibly indicated, and every precaution must be taken to delimit the area in which liquid is found cryogenic and to prevent spills, splashes or accidental jets of cryogenic liquid or its own vapors, also considering the possible presence of untrained staff in the laboratory which could accidentally interfere with the dewar and transfer tubes. In these cases they must be taken considering physical barriers or possibly the ban on access to the laboratory at untrained staff.

A.3.7 Storage of dewar or tanks containing cryogenic liquids

Cryogenic liquids must be stored and handled in containers that have been designed to cope with the pressures and temperatures to which they can be subjected. Avoid contact with unsuitable materials, which could become very brittle at low temperatures. Indicate clearly, with a special sign, the dewars or tanks containing cryogenics liquids.

In the case of dewar or storage tanks of LN_2, always put a cap (making sure that there is always a way of venting the steam that is generated by spontaneous evaporation or use gravity caps) so that LN_2 is not directly exposed to the air. Indeed, since the point of evaporation of oxygen is higher than that of nitrogen, the oxygen in the air would condense in LN_2, making the mixture potentially explosive.

When the dewar or tanks are hot, it is not necessary to provide any special information. If the supervisor/responsible considers it appropriate, it can also be signaled on the laboratory door, with a sign, the presence inside dewar or cold storage tanks using the appropriate signs. This type of signs allows the description of the type of danger present specifying the term "nitrogen" replacing the generic term "cryogenic liquids" or "liquid helium".

A.3.8 Transport and lifting of dewar or tanks containing cryogenic liquids

The transport of LHe must be done exclusively in dewar suitable for this type of cryogenic liquid.

The transport of LN_2 in dewar suitable for this type of cryogenic liquid and also in containers or tanks specifically designed for cryogenic, is allowed insofar as they are insulated, unsealed and equipped of gravity cap, which can allow venting when a slight overpressure develops in the tank or container.

A.3.9 In the event of an accident, spillage, emergency, natural disaster, evacuation

In case of cold burns

1. Emergency call or directly to single emergency number or health emergency if the urgency requires it;
2. If the injury is severe or extensive, or if it is the eyes, call single number for emergencies or health emergency and have the victim transported to the hospital;
3. Do not provide heat to the affected area;
4. Loosen clothes that can limit blood circulation;
5. Wash the affected areas with large volumes of warm water ($41\,^{\circ}$C to $46\,^{\circ}$C) to reduce the freezing; do not heat quickly, the thaw can last from 15 to 60 minutes and can continue until the pale blue color of the skin turns pink or red;
6. Cover the affected area with a sterile protective dressing or with clean sheets if the area is great, and protect the area from further injury. Do not cover injuries with oils or other ointments;

7. If a freezing or shock principle is detected, cover the victim with one blanket;
8. Do not give alcoholic beverages, which decrease blood circulation in the body frozen fabrics. If the victim wishes, administer lukewarm drinks; do not allow the victim to smoke;
9. Consult a doctor.

In case of asphyxia

1. Any rescuer can only intervene if the area is safe;
2. Alert the emergency number or directly single emergency number or health emergency according to the urgency;
3. If a person begins to falter or loses his senses while working in a liquid environment cryogenic, it is necessary to bring it immediately in a well-ventilated place;
4. Symptoms of an incipient asphyxia may be rapid or labored breathing, fatigue abnormal, nausea and vomiting, collapse or inability to move, unusual behavior or cognitive difficulties.

In the event of an accident with spillage or release of vapors

Evaporation of a large quantity of cryogenic liquid can cause mists that limit visibility. It is therefore necessary that all workers have clear position of the routes of escape and that these are free from encumbrance.

A spill of cryogenic liquid on the floor can cause a thin to freeze layer of water coming from atmospheric humidity, which makes the floor particularly insidious. Care should therefore be taken not to slip.

If the spill is limited, demarcate the area and ventilate, otherwise evacuate the room.

Pay close attention to the fact that a spill or a release of vapors can damage vacuum seals or insulating sleeves of electric wires, causing secondary accidents such as breakage of empty, short circuits, etc.

In case of emergency evacuation or natural disaster

- If possible, stop any transfer operations, depressurize the dewar or receptacles and leave the relief valves open;
- If possible, switch off any systems that require the cryogenic liquid as refrigerant and that could lead to an accident in case of sudden evaporation (for example superconducting magnets);
- Abandon the room by closing the door not to key, to facilitate the possible entry of emergency teams;
- If possible, turn on the forced air intake.

A.3.10 Work alone

The operations of transfer or handling of cryogenic liquids are not recommended in solitude. It is allowed to work alone for the ordinary operations of the equipment using cryogenic liquids, provided that the operator has some experience about these operations and is not exposed to further risks.

A.3.11 Interference with other workers in the same room

Workers who work in any capacity in premises where cryogenic liquids are used are exposed to all the risks described above even if they do not directly use nitrogen or helium liquids. And therefore it is mandatory that these workers are trained properly before they can access these rooms using this security procedure and any other ones relevant procedures specific to the laboratory and the activity. It is important to remember that such workers include cleaning staff, installers and maintenance technicians, fellows, students and other workers free of charge, in addition to the staff who more or less regularly access the local for their duties.

It is also necessary:

1. Clearly identify the dewar, tanks, vessels, cryostats and machinery used for cryogenic liquids, for example with the signage previously reported;
2. Clearly identify the dewar or storage tanks containing cryogenic liquids (better if they are easily distinguishable from the empty ones and therefore do not present dangers), for example with the same signage;
3. Identify clearly, and if possible demarcate, areas that might be cold or affected by vapors of cold vapors;
4. Make sure that vents, steam jets or spills cannot interfere with escape routes, with other workstations, with other electrical equipment or devices;
5. Make sure there are no pipes, valves or other components that can be knocked out or accidentally tampered with by unqualified personnel, causing breakages, spills or spills of cold steam jets.

For workers subject to interferential risk, the same rules apply as for workers directly involved in the use of cryogenic liquids, also regarding the rules of clothing and conduct to be kept in case of accident or evacuation.

A.3.12 Normative and bibliographic references

1. INRIM - IO SPP 012: Istruzione Operativa Sicurezza in Criogenia, Ed: , Rev. 0, 09/05/17 (in Italian).
2. Safety Matters, Oxford Instruments.
3. Practical Cryogenics, An introduction to Laboratory Cryogenics, by N.H. Balshaw, Oxford Instruments.
4. Jefferson Lab, Oxygen Deficiency Hazard Safety Booklet, version July 2008.

http://www.acqpro.cmi.cz

Javier Díaz de Aguilar, Raúl Caballero, Yolanda A. Sanmamed, Martin Šíra, Patryk Bruszewski, Andrea Sosso, Vitor Cabral, Luís Ribeiro, Helge Malmbekk, Jonathan M. Williams, Ralf Behr, Oliver Kieler, Recep Orhan, Grégoire Bonfait

Good Practice Guide on the operation of AC quantum voltage standards

Published by Czech Metrology Institute
Okružní 31, Brno, 636 00, Czech Republic
Typeset by Martin Šíra using pdfLaTeX

First edition, 21.6.2018
ISBN 978-80-905619-2-2
2018